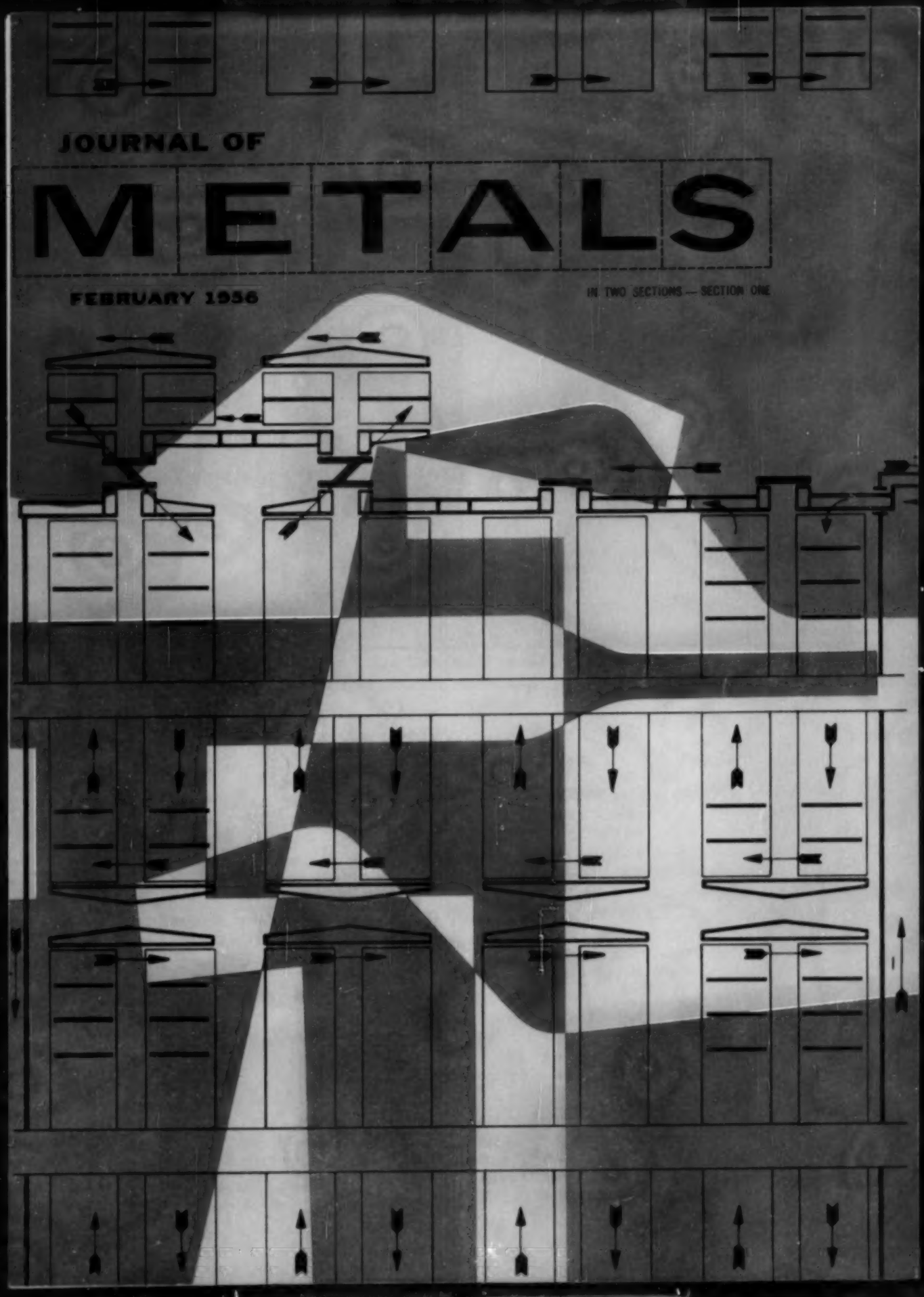
JOURNAL OF
METALS
FEBRUARY 1956
IN TWO SECTIONS — SECTION ONE

Furnace additions of ELECTROMET *silicomanganese give you many advantages . . .*

• **Combination Alloy** – In making steel, silicon and manganese are much more effective deoxidizers in combination than when used separately. ELECTROMET silicomanganese is designed for the simultaneous addition of silicon and manganese in the correct proportion.

• **Fast Solubility** – Because of the concentration of active elements in ELECTROMET silicomanganese, less time is required for solution in molten steel than when equivalent amounts of silicon and manganese are added separately.

• **Savings in Furnace Time** – Because of the low carbon content of silicomanganese, the carbon in the bath need not be reduced so much as would otherwise be necessary. This results in a saving in furnace time.

• **Cleaner Steel** – Since silicomanganese has a low carbon content, it is not necessary to drive the carbon as low (or make the oxygen as high) as when standard ferromanganese is used. The final steel is, therefore, cleaner and has better working properties.

CHOICE OF THREE GRADES

You have a choice of three grades of ELECTROMET silicomanganese:

Max. 1.50% Carbon Grade	Manganese	65 to 68%
	Silicon	18 to 20%
Max. 2.00% Carbon Grade	Manganese	65 to 68%
	Silicon	15 to 17.50%
Max. 3.00% Carbon Grade	Manganese	65 to 68%
	Silicon	12 to 14.50%

"ELECTROMET" SERVICE IS AVAILABLE TO YOU

Our metallurgists will be glad to assist you in the application of ELECTROMET silicomanganese to your specific requirements.

For further information please get in touch with the nearest ELECTROMET office.

The term "Electromet" is a registered trade-mark of Union Carbide and Carbon Corporation.

ELECTRO METALLURGICAL COMPANY
A Division of Union Carbide and Carbon Corporation
30 East 42nd Street UCC New York 17, N. Y.

OFFICES: Birmingham • Chicago • Cleveland • Detroit
Houston • Los Angeles • New York • Pittsburgh • San Francisco

In Canada: Electro Metallurgical Company, Division of Union Carbide Canada Limited, Welland, Ontario

JOURNAL OF

METALS

Published to provide a continuing, authoritative, and up-to-date record of technological, engineering, and economic progress in all branches of the metals industry by the
Metals Branch
American Institute of Mining and Metallurgical Engineers, Inc.
29 West 39th Street, New York 18

• • •

RIXFORD A. BEALS
Editorial Director

• • •

M. SNEDEKER G. M. ZILL
N. FRANKEL
Assistant Editors

• • •

METALS BRANCH COUNCIL

J. H. Scaff — Chairman
R. W. Shearman — Secretary
J. S. Smart, Jr. — IMD Chairman
A. W. Thornton — ISD Chairman
A. W. Schlechten — EMD Chairman
P. T. Stroup — M. E. Volin
J. S. Marsh — D. S. Eppelsheimer

EDITORIAL ADVISORY COMMITTEE

J. S. Smart, Jr. — Chairman
W. A. Dean — Evan Just
J. C. Kinnear, Jr. — John Marsh
T. D. Jones — M. Tenenbaum

TECHNICAL PUBLICATIONS COMMITTEES

N. Arbiter — AIME Chairman
H. B. Emerick — ISD Chairman
S. J. Dickinson — EMD Chairman
P. A. Beck — IMD Chairman
E. J. Kennedy, Jr. — Secretary

• • •

STAN TUCKER
Advertising Director

• • •

GRACE PUGSLEY — Production Manager
W. J. SEWING — Asst. Prod. Mgr.
WARREN V. SMITH
Eastern Advertising Manager
BOB WILSON
Western Advertising Manager
Millard Ave., Fox River Grove, Ill.

• • •

Journal of Metals
Mining Engineering
Journal of Petroleum Technology
The AIME Publishes:

VOL. 8, NO. 2 — FEBRUARY, 1956

COVER

Artist Harry Brocke finds an interesting pattern in the busbar system that is the electric driving system of Mufulira's electrolytic copper refinery. The full story of this plant will be found beginning on page 234.

NEWS

Personnel Service	218	AIME News	289
Books for Engineers	224	Personals	294
Drift of Things	231	Coming Events	296
Reporter	233	Advertisers' Index	296

Mufulira's Electrolytic Copper Refinery 234
R. H. Bauld, G. E. Rowe, G. N. Healey, A. A. Haynes, and P. C. Lockyer
Introduction: The Economic Factors
Refinery Design
Anode Dept.
Tankhouse Operations
Electrical Distribution—Boiler Plant—Yard and Transportation

TRANSACTIONS

Kinetic Study of the Oxidation of Sphalerite 257
J. N. Ong, Jr., M. E. Wadsworth, W. M. Fassell, Jr.

Intermediate Phases in Binary Systems of Certain Transition Elements 265
P. Greenfield, P. A. Beck

Influence of Holes and Electrons on the Solubility of Lithium in Boron-Doped Silicon 276
H. Reiss, C. S. Fuller

Preparation of Metallic Titanium by Film Boiling 284
A. W. Petersen, L. A. Bromley

TECHNICAL NOTES

Filtering Apparatus for Study of Liquid-Solid Equilibria in Alloy Systems 263
L. A. Willey

Effect of Stress on the Martensitic Transformation in the Cu-Zn System 283
E. J. Scanlon, R. M. Genevoy, M. B. Bever

Liquid Emulsion Autoradiography of Metals 286
J. C. Bokros, P. C. Rosenthal

Effect of Cooling Rate on Hardness of Commercial Titanium Alloys 288
H. Martens

This issue of JOURNAL OF METALS is in two Sections:
Section 1—Magazine Section 2—Transactions Section

Published the first day of each month by the American Institute of Mining and Metallurgical Engineers, Inc., 29 West 39th Street, New York 18, N. Y. Telephone: PEnnsylvania 6-9220. Subscription $8 per year for non-AIME members in United States and North, South and Central America; $10, foreign; $6 for AIME members, or $4 additional in combination with a subscription to "Mining Engineering" or "Journal of Petroleum Technology." Single copies, 75 cents; single copies foreign, $1.00; special issues, $1.50.... The AIME is not responsible for any statement made or opinion expressed in its publications.... Copyright 1956 by the American Institute of Mining and Metallurgical Engineers, Inc.... Registered cable address, AIME New York.... Indexed in Engineering Index, Industrial Arts Index and Chemical Abstracts.... Reentered as second-class matter Sept. 21, 1949, at the post office at New York, N. Y., under the Act of March 3, 1879. Additional entry established at Manchester, N. H.

— PERSONNEL SERVICE —

THE following employment items are made available to AIME members on a nonprofit basis by the Engineering Societies Personnel Service Inc., operating in cooperation with the Four Founder Societies. Local offices of the Personnel Service are at 8 W. 40th St., **New York 18**; 100 Farnsworth Ave., **Detroit**; 57 Post St., **San Francisco**; 84 E. Randolph St., **Chicago 1**. Applicants should address all mail to the proper key numbers in care of the New York office and include 6c in stamps for forwarding and returning application. The applicant agrees, if placed in a position by means of the Service, to pay the placement fee listed by the Service. AIME members may secure a weekly bulletin of positions available for $3.50 a quarter, $12 a year.

——POSITIONS OPEN——

Metallurgist, 22 to 45, engineering degree, to supervise activities of a section of the laboratory, plan and direct development projects, investigate and consult on fabricational problems encountered in production of aircraft engine components. Salary, $5000 to $8500 a year. Location, Iowa. C4263.

Instructor to Professor, Ph.D., 25 to 55, to teach and do research work of metallurgy at graduate and undergraduate level. Must have knowledge of metallurgy or metal physics. Salary, $4,000 to $10,000 a year. Location, Chicago. C4306.

Research Metallurgist, M.S. metallurgy, up to 40, for normal research work on metals and alloys for shop usage for refinery of petroleum. Must have at least five years experience in metallic research work. $7800 a year. Location, Calumet District. C4250.

Materials Metallurgist, to 40, for research work on metal failures for refinery of petroleum. Must have at least five years experience in materials selection, failure analyses, etc. Salary, $6000 to $7200 a year. Location, Calumet district. C4249.

Metallurgist, up to 35, for inorganic nonferrous research and development for refiners of base and precious metals. Must have knowledge of physical metallurgy. Salary, up to $6000 a year. Employer will pay placement fee. Location, Chicago. C4095.

Engineers. (a) Metallurgists, B.S., M.S., or Ph.D. graduates, with 1 to 10 years experience. Appropriate background in physical, process, extraction, light alloy development, welding, or powder metallurgy. (b) Minerals engineers, B.S. or M.S. graduates, with 1 to 10 years experience. Appropriate background in minerals processing, extraction, hydrometallurgy, pilot plant operation, and plant process improvement. Salaries, $5400 to $9600 a year. Location, Midwest. W2732.

Sales Engineer, recent graduate, with degree in metallurgical, chemical, or mechanical engineering, for company producing ferrous and nonferrous alloys. Territories open in Midwest and on East Coast. W2729.

Chemical-Metallurgical Engineer and Lubrication Engineer for field test and exploit commercial developments in metal working, wire drawing, lubricants, automotive chemicals for laboratory. Salary open. Employer will pay placement fee. Location, New Jersey. W2693.

Process Engineer, recent graduate (will consider nongraduate); several years experience in mechanical engineering or metallurgy. Company offers one year training program in methods and process engineering, etc. Salary, to $6500 a year after training period. Location, New York, N. Y. W2668.

Metallurgical Engineer, young, to assist chief metallurgist in laboratory and production problems. Nonferrous metals, including brass and aluminum subjected to cold working and annealing processes. Technical degree. Salary, $6000 to $7200 a year. Location, Pennsylvania. W2456(a).

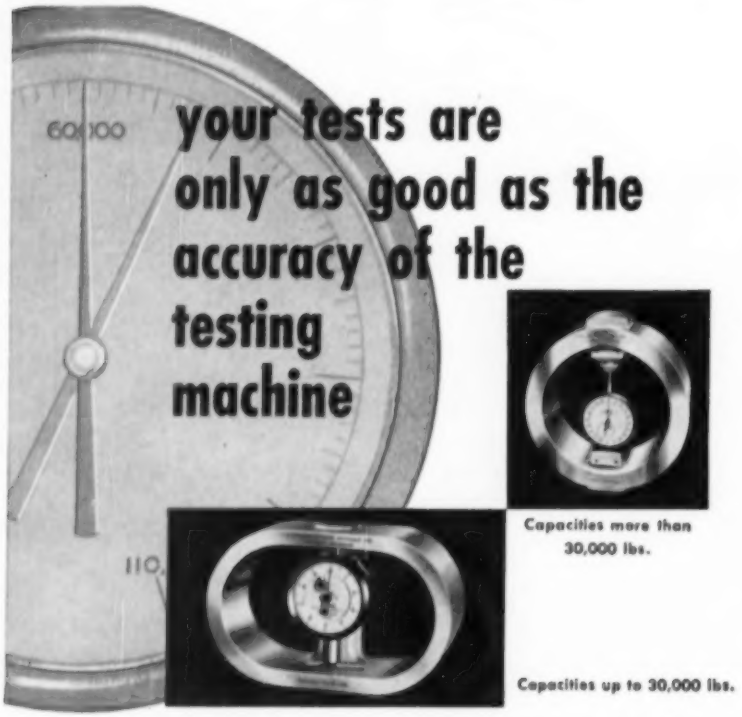
your tests are only as good as the accuracy of the testing machine
Capacities more than 30,000 lbs.
Capacities up to 30,000 lbs.

Steel City Proving Rings, calibrated by the National Bureau of Standards, *check* the accuracy of your equipment.

Steel City Proving Rings are of the direct reading type . . . indicator graduations are in .0001", and the resultant readings are translated into pounds or kilograms by calibration reports furnished with the rings. No adjustments are necessary . . . do not require experienced operator to get accurate results. Used for checking loads on Brinell, Universal, other testing machines and presses.

Steel City has qualified sales representatives in *all* major metal-working areas to give you *personal* attention.

Manufacturers of machines for testing physical properties of metals, including:

Steel City Testing Machines Inc.
8825 Lyndon Ave., Detroit 38, Mich.

Brinell Hardness | Ductility | Tensile | Compression
Transverse | Hydrostatic | Proving Instruments | Flex-Tester
. . . and Special Testing Machines.

Editorial Assistant with mechanical engineering training and metal products experience, for technical writing and editorial work. Salary, $4500 to $5200 a year. Location, Westchester County, N. Y. W2664.

Metallurgist, young, with nonferrous metallographic and mechanical testing experience. Salary, $4800 to $6000 a year. Location, New Jersey metropolitan area. W2472.

Engineering Geologist to study and develop present and future raw material sources for a cement company. Location, Pennsylvania. W2470.

Research Metallurgist, graduate, with 6 to 10 years of good experience, including research metallurgy on heavy sulfide ores. Some operating experience desirable, but not absolutely necessary. Salary open. Location, Mediterranean area. F2469.

Metallurgist with X-ray and spectrographic laboratory experience. Salary, $6000 a year. Location, Long Island, N. Y. W2455.

Metallurgical Engineer, young, graduate, with at least three years experience covering welding, heat treating, testing, and/or manufacturing of ferrous and nonferrous equipment. Location, upstate New York. W2147(a).

Field Engineer, young, with equipment experience in chemical, metallurgical, or process industry for service work covering equipment improvements. Considerable traveling. Salary, $4800 to $6000 a year. Location, eastern states. W2144.

Assistant Metallurgist, B.S. engineering, 22 to 32, for the development, piloting through production, and production control of automatic and semi-automatic welding rods and/or their fluxes. Must have had some experience with welding and knowledge of metallurgy and welding. Salary, $4800 to $6000 a year. Employer will negotiate placement fee. Location, south Chicago. C3907.

MEN AVAILABLE

Metallurgist, M.S. degree. Six years diversified experience nonferrous metallurgy. Work on applied research of creep phenomena, various alloy development, extrusion problems, investigation of modification of phase changes, use of vacuum techniques, etc. Desires position with opportunity to advance. M-148.

METALLURGIST

.....needed as Process Metallurgist and Quality Control in brass mill manufacturing beryllium-copper, phosphor-bronze and nickel-silver in the form of strip, wire and rod.

Reply fully in writing, giving age, experience and salary desired to: Personnel Department, The Riverside Metal Company Division, H. K. Porter Company, Inc., Riverside, New Jersey.

PROJECT ENGINEER WANTED

Major West Coast engineering firm offers outstanding opportunity to well qualified engineer with degree in metal mining, metallurgical, or mechanical engineering—age 35 to 50.
Must have broad design and operation experience in basic industries such as cement, metal mining, ore dressing, smelting, metallurgical milling.
Please write furnishing complete chronological experience record and salary history. Also show details regarding education, salary desired, business and character references.

Box B4-M AIME
29 West 39th Street, New York 18

Metallurgist—B.S. or M.S. degree with some experience for diversified responsibility involving manufacturing control, metallography, development and application. Position involves work on high temperature applications, precision casting processes and mold materials, application and control on quality die steels, and laboratory testing and failure analysis. Experience in any of these phases of metallurgy is helpful but not essential. Company is one of the oldest and best known in its field and is located in the Southern Tier of New York State.

Box B5-M AIME
29 West 39th St., New York 18

RESEARCH METALLURGISTS

Research and development engineers with experience and a desire to use their talents are needed for challenging work in the fields of alloy development, primary metal forming and metal processing.

These new positions in the Department of Metallurgical Research, Kaiser Aluminum and Chemical Corp., have been created as a result of a current research expansion to meet the demands of the rapidly expanding aluminum industry. Attractive salaries, insurance and retirement benefits. Expenses connected with interview and relocation will be paid.

For further information and application forms, please write to:
M. C. Fetzer
Department of Metallurgical Research
Kaiser Aluminum and Chemical Corp.
Spokane 69, Washington
Replies will be held confidential.

SENIOR ENGINEER
METALLURGICAL RESEARCH

For materials research and Radiations Studies Group of the Aircraft Nuclear Propulsion Department.

A senior research position is now open in an advanced project . . . the application of nuclear energy to the field of flight. The engineer who qualifies will be responsible for research designed to provide improved metals and alloys for use in an aircraft nuclear power plant.

The job requires a degree in physical metallurgy or metallurgical engineering and 8 to 10 years experience in working with high temperature or corrosion resistant metals and alloys. (If directly related, time spent on obtaining an advanced degree may be considered part of this experience.)

PUBLICATION OF RESEARCH RESULTS IN THE APPROPRIATE CLASSIFIED OR OPEN LITERATURE IS ENCOURAGED.

Openings in
Cincinnati, Ohio and Idaho Falls, Idaho
Address replies to location you prefer

Aircraft Nuclear Propulsion Dept.
ATT: W. J. Kelly
ATT: L. A. Munther

GENERAL ELECTRIC

P.O. Box 132, Cincinnati, Ohio
P.O. Box 535, Idaho Falls, Idaho

RESEARCH AND DEVELOPMENT
THE NEW JERSEY ZINC COMPANY (OF PA.)
RESEARCH DEPARTMENT
PALMERTON, PENNA.
PROCESS METALLURGISTS
PHYSICAL METALLURGISTS

Research and Development program on processing of raw materials, manufacture and applications of zinc, titanium, metals and alloys and new products. Smelting, electrometallurgy, alloy development, and corrosion.

Advanced degrees or research experience desirable for Research; not required for Development. We have openings for men without experience or with up to five or ten years' experience.

These openings are for permanent staff positions in a well-established research organization. Excellent laboratories and working conditions. Ideal location in Eastern Pennsylvania.

Morgan Quality in Action

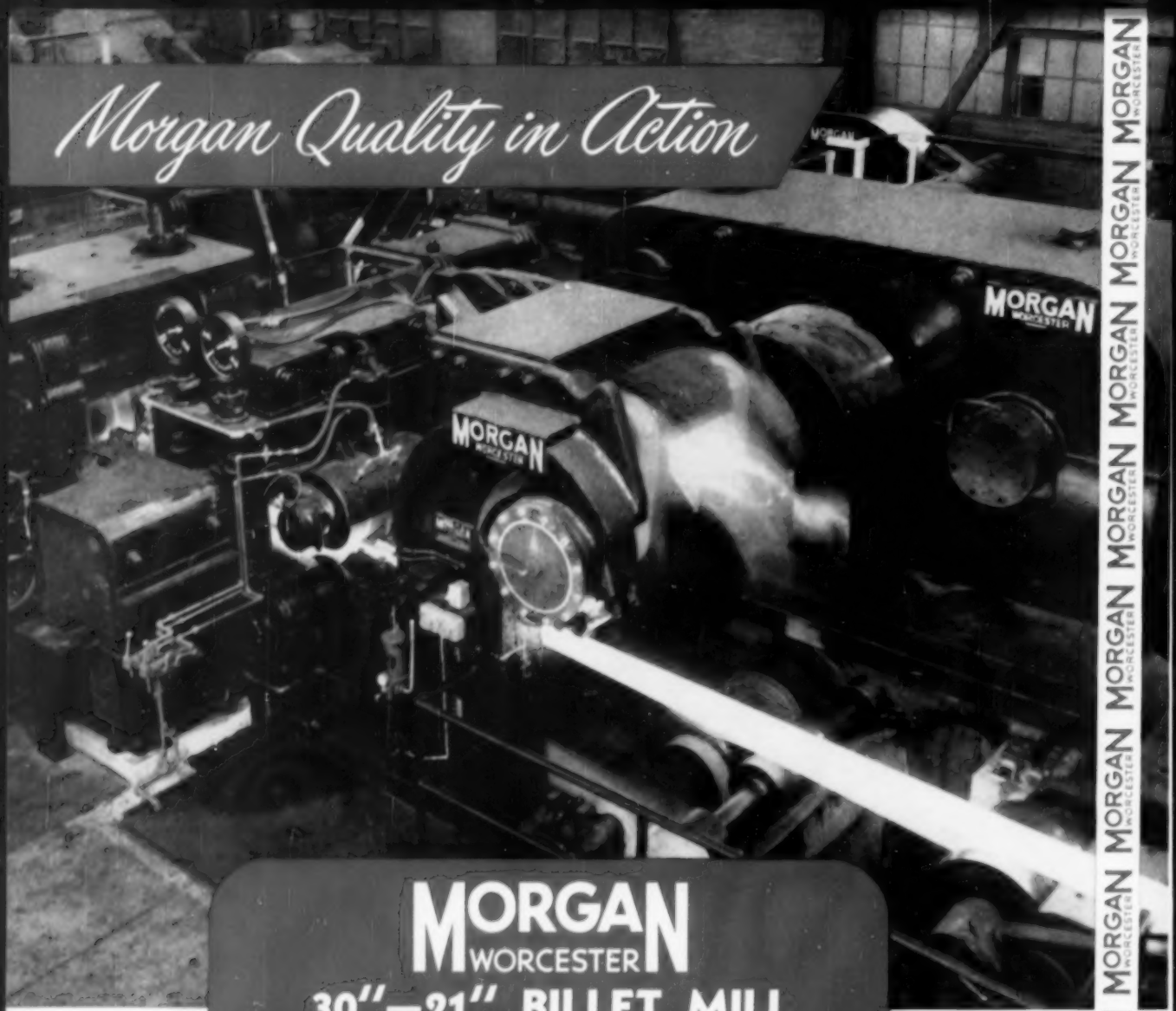

MORGAN WORCESTER

30"—21" BILLET MILL

with No.5 Electric Flying Shear in Action

Every Morgan Mill is developed by highly skilled technical engineers to answer the exacting demands of mass production. Morgan introduced the first successful continuous rolling mill in this country—and has consistently maintained leadership in producing quality, high production mills in this country and abroad.

MORGAN CONSTRUCTION CO.

WORCESTER, MASSACHUSETTS

ROLLING MILLS MORGOIL BEARINGS GAS PRODUCERS
WIRE MILLS EJECTORS REGENERATIVE FURNACE CONTROL

English Rep., International Construction Co., 56 Kingsway, London W. C. 2, Eng.

RM-68

MORGAN WORCESTER MORGAN WORCESTER MORGAN WORCESTER

for accurate analytic results
use Leitz *precision equipment*

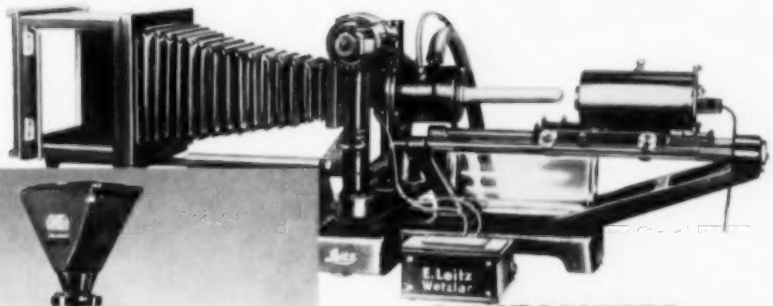

Leitz **DILATOMETER**

for accurate metal analysis

Researchers consider dilatometric analysis the most sensitive and reliable method for precise determination of the expansion coefficient of metals, alloys, etc. The *DILATOMETER* records volume changes in relation to its own temperature (absolute curve), yielding data from which the expansion coefficient may be determined.

Leitz **METALLUX** *microscope*

for easier, quicker metallography

Metallography is easier with the METALLUX—unobstructed upright stage, inclined eyepieces, unique quintuple nosepiece, built-in light and low position controls for relaxed operation. Accessory equipment available for phase contrast, material testing and photography.

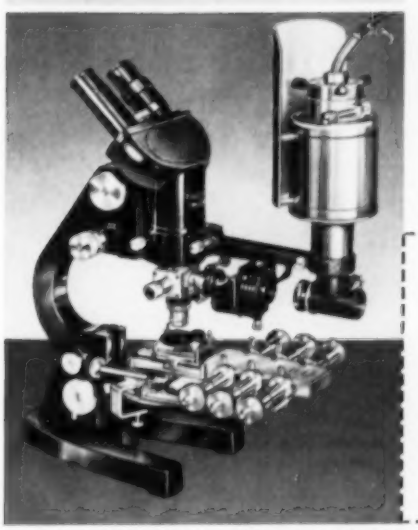

Leitz **KPM** *microscope*

for precise coal petrography

Engineered specifically for coal petrographic investigation, including examination by polarized or ordinary light, quantitative analysis and microscopic measurement. Fusain analysis readily accomplished by coal slide-comparison eyepiece with revolving disc.

68788

E. LEITZ, INC., Dept. JM-2
468 Fourth Ave., New York 16, N. Y.

Please send me additional information on the

☐ *DILATOMETER* ☐ *METALLUX* ☐ *KPM*

Name_____

Street_____

City_____ Zone_____ State_____

E. LEITZ, INC., 468 FOURTH AVENUE, NEW YORK 16, N. Y.
Distributors of the world-famous products of Ernst Leitz, Wetzlar, Germany
LENSES • CAMERAS • MICROSCOPES • BINOCULARS

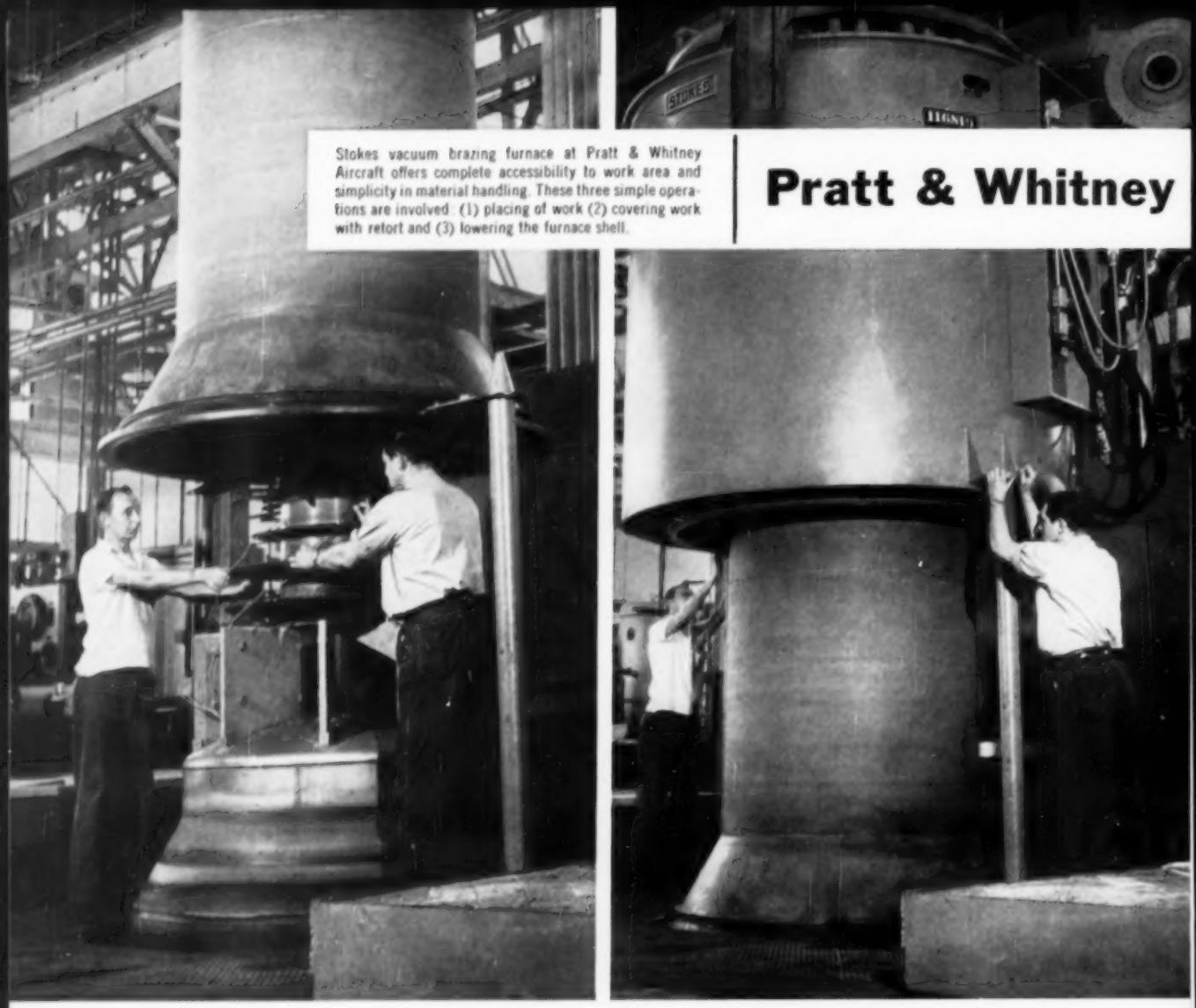

Stokes vacuum brazing furnace at Pratt & Whitney Aircraft offers complete accessibility to work area and simplicity in material handling. These three simple operations are involved: (1) placing of work (2) covering work with retort and (3) lowering the furnace shell.

Pratt & Whitney

THE COMPLETE LINE OF STOKES

Stokes manufactures a complete line of vacuum pumping equipment. This includes mechanical vacuum pumps, diffusion and booster pumps, vacuum valves and gages, and complete vacuum instrumentation. In engineered high vacuum equipment, Stokes builds vacuum metallizers, vacuum furnaces and other vacuum processing equipment.

Stokes has for many years been active in vacuum research. Vacuum experience among our engineers covers the range from laboratory equipment to some of the largest vacuum equipment in service. This experience is available to help solve your vacuum problems.

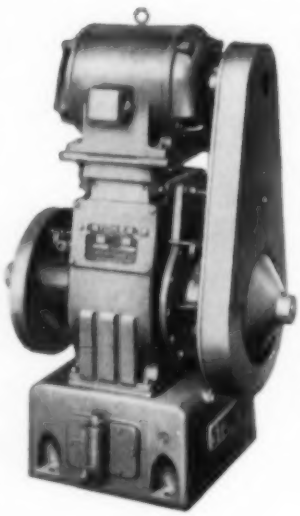

STOKES MECHANICAL VACUUM PUMPS

For vacuum processing systems and for maintaining low forepressures in high-vacuum systems, the Stokes Microvac pump provides efficient, economical operation. Designed with fully automatic lubrication and a long-lasting exhaust valve assembly, every Microvac pump is assured of smooth, trouble-free operation. Six sizes give capacities from 15 to 500 cfm. Send for catalog listed at right.

Aircraft Uses Stokes Furnace to Investigate Vacuum-Brazing of Jet Engine Components

Versatile new furnace design also can be used for heat-treating and outgassing at high vacuum or under controlled atmospheres.

A logical development of vacuum metallurgy, high-vacuum brazing, presently being investigated by numerous firms throughout the country, promises to produce superior products more economically than brazing methods used heretofore. Tests of vacuum brazed components indicate the greater strength, ductility and uniformity of assemblies produced by this method.

Typical of firms currently carrying on investigations in this field is Pratt & Whitney Aircraft, East Hartford, Conn. The firm is using a Stokes furnace in experimental work on the application of vacuum brazing to the production of jet engine components.

Stokes' furnace design for vacuum brazing is practical . . takes into account the problems of large-scale production. The Stokes dual-chamber design, with a smooth-contour retort completely enclosing the work, permits faster vacuum pumping cycles; provides complete accessibility of the work area and a large, uniform temperature zone.

Stokes engineers have a wealth of practical experience in the field of vacuum metallurgy We'll be glad to discuss the application of this fast-growing science to your production. Write for Catalog 790 containing valuable information on Stokes High-Vacuum Furnaces.

F J Stokes Machine Company, 5504 Tabor Road, Philadelphia 20, Pa.

SEND FOR TECHNICAL LITERATURE:

- Microvac Pumps—Catalog 750
- Diffusion and Booster Pump Specification sheets and performance curves
- The Story of the Ring-Jet Pump
- Complete Vacuum Processing Systems—Catalog 730
- How to Care for Your Vacuum Pump—Booklet 755
- Vacuum Impregnation—Catalog 760
- Vacuum Drying—Catalog 720
- Vacuum Furnaces—Catalog 790
- Vacuum Metallizing—Catalog 780
- Vacuum Calculator Slide Rule

VACUUM EQUIPMENT

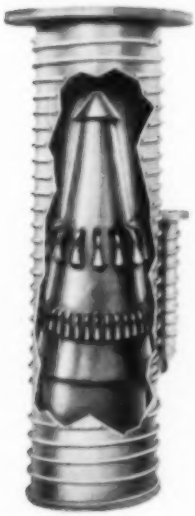

STOKES RING-JET DIFFUSION AND BOOSTER PUMPS

The new Stokes Ring-Jet Pumps embody a new concept of the diffusion principle. Size for size, they have pumping speeds of 10% to more than 100% above any other diffusion pump for a given heat input. Ring-Jet Diffusion Pumps are available in sizes of 4, 6, 10, 14 and 16 inches; Booster Pumps in sizes of 4, 6, 10 and 16 inches. Send for information listed.

STOKES VACUUM VALVES

To control vacuum safely and surely, Stokes vacuum valves are available in 4, 6, 10 and 16-inch standard flange sizes.

STOKES-McLEOD VACUUM GAGES

For measuring vacuums from fractions of a micron up to 50 mm, Stokes-McLeod gages are the standard of reference. Four sizes available.

STOKES

OFFICES IN PRINCIPAL CITIES, REPRESENTATIVES THROUGHOUT THE WORLD

Books for Engineers

ORDER YOUR BOOKS THROUGH AIME—Address Irene K. Sharp, Book Dept. AIME members given 10 pct discount whenever possible. Please order Government publications direct from the agency concerned.

Principles of Physical Metallurgy, by Morton C. Smith, *Harper & Brothers,* $6.00, 417 pp., 1956.—The science of metal behavior as an integrated, consistent, and satisfying chain of reasoning is developed and presented. It begins with the necessary background in physics, chemistry, and thermodynamics. It then discusses in detail the crystallography, crystal structures, and crystal mechanics of metals with an extensive treatment of crystal imperfections, deformation behavior, and the general effects of elevated temperatures.

Alloy Series in Physical Metallurgy, by Morton C. Smith, *Harper & Brothers,* $6.00, 338 pp., 1956.—This book begins where the *Principles of Physical Metallurgy* ends. It starts with the phase rule and binary constitutional diagrams in general and considers all of the solidification and solid state reactions commonly encountered in metallic systems.

Atomic Physics, by G. P. Harnwell and W. E. Stephens, *McGraw-Hill Book Co., Inc.,* $8.00, 401 pp., 1955.—Fundamental physical ideas relating to the nature of matter and radiation, atomic structure, electron spin, poly-electronic atoms, and molecular structure are presented.

High Vacuum Technique, third edition, by J. Yarwood, *John Wiley & Sons, Inc.,* $5.50, 208 pp., 1955.—New material in this edition includes an analysis of American and British vacuum pumps, details of large diffusion pumps, and information on a number of innovations in methods. Among the applications discussed are exhausting radio tubes, deposition of metal films, and evaporation. The book is a concise presentation of standard techniques for producing and measuring high vacuums and a description of the latest developments in apparatus, materials, and applications.

ASTM Specifications for Steel Piping Materials, *ASTM,* $4.00, 425 pp., 1955.—This edition contains the latest approved form of 58 ASTM specifications for ferrous pipe, tubes, castings, fittings, and bolting materials.

An Introduction to Reactor Physics, by D. J. Littler and J. F. Raffle, *McGraw-Hill Book Co., Inc.,* $4.50, 196 pp., 1955.—This is a detailed presentation of the calculations used in evaluating the critical size of a gas cooled, graphite moderated, natural uranium reactor of the type intended for use in the nuclear energy power program of the United Kingdom. It also includes an account of nuclear physics essential for an understanding of the construction principles and sufficient theory for an understanding of the problems involved in construction of other types of reactors.

Superior
BLAST FURNACE
COPPER CASTINGS
Hot Blast Valves and Valve Seats
Blast Furnace Tuyeres. Licensed Manufacturers of all Leading Designs
Cooling Plates of all kinds including Heavy Nose Super Cooled Bosh Plates.
SMEETH-HARWOOD COMPANY
8524 Vincennes Ave., Chicago 20, Ill.
In Canada—The William Kennedy & Sons, Ltd., Owen Sound, Ontario
Blast Furnace Copper Castings—also Brass and Bronze Mill Castings

Metallographie, in German, by Hermann Schumann, *Fachbuchverlag Leipzig,* 30 marks (about $8.10), 374 pp., 1955.—During the course of time the microscopic examination of metals has found entrance into alloy production and metal working on a qualitative technical basis. This book is written not as a study book, for metallography, in the author's opinion, cannot be learned through self study or through listening to lectures. The reason for this work is to acquaint the reader with some important special metallographic work in order to show in the clearest possible form the relation between the phase diagram of the alloy and its structural interpretations. The text is interspersed with formulas and a moderate number of calculations as well as tables.

Hydrology, edited by Oscar E. Meinzer, *Dover Publications, Inc.,* $4.95, 712 pp., 1955 Edition.—Included is material on the whole hydrologic cycle: distribution of rainfall, effects of wind and heat, water table fluctuations, soil moisture, flood control, effects of the internal motion of glaciers, etc. It contains 165 illustrations and 23 tables. Twenty four experts have pooled their knowledge to make this the most up-to-date handbook available on the subject.

Bibliography on Machinery Foundations; Design, Construction, Vibration Elimination, compiled by Engineering Societies Library, $2.00, 25 pp., 1955.—This is a revised list of 175 annotated references of selected books and articles published from 1924 to 1955. Subjects covered are: theory, design, and construction of machinery foundations; specific problems such as heavy machinery foundations on unstable soils; and vibration as related to foundations of oil engines, turbines, presses, machine tools, etc.

Annual Review of Nuclear Science, Vol. 5, edited by J. G. Beckerley, *Annual Reviews,* $7.00, 448 pp., 1955.—Typical papers deal with radiation shielding, nuclear particle detection, design comparison of reactors for research, and mass spectrometry. Author and subject indexes to Vol. 5 and chapter author and title indexes to Vols. 1 to 5 are included.

Aeroelasticity, by R. L. Bisplinghoff, Holt Ashley, and R. L. Halfman, *Addison-Wesley Publishing Co., Inc.,* $14.50, 860 pp., 1955.—The first part of this book presents analytical methods for dealing with problems of aircraft structures under load and problems of two and three dimensional incompressible flow, compressible flow, and three dimensional unsteady flow. In the second part these methods are applied to problems of static aeroelasticity, flutter, and dynamic response phenomena.

Experimental model of Bell's new high-frequency transistor. It has a cut-off frequency of at least 500 mc and can be used to amplify 2500 independent voices simultaneously.

THE TRANSISTOR
that smashed a frequency barrier

A new transistor invented at Bell Telephone Laboratories can provide broadband, high-frequency amplification never before possible with transistors. The big leap in frequency is made possible by a diffusion process that earlier enabled Laboratories scientists to create the Bell Solar Battery.

This transistor is a 3-layer semiconductor "sandwich." High-frequency operation is obtained by making the central layer exceedingly thin. This was difficult to do economically by any known method.

The new diffusion process, however, easily produces microscopic layers of controllable thickness. Thus it opens the way to the broad application of high-frequency transistors for use in telephony, FM, TV, guided missiles, electronic brains and computers.

The new transistor shows once again how Bell Laboratories creates significant advances and then develops them into ever more useful tools for telephony and the nation.

A Bell scientist checks temperature as arsenic vapor diffuses into germanium, creating 4/100,000-in. layer.

BELL TELEPHONE LABORATORIES

IMPROVING AMERICA'S TELEPHONE SERVICE PROVIDES CAREERS FOR CREATIVE MEN IN SCIENTIFIC AND TECHNICAL FIELDS

JPL . . . an Established Center of Research and Development

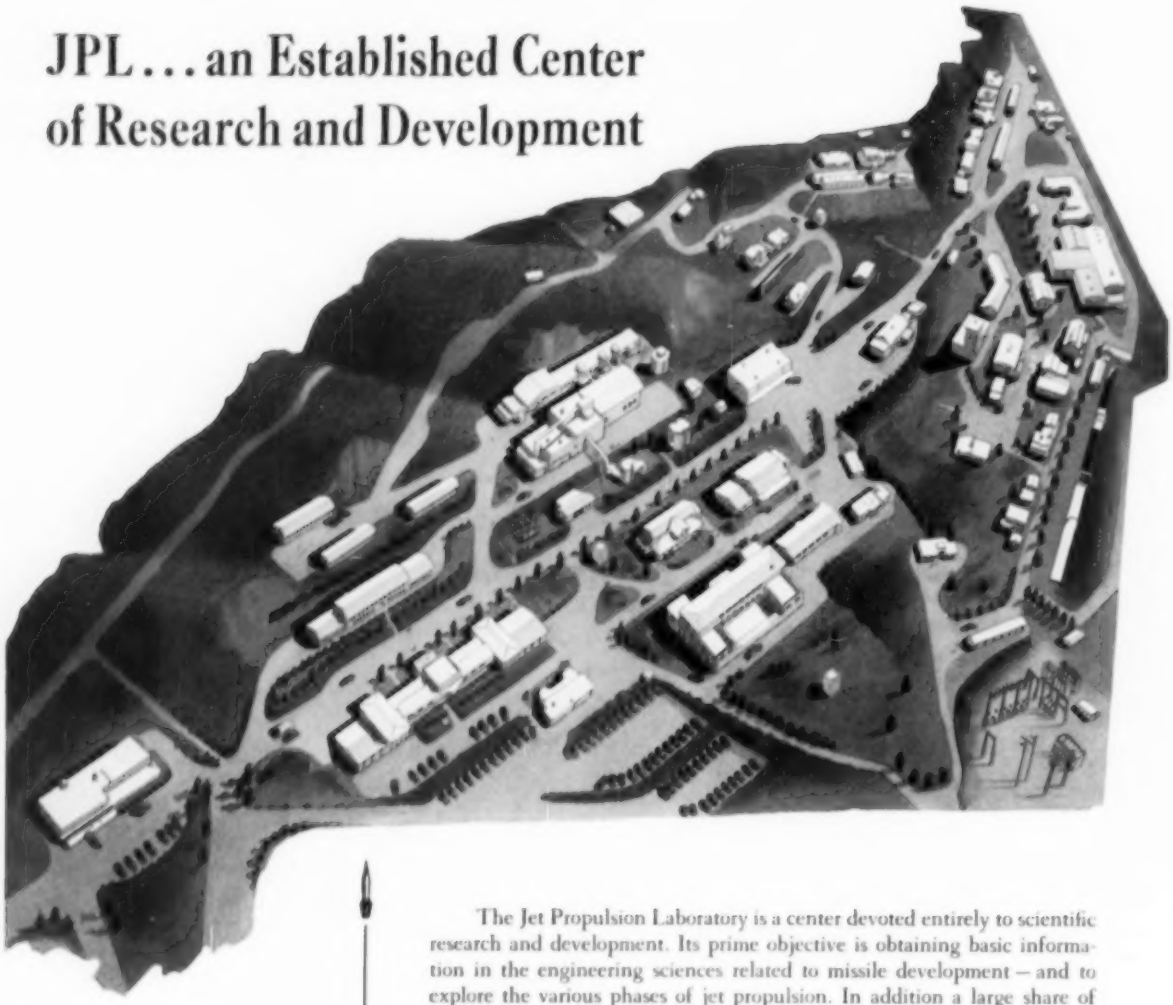

The Jet Propulsion Laboratory is a center devoted entirely to scientific research and development. Its prime objective is obtaining basic information in the engineering sciences related to missile development — and to explore the various phases of jet propulsion. In addition a large share of its program is devoted to fundamental research in practically all of the physical sciences.

The Laboratory extends over more than 80 acres in the foothills of the San Gabriel mountains north of Pasadena. It is staffed entirely by personnel employed by the California Institute of Technology and conducts its many projects under contracts with the U.S. Government.

Exceptional opportunity for original research coupled with ideal facilities and working conditions have naturally drawn scientists and engineers of a very high caliber. These men, working in harmony, are building a very effective task force for scientific attack on the problems of the future.

An unusual atmosphere of friendliness and cooperation is apparent at the "Lab" and newcomers soon sense the warmth of their acceptance. New advanced projects are now providing some challenging problems — and good jobs for new people.

If you would like to develop your skill and knowledge at the "Lab" and, at the same time, help us solve some of our problems — write us today.

★ At this time we are particularly interested in interviewing graduate engineers and scientists in the fields of aerodynamics, aircraft structures, mechanical engineering, chemistry, chemical engineering, heat transfer, electronics, systems analysis, electromechanical instrument design, instrumentation, metallurgy, nuclear physics and solid state physics.

These men should be definitely interested in scientific research and development relating to the problems of the future.

CALTECH jpl JET PROPULSION LABORATORY

A DIVISION OF CALIFORNIA INSTITUTE OF TECHNOLOGY

PASADENA, CALIFORNIA

AS PARTNERS IN
YOUR PROGRESS . . .

ENCLOSED STORAGE SILOS
MORGANTON, N. C., PLANT

OUR RAW MATERIAL UNIFORMITY – is a *plus* factor!

The extensive background of experience of Great Lakes Carbon Corporation in industrial carbons and other raw materials is an unique *plus* factor in the uniformity which distinguishes GLC electrodes, anodes, carbon brick and mold stock.

The high degree of integration between discoveries in our research laboratories, refinements in processing raw materials, and improved manufacturing techniques is further assurance of excellent product performance.

ELECTRODE
GLC®
DIVISION

Great Lakes Carbon Corporation

GRAPHITE ELECTRODES, ANODES, MOLDS and SPECIALTIES

ADMINISTRATIVE OFFICE: 18 East 48th Street, New York 17, N. Y. PLANTS: Niagara Falls, N. Y., Morganton, N. C. OTHER OFFICES: Niagara Falls, N. Y., Oak Park, Ill., Pittsburgh, Pa. SALES AGENTS: J. B. Hayes Company, Birmingham, Ala., George O. O'Hara, Wilmington, Cal. SALES AGENTS IN OTHER COUNTRIES: Great Northern Carbon & Chemical Co., Ltd., Montreal, Canada; Great Eastern Carbon & Chemical Co., Inc., Chiyoda-Ku, Tokyo, Japan

New

1715 AB ELECTRO POLISHER FOR METALLURGICAL SAMPLES

New **GREATER POWER**
0-5 amps usable D.C.

New **BUILT IN RECTIFIER**
Requires only 110 V., 60 C., 1 Phase.

New **IMPROVED CORROSION RESISTANCE**
Vitreous covered cell housing.

New **MODERN DESIGN**
Convenient separate units.

New **EXTRA VERSATILITY**
Power source suitable for present and future AB cells, open beaker or other polishing or etching cells.

New **IT'S ALL NEW**
Except the dependable Buehler name and service and the "made in U.S.A." quality.

Buehler Ltd. **METALLURGICAL APPARATUS**
2120 GREENWOOD STREET, EVANSTON, ILLINOIS

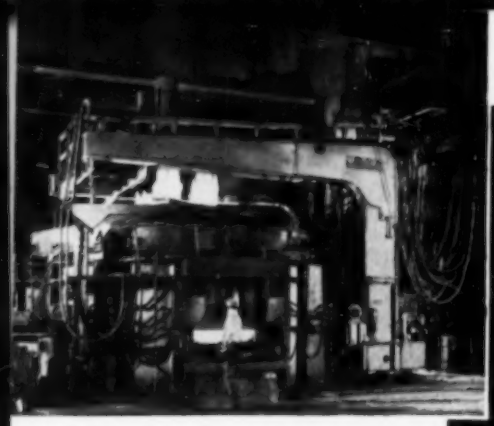

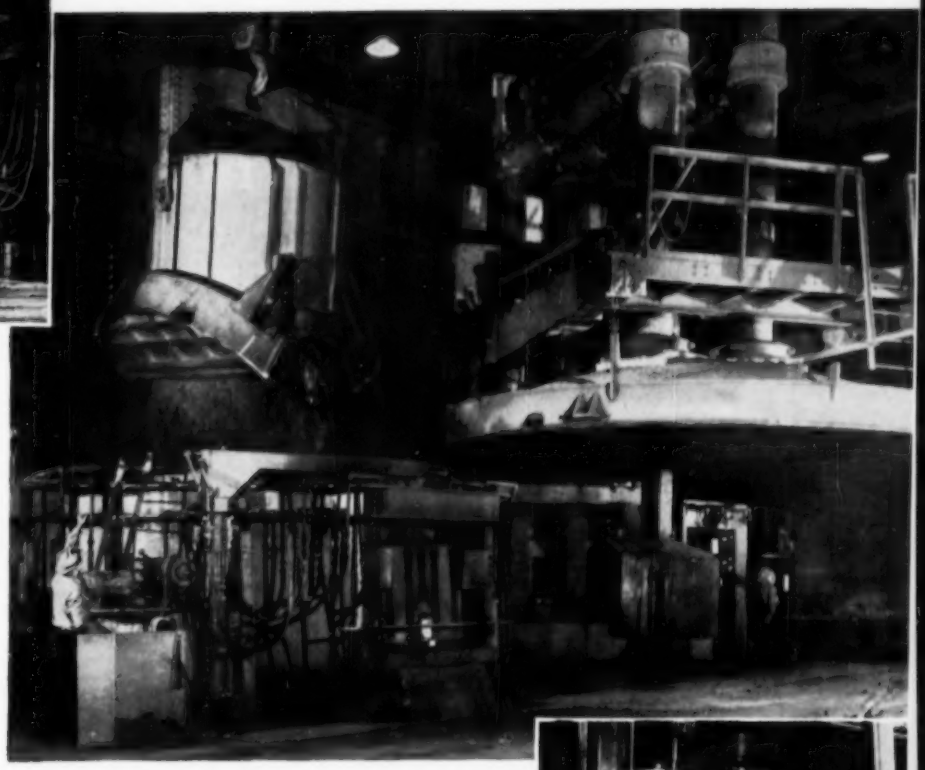

Shown above is a 20′ diameter shell Top-Charge Heroult Furnace. At right, the same furnace is shown with swing-type roof removed for charging. Smaller picture at lower right, shows tilting mechanism for 20′ diameter Heroult.

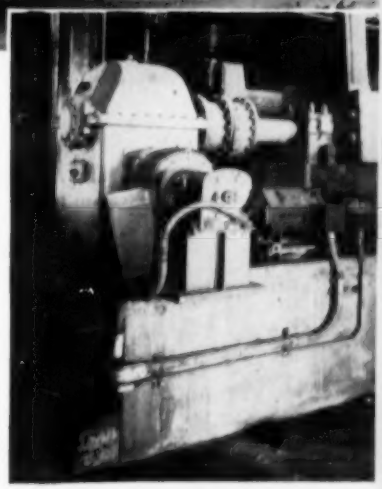

Heroult Electric Furnaces for faster, high quality steel making - -

To keep pace with modern steel making methods . . . to produce better quality steel faster, and more economically, it will pay you to consider the addition of electric furnaces to your existing facilities.

In the light of the experience of some of the nation's most successful mills, Heroult Electric Furnaces should easily prove a big time and labor saver, *and quality up-grader* for you.

Embodying the latest in mechanical and electrical equipment, these widely used furnaces are noted for their efficient performance, and low operating and maintenance costs.

Available in sizes of shell diameter ranging from 7′0″ up to 24′6″, and with rated charge capacity of from 8000 lbs. up to 400,000 lbs. They are usually equipped with roof-moving mechanism to permit top charging. Both gantry and swing-type roof-moving mechanisms are available. Door-charging furnaces and furnaces of special design, including units equipped with austenitic steel bottoms to permit inductor stirring, can also be supplied.

We welcome an opportunity to help you select and install the Heroult Electric Furnace best suited to your particular requirements.

THIS CATALOG

contains up-to-date information on Heroult Electric Furnaces — types, sizes, capacities, rating, etc. For free copy, write to our Pittsburgh office.

AMERICAN BRIDGE DIVISION

UNITED STATES STEEL CORPORATION, GENERAL OFFICES: 525 WILLIAM PENN PLACE, PITTSBURGH, PA.

Contracting Offices in New York, Philadelphia, Chicago, San Francisco and other principal cities.

United States Steel Export Company, New York

USS

UNITED STATES STEEL

From Molten Aluminum to 3/8" Diameter Rod in 1½ Minutes!

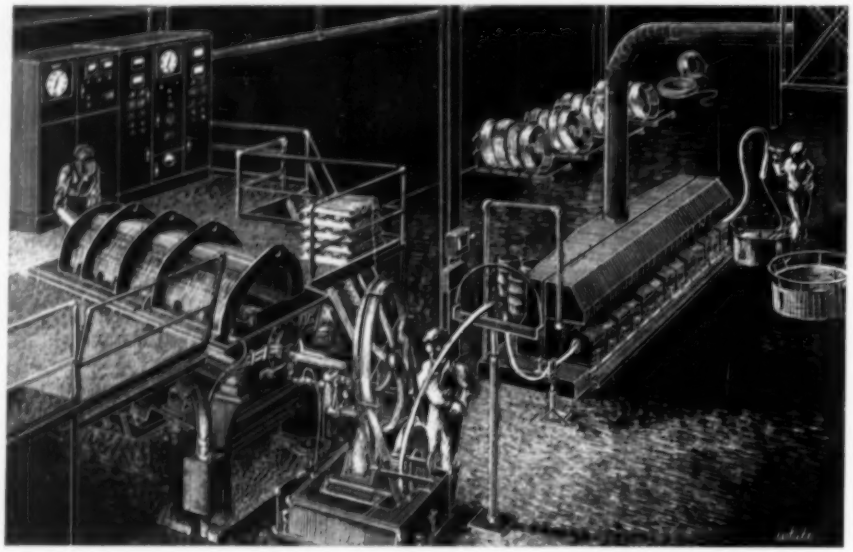

Rome Cable Corporation

uses **AJAX INDUCTION FURNACES** for

MELTING ALUMINUM FOR CONTINUOUS CASTING AND ROLLING OF HIGH CONDUCTIVITY ROD

The picture above, a drawing made at the Rome Cable Corporation, Rome, N. Y., shows one of the most modern installations in the country for the continuous casting and rolling of aluminum rod directly from molten metal. From left to right are shown the electric controls of the adjacent 450 kW. AJAX low frequency induction combined melting and holding furnace which is pouring molten metal into the Properzi continuous casting machine in the foreground, and the rolling mill from which the coiled rod is emerging.

This installation casts at the rate of about one ton per hour. The furnace feeds a continuous stream of molten aluminum at automatically controlled temperature into a rim cavity on the slowly revolving wheel of the Properzi machine. Metal loss from pig to rod averages less than 1 pct. Mechanical properties and electrical conductivity are excellent; the material is sound and fine grained. The men work under cooler, cleaner conditions because the only heat generated is within the melt itself. Due to melting conditions inherent in AJAX furnaces, the operation is continuous and no fluxing is required.

AJAX TAMA-WYATT

AJAX ENGINEERING CORP., TRENTON 7, N. J.

INDUCTION MELTING FURNACE

AJAX ELECTRO METALLURGICAL CORP., and Associated Companies
AJAX ELECTROTHERMIC CORP., Ajax Northrup High Frequency Induction Furnaces
AJAX ELECTRIC CO., The Ajax Hultgren Electric Salt Bath Furnace
AJAX ELECTRIC FURNACE CORP., Ajax Wyatt Induction Furnaces for Melting

Drift of Things

New Headquarters to be Selected on a National Basis

The Committee of Five Presidents in its report dated Feb. 2, 1955, and amplified in its report of Apr. 4, 1955 (signed by four presidents), recommended that the new Engineering Center be located on the Schenley Park site in Pittsburgh, basing their recommendation on an offer of cash and site by a public-spirited Pittsburgh group, which resulted in the lowest estimated capital cost and annual expenditure of the four sites considered in detail, viz., Chicago, New York, Philadelphia, and Pittsburgh. The AIEE approved this recommendation, and the AIChE approved without commitment.

The committee of five presidents necessarily gave major consideration to the liberality of local groups with substantial offers of cash and site. These offers received careful study on a cost basis, and meanwhile the societies developed data as to their present and future needs.

Then, on June 8, 1955, a proposal referred to as the Kelly letter,* was received by United Engineering Trustees and the five societies—AIME, ASCE, ASME, AIEE, and AIChE. This letter, signed by 21 leaders in national engineering education and industrial fields, urged the societies to choose their new headquarters on a national basis.

* The complete text of this letter appeared in JOURNAL OF METALS, page 924, August, 1955.

The Kelly letter went on to state: "If such a choice is made, a group of the undersigned will organize a large national committee, representing all sections, all technologies in your Societies, and a variety of industries to conduct a nationwide drive for funds." In addition, the group offered to finance the cost of a study by an independent consulting firm. The five societies decided that this study should be at the cost of the societies and formed a 15-member Special Task Committee.

Excerpts from a guidance memorandum of this committee follow:

"This Special Task Committee is charged with the duty of recommending a specific site with improvements for the Engineering Societies Center, based upon a review and comprehensive additional study of feasible locations.

"The predominant consideration throughout this work should be the long range welfare of the entire membership over the years, so that a similar committee two generations hence will agree that the site now selected was well done and their only problem will then be to plan extensions and provide for healthy growth and more effective unification and coordination of the engineering profession for the newer and enlarged services to enrich mankind in their day.

"The plans carried out by our predecessors fifty years ago have served us well, but there is urgent need for additional space which is not feasible on the present site. Let us, therefore, plan for the future with the realization that our final judges have not yet been born."

A nationally known management consulting organization, McKinsey & Co., with offices in New York, Chicago, Los Angeles, San Francisco, and Washington, D. C. has been selected. This organization will serve as staff for the Special Task Committee.

The committee has requested the Boards and Councils of the Societies to extend the deadline for its report to May 1, 1956 and has asked the Pittsburgh Engineering Trust to extend its generous offer of site and cash to Oct. 1, 1956.

H. DeWitt Smith

Twice the life of materials previously used is reported for this group of Ni-Vee bronze half bearing castings used in the first six or eight rolls each side of rollout table on large reversing mills. Ni-Vee type bronze castings are used for various heavy duty steel mill maintenance jobs. Castings shown on this page were produced by A. W. Cadman Manufacturing Company, Pittsburgh, Pa. under their trade name "NICUITE."

NI-VEE bronzes double life of parts in rollout tables and other mill machines

STRENGTH UP TO 90,000 psi and high resistance to wear, impact and galling characterize Ni-Vee bronzes.

Other advantages include easy castability, low shrinkage, pressure tightness, fine grain, economy and versatility.

Containing 5 per cent nickel and 5 per cent tin, Ni-Vee bronzes increase life of gears, cams and similar "constructional" castings. Likewise, the life of "pressure" group castings such as pumps, valves and fittings.

And for bearings, bushings and anti-friction metal, leaded Ni-Vee bronzes process into hard, wear-resistant products that are unmatched by the usual lead-free compositions.

Ni-Vee bronzes are produced by authorized foundries in industrial areas from coast to coast.

Get the facts about nickel-tin bronzes and see how they can save you money. Write now for the valuable data-packed booklets entitled, "THE NI-VEE BRONZES." They are yours for the asking.

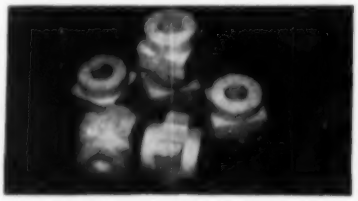

Four times life of replaced tin bronze and still good. That's the status of Ni-Vee bronze feed screw nuts cast by A. W. Cadman Mfg. Co., for Babcock & Wilcox, Beaver Falls, Pa.

2,000,000 tons of steel were rolled by a 40" blooming mill, before its Ni-Vee bronze screw box nuts . . . such as the one shown above . . . called for replacement.

INCO THE INTERNATIONAL NICKEL COMPANY, INC. 67 Wall Street New York 5, N. Y.

Titanium sheet production is expected to increase considerably in 1957 since orders for two Sendzimir cluster cold-reducing mills have been placed. One mill is to be installed at the Midland, Pa., plant of Crucible Steel Co. of America for rolling both stainless and titanium strip in widths up to 50 in. The other, to be used exclusively for titanium, is a 49-in. mill to be installed for the Titanium Metals Corp. of America at an Allegheney Ludlum Steel Corp. plant in the Pittsburgh area.

Recommendation that the U. S. Government reduce its scheduled purchases of nickel for the strategic stockpile was made by the Business & Defense Services Administration of the Commerce Dept. During 1955 the Government diverted 24 million lb of scheduled stockpile purchases to industry to allow continued high level operation. The BDSA expects industrial demand for nickel to be substantially higher in 1956.

The largest open hearth furnace ever to be constructed has been ordered by Weirton Steel Co. from Loftus Engineering Corp. The furnace, to be installed at the Weirton, W. Va., plant, will produce 500 tons of steel in one heat.

The Canadian steel industry completed a record breaking year in 1955 with steel ingot output rated at 4.4 million net tons. As the first phase of its 25 pct expansion program, the Steel Co. of Canada hopes shortly to commence erection of a slabbing mill, a cold reduction mill, and a second electrolytic tinning line.

The British steel industry, in spite of raw material supply difficulties and a three-week work stoppage, produced more ingots in 1955 than ever before, 22.2 million net tons. Europe's largest blast furnace, with a hearth diameter of 29 ft 6 in and a daily capacity of almost 1700 tons, has just been blown in at the Margam works of the Steel Co. of Wales.

Steel output in the European Coal & Steel Community topped all previous records with an ingot production of 57.75 million net tons. Every country in the Community produced more steel in 1955 than during any previous year....On the other side of the Iron Curtain, Poland's first continuous hot wide-strip mill is undergoing trial runs at the new steel plant at Nowa Huta near Krakow. The mill, with a capacity of 1.2 million net tons, is to supply coils for the galvanizing and tinplate mills.

THE MUFULIRA

Electrolytic Copper Refinery

Design—Construction—Operation of the Anode Dept. and of the Refinery Tankhouse

Introduction—The Economic Factors

R. H. BAULD, Consulting Metallurgical Engineer

FROM the inception of operations in 1933 to the end of World War II, Mufulira had produced about three quarters of a million short tons of blister copper through a single fire refining operation. This blister was turned into eminently satisfactory wire bars, cakes, billets, and ingots—largely at two fire refineries in the United Kingdom. However, it was realized that the market for fire refined copper was not limitless.

An analysis by R. L. Prain, managing director, and R. M. Peterson, technical director resulted in a decision to enlarge the scope of Mufulira's Rhodesian operations through construction of an elecrtolytic refinery.

Some of the factors behind this decision were the rising costs of fire refining in the United Kingdom, the rising costs of electrolytic refining in the U. S., and more specific considerations of limits upon increasing flotation and overall recovery at the mine itself. The latter problem arises because when recovery is increased there is a failure to reject certain impurities which are only partially removed in subsequent smelting, converting, and fire refining operations. There is also an appreciable amount of nickel in the coal used in the Rhodesian operation, and increased recovery through lowered concentrate grade would raise the nickel contamination per unit of copper smelted. The safety factor of having an electrolytic refinery loomed large in all considerations, and although virtually no by-product recovery incentive existed, electrolysis appeared a premium necessity for adapting increasing tonnages to the widest market.

Location of the new plant was determined by the economy of integration with existing organization, making possible extension of already existing housing, hospital, welfare, and allied facilities.

The studies begun in 1945 resulted in a decision to go ahead with the electrolytic plant in 1947 and first cathodes were produced in 1953. Work is now in hand to increase annual tankhouse capacity 105,000 tons.

In the last fiscal year the property produced 60,381 tons of blister and 40,755 tons of cathode copper. The overall Mufulira enterprise—representing a historical capital investment of about £20 million—expects to maintain at least this rate for many years ahead.

Background of Plant Design

G. E. ROWE, Design Engineer and
G. N. HEALEY, Consulting Mechanical and Electrical Engineer

In designing the electrolytic refinery in Rhodesia for Mufulira, it was desired to take full advantage of the past experience gained by the Carteret refinery of U. S. Metals Refining Co. It was therefore agreed that all design should be carried out by the London engineering dept., of the Selection Trust Ltd., but working in close cooperation with Mr. Hilbert, who in 1947 was chief design engineer of U. S. Metals.

Early in 1948 Mr. Hilbert in company with W. Brytczuk then refinery metallurgist at Carteret, visited Rhodesia to determine the location and layout most suitable to facilitate further extensions.

The general layout of the refining plant and future installations is illustrated in Fig. 2. Initial tankhouse capacity is 36,000 long tons of cathode copper, and extensions can easily be made to provide for an ultimate rated annual capacity of 144,000 long tons of copper.

Primarily because slow delivery of plant and equipment in the United Kingdom since the close of World War II, it was decided to produce and ship cathode copper, pending construction of a refined copper casting plant to produce wire bars, cakes, and billets.

Table I. Plant Cost

Anode casting plant	£	164,400
Tankhouse		656,700
Substation		135,600
Track and storage system		128,000
General		107,300
Total	£	1,192,000

All equipment was obtained from the United Kingdom, with the exception of certain specialized machines obtained from U. S., and the total cost of the initial 36,000 long ton installation for cathode production was £1.192 million. The mine construction dept. at Mufulira carried out the refinery construction.

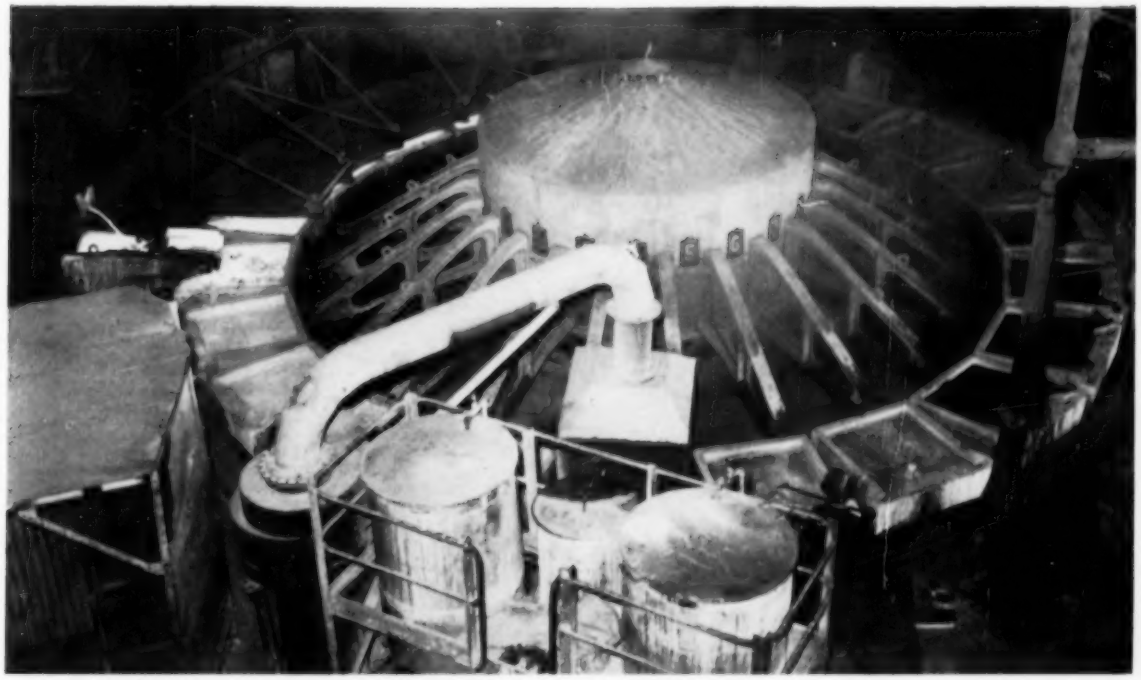

CASTING WHEEL: General layout shows mold wash tanks in foreground with vapor hood connected to exhaust system. The casting cabin is at left, and behind that is the casting spoon. Previously poured anodes extend from under the canopy to the takeoff point.

The Anode Dept.

A 22-mold casting wheel is fed from a 220-ton furnace to supply 37 tph of anodes to the electrolytic refinery.

THE smelter has a rated capacity of 10,000 short tons of copper per month. Two products are made: blister copper cakes with a bismuth content of less than 0.0020 pct for direct shipment overseas, and anodes for the refinery. The proportion of blister cakes to anodes now produced is about 1.5:1 but when a second anode furnace is added, only a small tonnage of blister cakes will be made.

Operations are influenced by the necessity of eliminating bismuth, which involves the control of the matte grade, the converter temperatures, and the time of scrap additions to the converters. Matte grade remains the same for all converter charges since a variation is impracticable, and the converter charges destined for the anode furnace follow the same routine as blister charges except for temperature control and finishing of the blow. Matte grade will be higher (unless the treatment of foreign concentrate to be undertaken later affects the grade) and converter practice modified when the end product becomes almost exclusively anodes.

Four converter charges normally constitute one anode furnace charge, and converter charges started on the night shift and early on the subsequent day shift are prepared for the anode section. The last two converter charges for the anode furnace are overblown to produce a hot thin slag, comprising largely cuprous oxide, which is skimmed off before transferring the copper. This slag is chilled, broken up, and returned to the reverberatory furnaces together with other converter aisle reverts.

Overblowing prevents slag build-up in the converters, and a secondary advantage is the lowering of compressed air consumption and decrease in time required for the oxidizing stage in the anode furnace. Overblowing is controlled to produce just the necessary amount of hot thin slag. Blowing beyond this point produces still more high oxide slag which, in turn, increases the iron pyrites additions to the reverberatory furnace charge to control the matte grade. This hot thin slag is not returned to the reverberatory furnaces in a fluid state as it tends to pass through without completely reacting with the charge and thus would increase the copper loss in the slag. Copper for the anode furnace may be stored in the blister holding furnace.

BASED on papers by A. A. HAYNES, Smelter Superintendent; G. E. ROWE, Design Engineer; and G. N. HEALEY, Consulting Engineer. Mr. Haynes prepared the material on Anode Production operations; and Mr. Rowe and Mr. Healey prepared a joint paper covering design of the department.

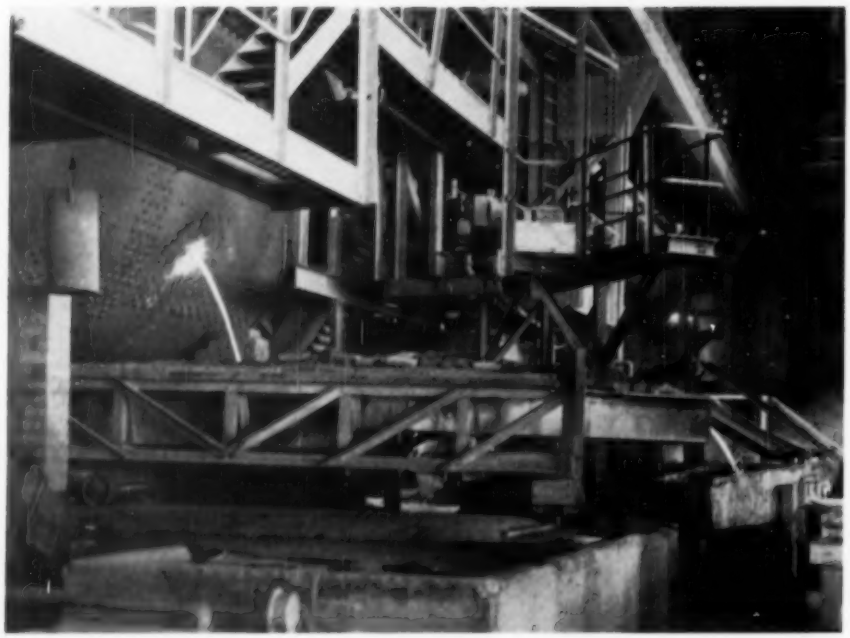

Molten copper is discharging from the 220-ton anode furnace to the launder leading to the casting spoon.

Anode Furnace and Casting Wheel Design

The anode dept. comprises a 120 ft extension to the existing converter aisle and blister copper casting shed, Fig. 1. The 13-ft diam anode furnace which receives molten converter copper is 30 ft long, lined with magnesite brick. There are three shell openings: one for receiving the charge, one for poling and one for slag skimming. The furnace is capable of a 360° rotation, but rotates 107° for normal charging and emptying. The charge door is opened and closed automatically, and the furnace delivers anode copper via a dogleg shaped launder to a tilting spoon which feeds the anode molds.

The anode wheel accommodates 22 molds which rest directly on the wheel arms and are water cooled by sprays. At the point farthest from the tilting spoon, the partially cooled anodes are automatically lifted from the mold by a push-pin actuated by a cam ramp and are removed by an air lift jib crane to the anode bosh tank where they are automatically positioned.

The bosh tank accommodates 51 anodes at 4½-in. pitch and a 10-ton capacity overhead crane lifts the anodes in batches of 32 for loading the anode cars.

Furnace Operation

To date, anode casting has been conducted in quarterly campaigns, with each campaign starting at the beginning of the quarter and continuing for about 10 weeks; blister cakes only being cast for the remaining three weeks of the quarter. Ultimately, anode casting will be on a continuous basis with casting on two shifts. At the end of each campaign minor repairs are effected to the furnace brickwork in the region of the skimming and poling doors. It is proposed to line these openings with castings of

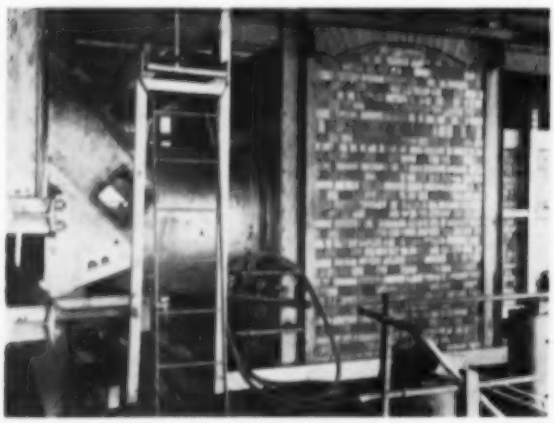

Closeup shows gooseneck connecting the furnace to the 85-ft stack. Draft is controlled by door at base of stack.

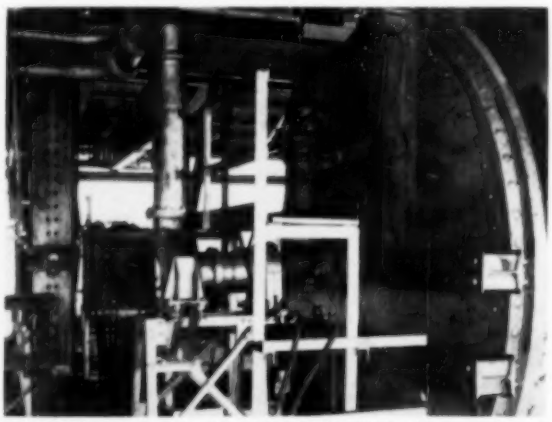

Pulverized coal fuel is fed through this 10-in. burner equipped with 6-in. primary air and coal line, and 9-in. secondary air line.

Anode Casting Plant—Plan and Section

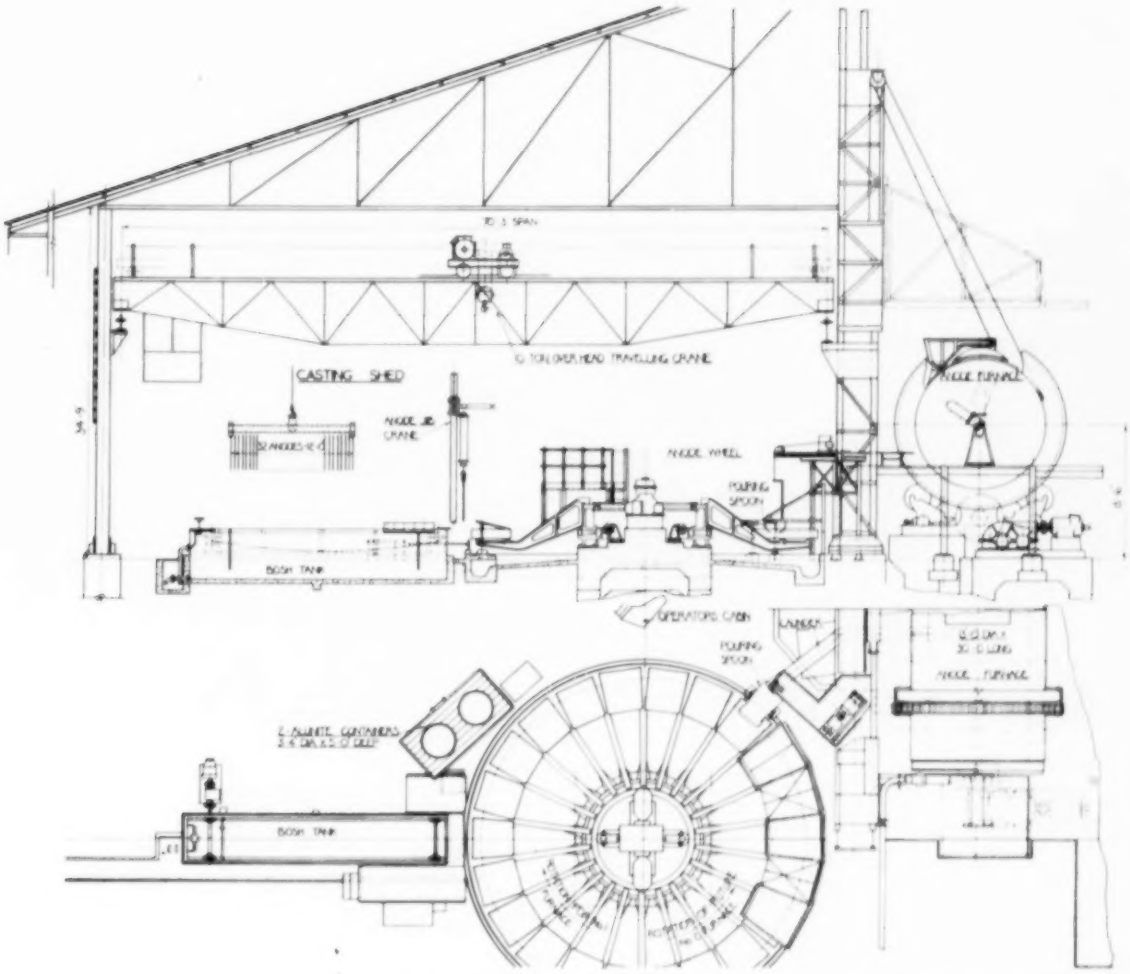

Fig. 1—The converter aisle is just to the right of these views. The whole Anode Dept. is housed in a 120-ft addition to existing converter aisle and blister copper shed.

28 pct chromium steel to preserve the brickwork and the furnace shell at these points.

The furnace is coal fired and the fuel, which has about 1.5 pct sulphur, is pulverized to 80 pct −200 mesh.

After a 220-ton charge has been transferred to the anode furnace the molten copper is blown with 50 psi compressed air. The air is introduced via two ¾ in. steel pipes, lagged with an asbestos fireclay cement mixture, which are forced into the bath through the poling door. Slag is skimmed by wooden bladed rabbles, falls down to a launder through a hole in the operating floor, to a prepared earth bed below where it is quenched, broken up and returned to the reverberatory furnace.

Blowing is continued until the bath is saturated with cuprous oxide and has been skimmed clean of slag. Spoon samples are taken towards the end of the oxidizing period and heavy blowing is stopped when the samples display a definite shrinkage crack and expose a large pea hole when broken in two. The average oxygen content of the bath at this stage is about 0.9 pct. The bath is then kept agitated by a small stream of air till poling is started.

Poling—Reducing conditions are then established by adjusting the draft and secondary air to the burner and poling is started. An average of 10 poles is used per charge. The poles—freshly cut trunks of indigenous trees, mainly of the so-called *mixed mutondo group*—and are used in 20-ft lengths of 12 to 18-in. diam at the butt. As poling proceeds 8-lb rectangular test blocks are cast and poling is continued until a flat set is established. The oxygen content of the copper at this stage averages 0.10 to 0.15 pct. The furnace is then sealed, the coal rate reduced to the minimum, secondary air adjusted to give a neutral atmosphere, and casting started immediately to avoid prolonged exposure to the high sulfur

Portion of the anode casting wheel shows the take-off point and bosh tank. Workman in foreground is applying the pin sealing wash, while another man operates the mold wash pan at the vapor hood.

coal used as fuel. No coke or charcoal is spread on the bath prior to sealing.

During both the blowing and poling operations the bath temperature is maintained as close to 2200°F as practicable by varying the coal firing rate. No scrap additions are made after poling has started.

Casting

When casting starts at the beginning of the day shift, the molds have cooled to 100°F or lower, depending upon the season, and until the molds have heated up to normal operating temperature, the anodes do not present the best appearance. This warming up process usually requires two revolutions of the wheel, and during this operation and for a further two revolutions bone ash is used sparingly as the mold wash. Cooling water is applied on the third revolution. Most of the anodes cast during the first revolution are acceptable after dressing.

On the fifth revolution alumina sand mold wash of 1.04 Sp.Gr. is substituted for bone ash and a thicker paste of the same material is used as a dressing around the head of the lifting pin. The mold wash is applied by pouring about a gallon of wash onto the mold and the dressing around the lifting pin head is applied with a white-wash brush.

Copper is discharged through a 1¼-in.diam taphole and a brick-lined launder to the casting spoon, which holds 3000 lb of metal. In the casting spoon the copper passes under a bridge and over a pouring lip 20-in. wide into the molds. The spoon is firebrick-lined and the bridge and pouring lip are of a 4:2:1 artificial sand, sand, and cement mixture. The bridge and lip are changed after each day's cast and the spoon patched with cement.

The newly filled mould passes beneath a refractory canopy which is 7½ in. above the mold and extends four molds. This canopy was designed to prevent blistering of the copper as it chills and probably does assist in this direction as blisters are generally absent from the set surface of the anodes.

Cooling

The surface of the anode is frozen by the time the next anode has been poured. Cooling water is sprayed onto the underside of the molds starting from the fourth mold from the casting spoon. A top spray is used on the sixth mold only. The anodes are a dull red heat when removed at the fourteenth mold by a manually operated air hoist on a rotating jib and plunged into the bosh tank. The cooling water is roughly in the proportion of 800, 3,700 and 11,000 gph to the top spray, the underside sprays, and the bosh tank respectively. The water in the bosh tank is about 170°F at the overflow and the temperature of the molds is maintained at about 450°F.

The rate of casting is 37 tph on commercial anodes and somewhat in excess of this on stripper anodes. After the anode has been removed, the mold is inspected and cleaned by scraping and/or blowing with a jet of air to remove any caked mold wash, after which it is sprayed with mold wash.

Anodes are removed from the bosh tank by a cradle which picks up 32 commercial anodes (545 lb avg weight), or 30 stripper anodes (630 lb avg weight), and transfers them to the anode cars. The anodes are inspected for defects while in the cars and are gaged for thickness, the range being 1.15 to 1.40 in. for commercial and 1.25 to 1.52 in. for stripper. Any anodes below the low limits are rejected, but those commercial anodes just above, but still within a prescribed tolerance, are removed to a specially marked car which, when full, is sent to the tankhouse.

The molds, which weigh about 6000 lb. are made from anode copper in either open cast iron molds dressed with alumina sand, or in a mold press using a water-cooled copper core. The lifting pin hole is made by a steel pin core which, in the open cast method, is located in a hole in the base plate and secured by a bar across the mold box, and in the mold press is screwed into the copper core. The average life of a mold is about 600 tons of copper but this figure is slowly being improved upon.

Table II. Analyses

	Blister Copper, Pct	Anode Copper, Pct
Cu	99.58	99.77
O_2	—	0.22
S	0.012	0.0019
Fe	0.0026	0.0021
Co	0.0002	0.0002
Ni	0.008	0.007
As	0.0012	0.0008
Se	0.0016	0.0013
Sb	0.0011	0.0007
Te	Trace	Trace
Pb	0.0011	0.0004
Bi	0.0016	0.0015
Au	0.008*	0.008*
Ag	2.345*	2.469*

* oz per short ton.

Acknowledgment

Acknowledgment is recorded of the collaboration of D. L. Turnbull, assistant smelter superintendent; L. R. Verney and R. R. Neller, senior metallurgical assistants; in the preparation of this paper.

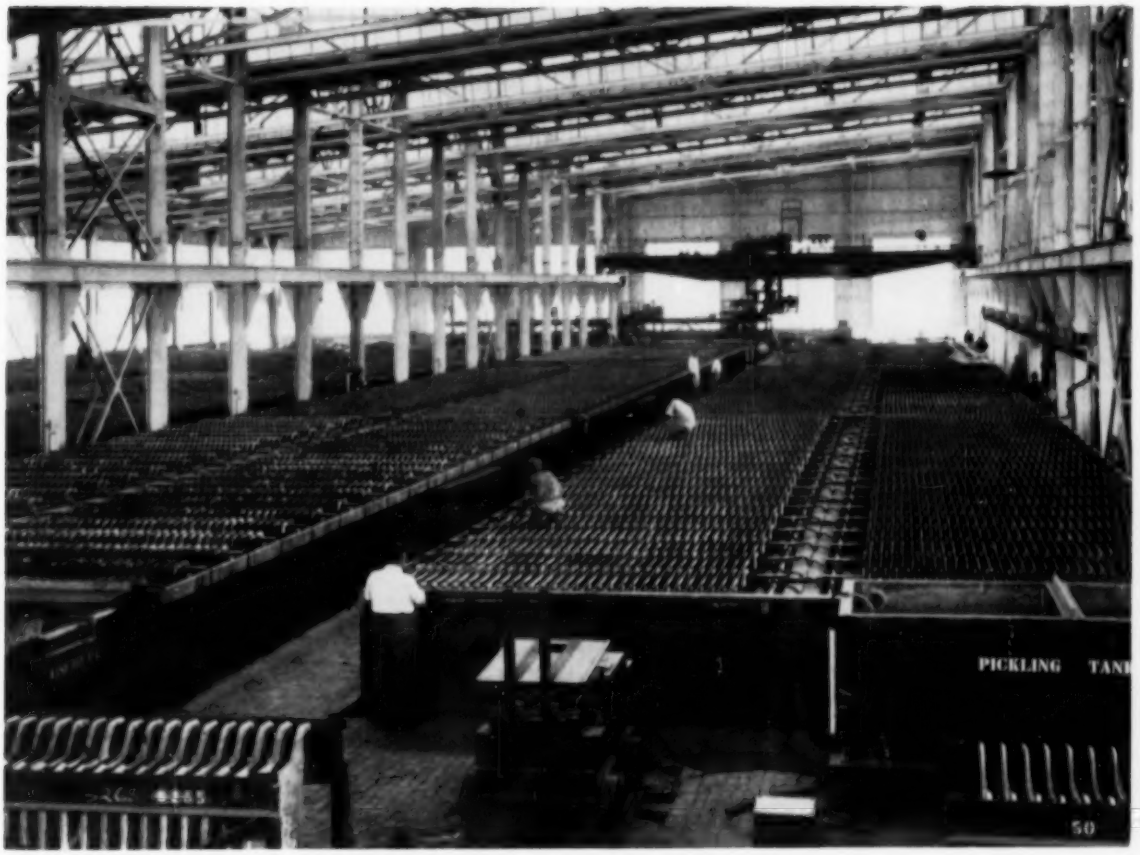

General view shows two of the tankhouse operating aisles.

THE MUFULIRA REFINERY

Refinery Tankhouse

Construction—Startup Methods —Tankhouse Operations

THE section of the tankhouse described in these articles may be considered the first quarter of a symmetrical tankhouse designed with two major axis. The center pump aisles form a North-South axis and the East-West axis is the traffic and copper handling system. Capacity of the initial section was 36,000 LT of cathode per year, and the design permitted addition of two more tank aisles east of the first pump aisle (which have already been built), to double capacity to 72,000 LT, since the initial pump aisle was adequate to handle two copper producing aisles on each side.

Traffic and copper handling on the East-West axis includes a 4-track, 3 ft 6-in. gage system along the south side of the present building. These facilities are sufficient not only for the eastern extension but for a possible doubling again of capacity to 144,000 LT per year, through construction of duplicate units to the south of the tracks.

BASED on papers by P. C. LOCKYER, Refinery Superintendent; G. E. ROWE, Design Engineer; and G. N. HEALEY, Consulting Engineer. Mr. Lockyer prepared the material on Tankhouse operation, while Mr. Rowe and Mr. Healey wrote a joint paper describing the design of this department.

Initial tankhouse construction provided three main aisles, each 396 ft x 72 ft 6 in., under a single roof deck. The two westerly copper producing aisles house 488 deposition tanks and the pump aisle on the east houses the ancillary equipment for heating, pumping, and conditioning the electrolyte as well as housing the slime treatment plant.

(Continued on page 243)

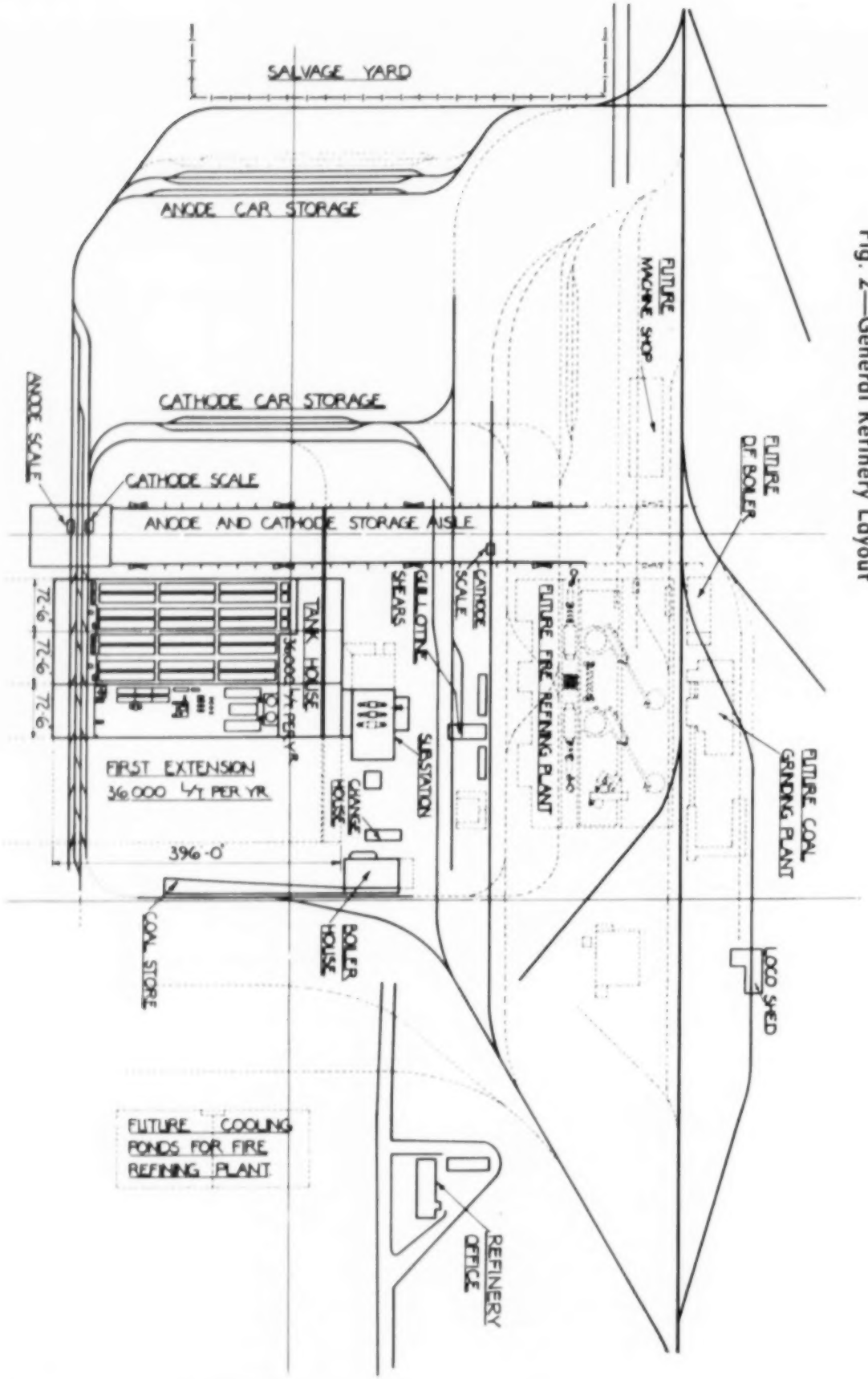

Fig. 2—General Refinery Layout

Fig. 3—Tankhouse Plan and Section

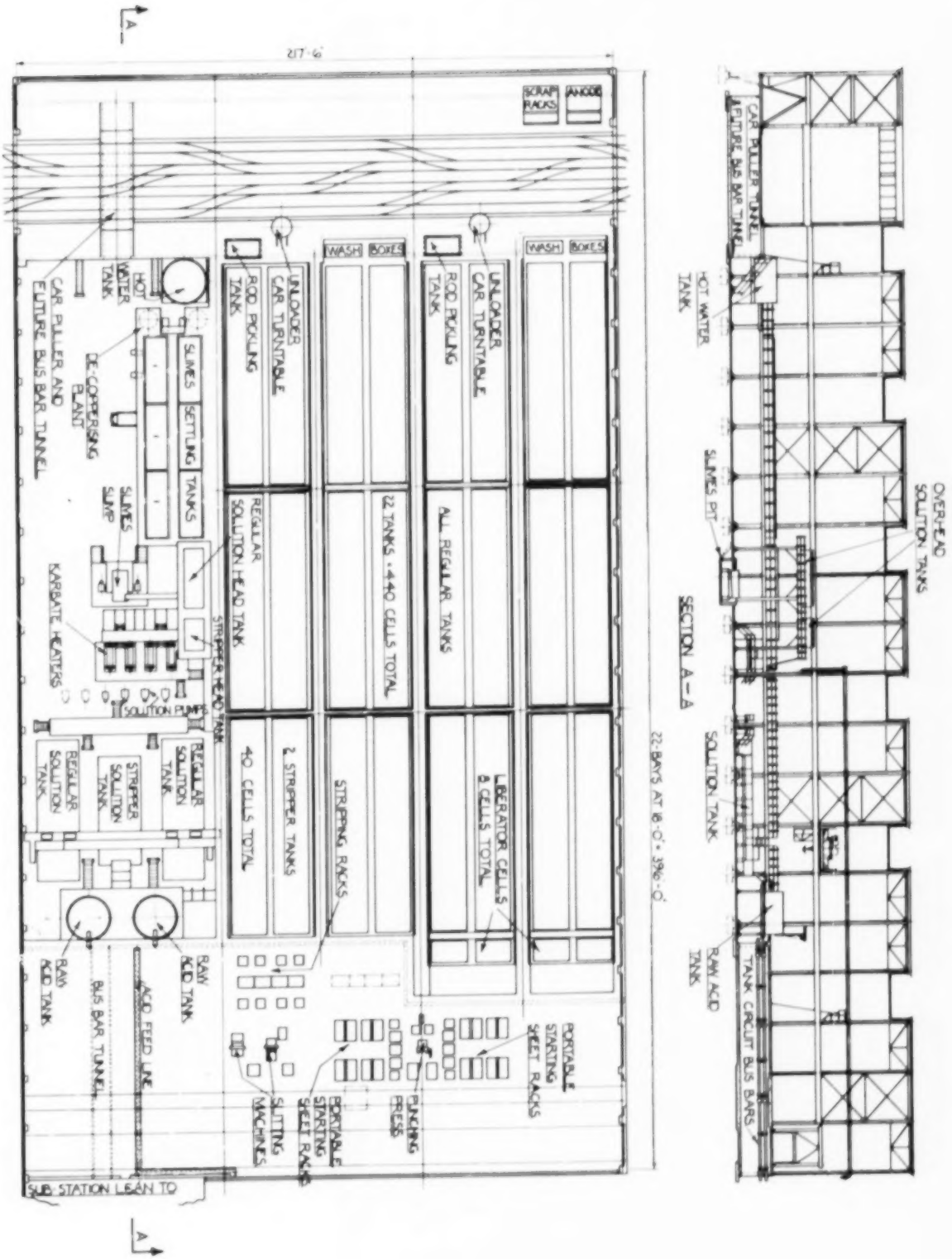

Fig. 4—Longitudinal Section, Electrolytic Tanks

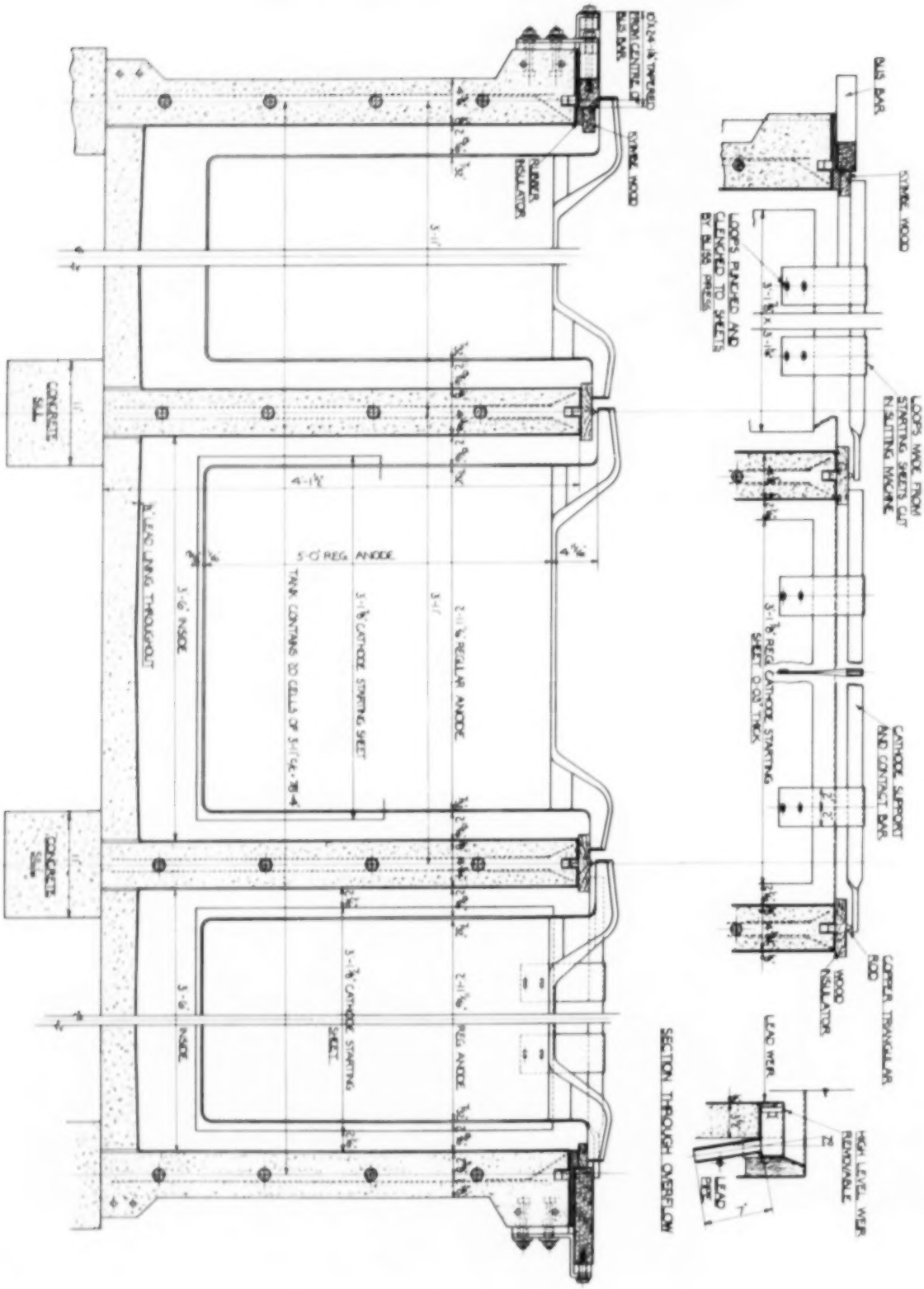

Tankhouse Construction

Design of the initial plant section provided for easy addition of future sections to double, and re-double the capacity.

The tankhouse is a steel frame structure 396 ft x 217 ft 6 in., and the first two-aisle addition increased this width 145 ft. A future addition to the south to double present capacity would require a 324 ft x 362 ft 6 in. duplicate of the present structure. Sides and gable ends of the building are of corrugated metal and the roof is 2 x 6 tongue-and-groove covered with Roc tropical roofing. Downpipes, gutters, and drains are designed for *a maximum rainfall of 12 in. per hr.*

The roof has alternate high and low spans, and maximum natural lighting is provided by glazing the 8 ft 8 in. step between the spans. High spans are fitted with 96 Robertson natural ventilators. In view of the acid laden atmosphere, steel design made appreciable use of broad-flanged beam sections to avoid double member columns. After erection all steel was coated with an acid resisting plant and trusses and lattice girders were designed to provide accessibility to all metal surfaces to facilitate inspection and repainting.

The tank aisles accommodate 440 commercial tanks and 40 stripper tanks in 11 commercial sections and a stripper section. One aisle also includes 8 tanks in two 4-tank liberator sections. These latter tanks are equipped with insoluble lead anodes to control electrolyte composition and space was allowed for two more sections.

Commercial and stripper tanks are assembled in banks of 20. Electrolyte tanks are built of precast 4-in. concrete slabs. All slabs have a double layer of 3-in. mesh expanded metal reinforcement and the end and partition sections have four 1⅛-in. tie rods. Front and back walls are secured by the tie rods, each wall having a matching zig-zag edge overlap, symmetrical around the line of each alternate set of partition tie rods, to ensure continuity of wall assemblies. The bottom slabs comprise three rectangular sections per tank, resting on reinforced concrete sills, supported by 10-in. square reinforced concrete columns. Each column is capped by a glass slab for electrical insulation, and lead flashing between the tank sill and glass protects the columns from electrolyte leakage.

All tanks are lined with 8-lb, 6 pct, antimonial lead. Dimensions of the tank inside the lead lining are approximately 12 ft 6 in. x 3 ft 6 in. x 3 ft 9 in. deep. Each tank has a 3-in. lead seat and plug for draining slime and liquor to the launder system below the tanks. These launders are V-section timber construction, with lead lining while the central collecting launders discharging to the slime sump are rectangular section. Walkways between sections have steelwork supporting concrete slabs and are surfaced by 2¼-in. thick acid proof brick laid on ¼-in. thick mastic.

The basement is 12 ft deep since solid ground did not occur above this level. This provides greater headroom than usual and facilitates inspection for leakage from tanks and launders. The cellar covers the complete area under the electrolyte tanks and the greater proportion of the machinery or pump aisle; the remainder of the building has its floor at the working level. The cellar floor is concrete with

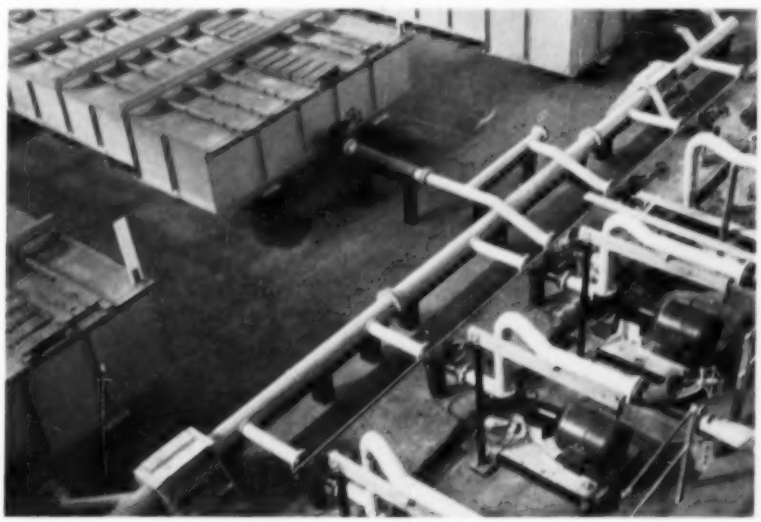

View looking down on the electrolyte pumps and sump tanks. Pumps are nickel chrome alloy construction LaBour centrifugals. Stripper and commercial electrolyte circuits are separate.

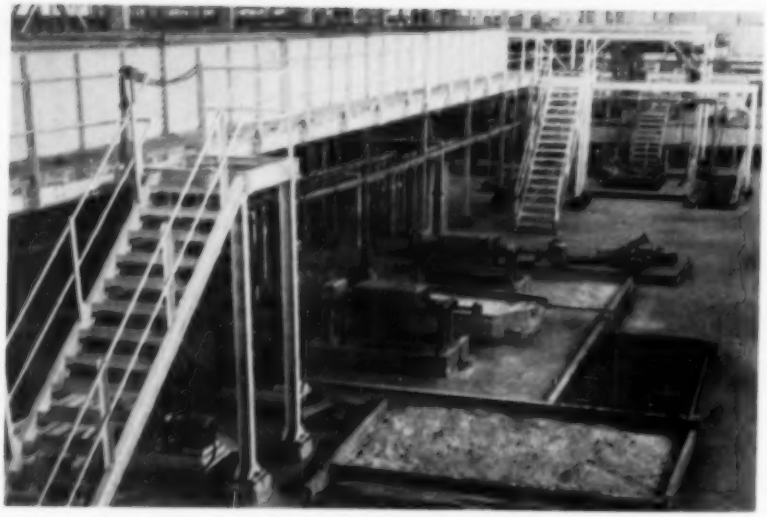

At left are the slime settling tanks from which the settled product is sent to decoppering tanks and then to the two filter presses at center. The 6-in. deep, steam-heated drying pan is of stainless steel construction.

⅛ in. per ft fall to the drains and acid proof brick is used only for local protection around the bases of the columns. Further protection was found unnecessary, except for lining the floor drains with bitsumastic compound, and the floor is maintained by frequent hot water washing using high pressure hoses. All wash water and spillage liquor within the tankhouse returns through the slime filter presses to the electrolyte circuit.

Solution Circuit

Solution is delivered to the bottom of each tank through a 3-in. pipe and overflows at the opposite end through an outlet box with an adjustable weir for varying the solution level. Solution enters the 3-in. inlet from a ⅝ in. bore Perspex 70° bend which is connected by a soft rubber pipe to the 4-in. diam solution feed main to the section. Solution return is through a 1¼-in. bore hard rubber pipe connected to the outlet box by a piece of flexible tubing. Return solution is collected in a 6 in. pipe which is provided with raised inlets or boots of oval section into which each 1¼ in. bore pipe is inserted through a porcelain plug resting on the raised aperture. The oval inlet together with the soft rubber section allows the solution return pipe to be readily withdrawn for inspection. Wooden or rubber splash guards cover the open portion of the oval boot.

Copper Handling

Each building aisle is served by a 10-ton, stiff-leg overhead electric traveling crane. These units which have approximately 69 ft span, handle 32 anodes or cathodes on bales fitted with stainless steel hooks, enabling a complete tankload to be withdrawn or inserted in one operation. The crane cab is located over the center of the aisle for maximum visability, and the stiff-leg feature allows accurate spotting over the tanks.

At the north end of the building a crane transfer car runs on a track at right angles to the main operating aisles. This device transports the stiff-leg cranes into whichever aisle they are needed, enables the crane service to follow the work load, and permits moving cranes to the pump aisle for repair or maintenance.

Cathodes, after washing, are dumped automatically from the stiff-leg cranes onto quadrant arm unloaders which stack the cathodes horizontally on the flat top cars.

Preparation Areas

Space at the north end of the building accommodates stripping racks for removal of starting sheets from blanks, racks for storage of starting sheets, sheet slitting machines, and a punching press. Eight starting sheet racks are provided, each accommodating 168 sheets in two compartments. Completed sheets in the racks are moved by shuttle car to the proper aisle and transported by the cranes to the tanks. Individual sheets are lifted from the racks and placed in the tanks by hand.

The two slitting machines to produce the suspension loops for the sheets handle 37⅞ x 37¼ in. copper sheet 1/32-in. thick. An arbor with three cutters trims edges and splits the sheets, and an arbor with ten cutters produces the 4 x 18-in. loops. A Bliss punching press secures the suspension loops to the starting sheets.

The area at the south of the building accommodates wash boxes for cathodes, pickling tanks, scrap anode racks, and the trackage system with car pullers for incoming anodes and outgoing cathodes.

Pump Aisle Equipment

The third aisle houses two 12,000-gal lead lined tanks for raw sulfuric acid; two 6700-gal return solution tanks; and one 5300-gal stripper return solution tank. The 16 pct H_2SO_4, 12 pct $CuSO_4$, electrolyte solution for the commercial tank circuit is handled by three multi-throat, single casing, LaBour centrifugal pumps of nickel chrome alloy construction. Each pump has 1000 gpm capacity at 50 ft head and one pump serves as standby for both commercial and stripper electrolyte circulation. A similar 300 gpm pump handles the stripper solution circuit.

The four Karbate heaters have ample capacity for maintaining electrolyte solution at 145°F. Two alloy centrifugal pumps deliver the electrolyte through the Karbate heaters to a head tank and a smaller pump draws from the stripper solution tank and similarly pumps through heaters to another head tank. The bottoms of both tanks are high enough to provide a constant gravity feed of 4 gpm.

Slime treatment equipment includes a collecting tank at the sump pit which has perforated stainless steel and lead screens to retain any sizeable pieces of copper scrap. A 300-gpm pump with standby transfers solution from the slime collection tank

alternately to two settling tanks 8 ft x 3 ft 6 in. deep x 72 ft long, each being subdivided into three compartments by weirs. After settling, clear solution is decanted through internal pipes extending 1 ft 2 in. above the tank bottom and returned via the filter press to the solution circuit. Sludge is drawn from the tank by a 60 gpm pump with standby, first to two decoppering tanks, and then to two 24-chamber filter presses. Each 19-in. square filter press has 96 sq ft of filtering area with frames and plates of Regulus metal. Two 30 gpm pumps supply clean wash water to the presses, the effluent and wash water being returned to the solution circuit.

The two batch decoppering units are 6-ft diam lead lined tanks fitted with paddle agitators driven by 5-hp motors. Clean solution, steam, and compressed air lines are proved at each tank. Filtered and washed slimes are dried on a steam heated stainless steel drying pan 10 ft x 5 ft x 6 in. deep.

Hot water for washing cathodes and anode scrap in the wash boxes is stored in a 16-ft diam lead lined tank. The tank is supplied with condensate from the Karbate heaters or with raw water heated by direct steam injection. Two 200-gpm pumps deliver the hot water for washing and general service.

Piping

Feed and return piping for the electrolyte solution is of antimonial lead in the following thicknesses:

⅝ to 3-in. bore — ⅛ in. thick
4 to 8-in. bore — 3/16 to ¼ in. thick
10-in. bore — 5/16 in. thick

The 650 tons of lead used for tank lining, piping, valve seats, etc., was furnished locally by Rhodesia Broken Hill Development Co. The piping, with the exception of the 10-in. tube was extruded in the supplier's works, but the 10-in. tube was made from sheet rolled and butt welded on the refinery site.

THE MUFULIRA REFINERY

Commissioning the Plant

Startup tasks included preparation of 400,000 gal of electrolyte in a dissolving tower and seasoning of starting sheets in an improvised deposition circuit.

The first operational phase, begun at the end of June 1952, was the preparation of the initial 400,000 gal of electrolyte. Hot dilute sulfuric acid was intermittently cascaded through a bed of blister copper fins in a lead lined steel cylinder into which air and steam were blown by two jet exhausters. This dissolving tower was originally in closed circuit with one of the electrolyte supply tanks, one LaBour pump, one Karbate heat exchanger, and a gravity head tank. Periodically, as the copper dissolved, deposition tanks were brought into the circuit with the addition of more water, more copper fins, and more concentrated sulfuric acid. It took 10 weeks to reach copper concentration of 35 grams per liter, suitable for the start of commercial deposition. Altogether 65 tons of copper fins were dis-

The 9x36-in. strips of cut cathode are tied in bundles by hand and secured with a center loop of wire. See text page 246.

Anode Instruction Sheet

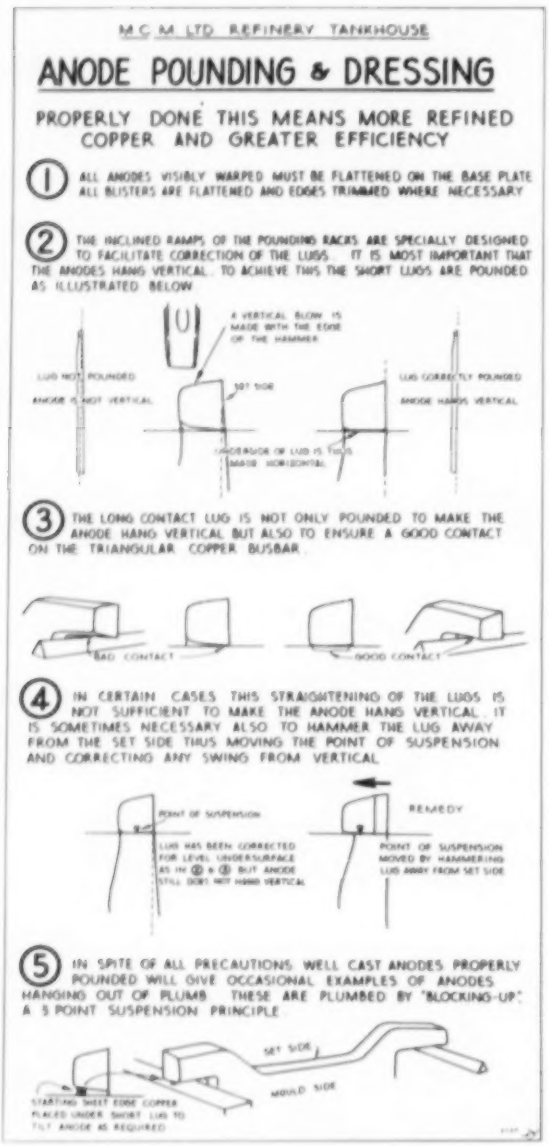
M C M LTD REFINERY TANKHOUSE
ANODE POUNDING & DRESSING
PROPERLY DONE THIS MEANS MORE REFINED COPPER AND GREATER EFFICIENCY
1 ALL ANODES VISIBLY WARPED MUST BE FLATTENED ON THE BASE PLATE ALL BLISTERS ARE FLATTENED AND EDGES TRIMMED WHERE NECESSARY
2 THE INCLINED RAMPS OF THE POUNDING RACKS ARE SPECIALLY DESIGNED TO FACILITATE CORRECTION OF THE LUGS. IT IS MOST IMPORTANT THAT THE ANODES HANG VERTICAL. TO ACHIEVE THIS THE SHORT LUGS ARE POUNDED AS ILLUSTRATED BELOW
A VERTICAL BLOW IS MADE WITH THE EDGE OF THE HAMMER
LUG NOT POUNDED
ANODE IS NOT VERTICAL
SET SIDE
UNDERSIDE OF LUG IS THUS MADE HORIZONTAL
LUG CORRECTLY POUNDED
ANODE HANGS VERTICAL
3 THE LONG CONTACT LUG IS NOT ONLY POUNDED TO MAKE THE ANODE HANG VERTICAL BUT ALSO TO ENSURE A GOOD CONTACT ON THE TRIANGULAR COPPER BUSBAR
BAD CONTACT
GOOD CONTACT
4 IN CERTAIN CASES THIS STRAIGHTENING OF THE LUGS IS NOT SUFFICIENT TO MAKE THE ANODE HANG VERTICAL. IT IS SOMETIMES NECESSARY ALSO TO HAMMER THE LUG AWAY FROM THE SET SIDE THUS MOVING THE POINT OF SUSPENSION AND CORRECTING ANY SWING FROM VERTICAL
POINT OF SUSPENSION
LUG HAS BEEN CORRECTED FOR LEVEL UNDERSURFACE AS IN 2 & 3 BUT ANODE STILL DOES NOT HANG VERTICAL
REMEDY
POINT OF SUSPENSION MOVED BY HAMMERING LUG AWAY FROM SET SIDE
5 IN SPITE OF ALL PRECAUTIONS WELL CAST ANODES PROPERLY POUNDED WILL GIVE OCCASIONAL EXAMPLES OF ANODES HANGING OUT OF PLUMB. THESE ARE PLUMBED BY "BLOCKING-UP" A 3 POINT SUSPENSION PRINCIPLE
SET SIDE
MOULD SIDE
STARTING SHEET EDGE COPPER PLACED UNDER SHORT LUG TO TILT ANODE AS REQUIRED

Labor force was carefully trained in correct pounding and dressing of anodes. This has proven important at Mufulira.

solved using 500 short tons of 66° Baume sulfuric acid to give the 400,000 gal of electrolyte. The tower and its pipe system were then dismantled.

Anodes were first received from the smelter July 26, 1952. At this time the main dc motor-generator equipment had not yet arrived at Mufulira. However, 22 tanks were rigged into one commercial section so that 500 amp dc from a paralleled group of three battery charging appliances could be passed through four anodes and three prepared stripper blanks in each tank. This gave a current density of about 8 amp per sq ft. The pounding and dressing of anodes was supervised carefully, and the preparation of the new stripper blanks was useful training for the growing labor force. The small deposition unit was used to coat the dressed blanks with sheets of a 48-hr copper deposit and served to school the operators.

By the end of August sufficient electrolyte had been prepared to start the main operation and 5300 tons of anodes had been received. By the end of September 880 stripper blanks had been prepared and coated with deposited copper for use and 2600 tons of anodes had been loaded into 8 of the 12 tankhouse sections. Approximately 20,000 starting sheets had been purchased from the neighboring refinery at Nkana.

The first M-G set had been installed and run on test and on October 2 the tankhouse operated for 2 hr with four commercial sections in circuit. The plant was then ready for operation, but startup was delayed by a fuel shortage and by an impending strike. On November 10 the first six sections went on line and by December 2 all were operating.

The stripper section was one of the first in circuit. At first these tanks were loaded with looped starting sheets, but as soon as satisfactory deposition was established, these sheets were progressively removed and the tanks charged with the precoated copper blanks seasoned in the improvised deposition plant. By November 18 the stripper section was fully operative. Full operating rate was achieved by November 22, and no blanks were damaged in this operation and stripper sheet rejection was below 2 pct within two weeks.

Additions of glue, Avitone, and salt were adjusted to give smooth dense commercial cathodes and tough starting sheets on the basis of the appearance of test strips of copper sheet which were carried in the end tanks of all sections.

The first cathode copper was pulled November 22, and December production was 3211 tons at 92.3 pct current efficiency.

Originally it was planned to ship cathode in 9 x 36-in. strips, packed in bundles of four, and secured by wraps of No. 10 wire. The guillotine shears provided a satisfactory operation, but the bundling and wire tying proved slow and difficult. The latter was speeded up with gravity roller conveyors for bundling, and soft wire ties, but the short ties securing the heavy, shallow 9-in. packs were never very satisfactory for the long rail and sea haul with its repeated handling. An improved method of hand tying with the wire looped through the middle of the pack was later introduced.

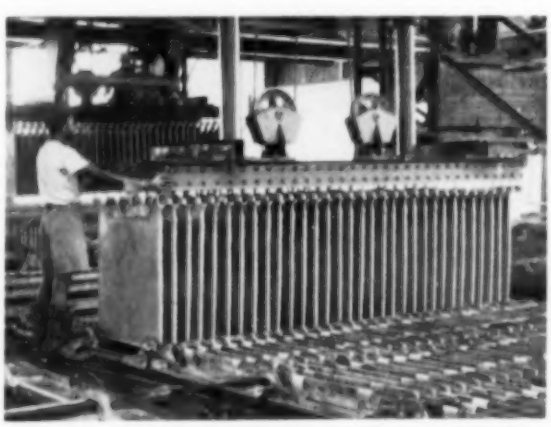

Startup period prior to full scale operation was used to train African crew in skilled handling of cranes and other refinery equipment.

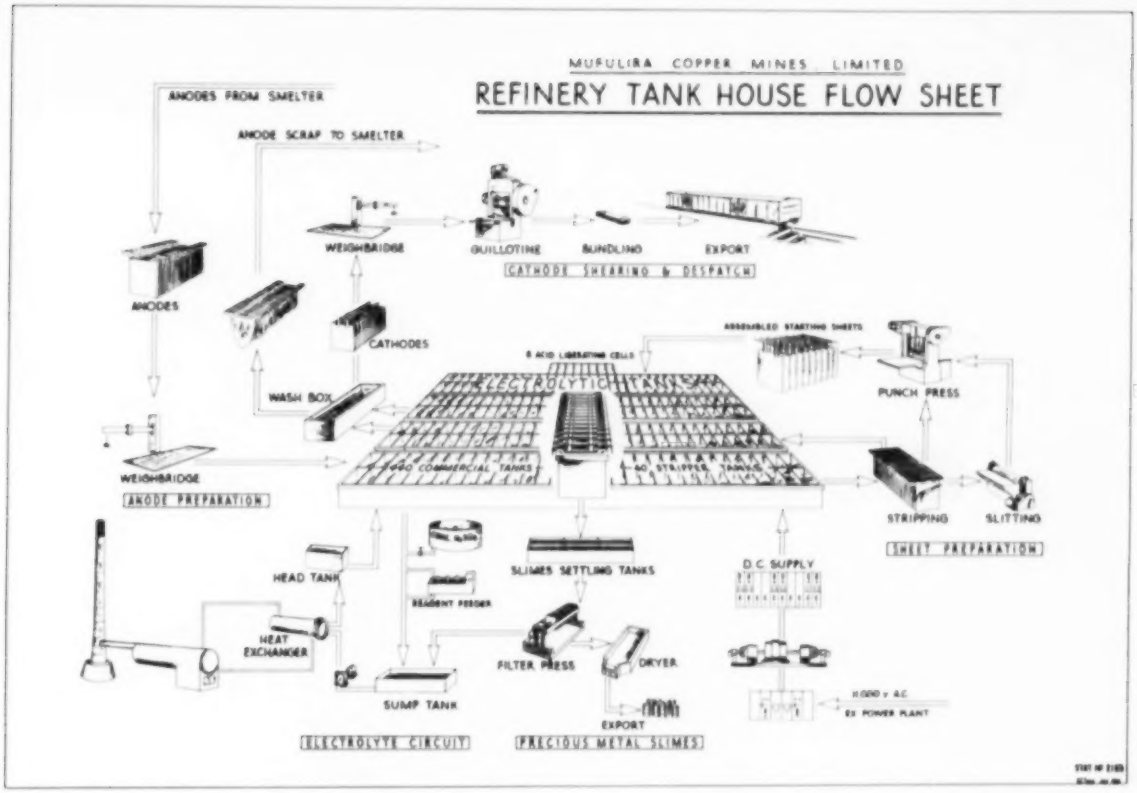

Tankhouse Operating Practice

Copper Handling—Deposition—Starting Sheets—Slimes—Control—Maintenance

COMMERCIAL anodes are received in 32 piece carloads from the Smelter Dept. via a Dennison weighbridge and either put in stock, or inspected, pounded, trimmed, and loaded to the tankhouse. Correct anode pounding is important at Mufulira and there are two pounding racks under the anode gantry. Bent anodes are straightened with sledge hammers. A dummy section of 40 racks made of concrete pillars and bull-nose rails enables the anode preparation gang to set up a section of dressed anodes in advance of tankhouse requirements without tying up anode cars.

On alternate days anodes are charged to 40 tanks. At present the tanks operate on 33 anodes and 32 cathodes in order to produce a uniform weight cathode, and one anode is left in the tank at each loading. Later, when the wire bar plant is commissioned, it is planned to change to 33-cathode, 32-anode, loading. The present 4½-in. electrode spacing will be closed to 4-in. at the same time. When the tankhouse extension is in operation, anode loading will be 40 tanks per day on a 6-day week and anode receipt and preparation will be on two shifts.

Tank loading begins at 5 am to permit efficient inspection during the first day under power. The anode electrical contact, or long lug, is ground on the underside and oiled before it is set in the tank. A section is loaded with anodes after the second crop cathodes have been removed, anode scrap taken out, and the tanks scavenged of pieces of dropped anode scrap. This operation is concurrent with the cleaning of slimes from 20 tanks. Dirty capping boards and dirty triangular bars are replaced when a section is loaded.

Cathodes: The tank loading crew removes the cathode pull from a section which has been locked out of the circuit by the night shift circulator. Cathodes are thoroughly washed by high pressure sprays of hot water in wash boxes, located two in each tank aisle. Two stiff-leg cranes handle the cathodes, one loading to wash boxes, while the other dumps washed cathodes on the quadrant arm unloader.

When the cathodes are in the horizontal pack, crossrods are withdrawn and stacked in stainless steel baskets ready for pickling and washing before reuse. Four sample cathodes from each section are taken from the tanks before the main pull, and the drillings from these are sent to the assay office for spectrographic analysis.

Cathodes which have been weighed out of the tankhouse are sent to the guillotine for cutting to 9 x 36 or 12 x 36-in. strips, or may be loaded direct as whole cathode. Cathode pulling is completed by about 7:00 am and spectrographic check assays are available by 8:30 am. Usually all cathode is in rail trucks ready for dispatch on the day it is produced.

Anode Scrap: After cathode copper has been removed from the section the anode scrap is taken out in crane lifts, washed, and returned to the smelter for remelting. Selected heavy scrap is used for *juggling*, i.e. replacing individual anodes which corrode prematurely. Juggling scrap becomes necessary on the 25th or 26th day of the anode cycle. A high efficiency deposition cycle usually necessitates between 150 to 400 of the 1320 anodes in a section being replaced by juggling in the last three days of the anode run.

Starting sheets with loops attached at the Bliss press and indented with a stiffening diagonal cross, are threaded with cathode cross rods and placed manually into open-ended steel racks which carry 168 sheets in two parallel lines.

Liberator Cathodes: There are eight liberator tanks with lead anodes, arranged in two sections of four. Operation of the liberators requires 1.8 v per

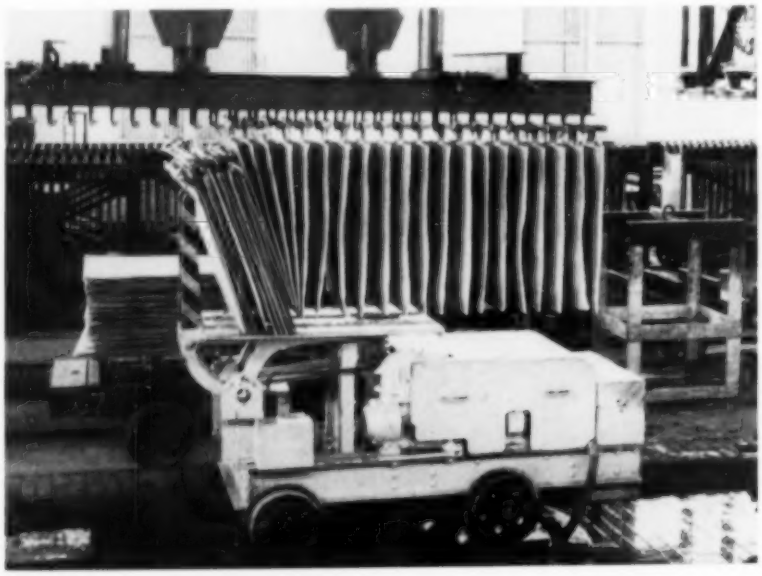

Tankloads of 32 cathodes or anodes are handled by the stiff-leg cranes through use of racks or bales fitted with stainless steel hooks. Unloader is seen here picking plates up from hooks.

The quadrant arm unloaders, shown above receiving cathodes from crane also stack the cathodes horizontally on flat cars as at left. Construction of the car is shown diagrammatically in Fig. 6, page 255.

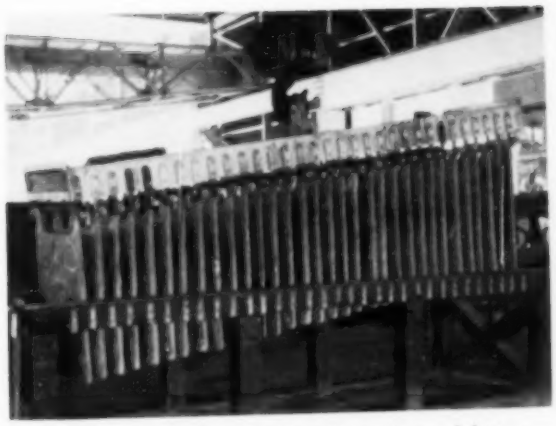

Special rack in the storage yard permits setting up of dummy anode section without use of anode cars.

tank (approximately the dissociation voltage for copper sulfate), so that a section of four tanks requires about the same power as 40 refining tanks. The electrolyte in liberator tanks is covered with a layer of thin machine oil which froths and blankets the objectionable mist of acid spray which would otherwise be formed.

The insoluble lead anodes are 2 ft 8 in. x 3 ft 3 in. x $\frac{3}{8}$ in. thick. Horizontal copper contact bars with lifting loops are riveted and sweated to the top of each anode and three porcelain insulators are attached to each anode face as a precaution against short circuiting.

Liberator cathodes are grown for a week only, when they are taken from the tanks individually by hand, to avoid locking out the liberator circuits. This cathode which is only oily and irregular in appearance and much lighter than the normal two-week commercial cathode, is returned to the smelter for remelting.

Deposition

Electrolyte Circulation: There are two electrolytes with independent circulation systems for the commercial cathode and sheet production operations. One of the liberator tanks is piped so that either commercial or stripper liquor can be fed to it and the resultant liberated liquor can be passed back to either the commercial or stripper circuits. A similar alternative feed device is available between one end tank of the stripper section and the next adjacent tank of a commercial section. These arrangements and the continuous sampling device give great flexibility and control over the acid and copper content of the electrolyte.

The electrolyte is pumped from the lead-lined steel sump tanks through a Karbate tube heat exchanger to a head tank from which it flows by gravity through lead pipe to the deposition tanks. Electrolyte flow at the tank is regulated to 3 gpm (Imperial) and checked systematically by timing the filling of 2-gal lead measuring pots at individual tank overflows on each section.

Feeds to the tanks are $\frac{3}{4}$ in. diam rubber with Perspex or Polythene 70° bends; overflows are $1\frac{1}{4}$ in. diam rubber with a hard rubber tube leading into ceramic sleeves in the main 6-in. section return pipes. Section feeds are articulated 4-in. lead pipe with *break* pieces of Polythene or PVC plastic for insulation.

Half the sections are temporarily covered with PVC blanket whenever possible, usually as soon as inspection work has been completed and throughout the night shift. This blanketing saves about 10 pct in the process steam used for heating the electrolyte; it cannot however be conveniently applied to more than half the sections as the considerable reduction in evaporation losses would make it impossible to reabsorb the normal daily intake of wash water and spillage. Wash water and evaporation are each normally about 3 pct by volume per day.

Sampling: Addition agents, made up once a day, are fed to the electrolyte by disk-and-thimble feeders. For the commercial circuit, glue and Avitone are added together from one compartment, and salt solution from a second compartment.

The end compartment of the reagent feeder is used as a continuous sampling device. Electrolyte is bled from one of the main pipelines into the compartment and overflows continuously to an open lead-lined trough which collects the reagents dispensed by the other disks and conveys them to the main return flow to the sumps. The disk in the end compartment carries an 8 cu cm ebonite sampling bucket at 1 rpm. This small sample is accumulated in a lead tank in the body of the feeder, and the whole sampling device is encased in a Perspex cover to prevent evaporation losses and contamination.

Inspection: Three methods of detecting electrical defects are regularly used: 1) Fingering the cathode cross rods indicates by hot contact when a rod is carrying excessive current due to a short circuit between the cathode sheet and anode, etc. 2) A gaussmeter indicates the comparative strength of the magnetic field above the cross rods. Beside a *normal* zone, the needle indicates a *short* zone caused by heavy short circuit currents, and a *stopped contact* zone resulting from low deposition currents possibly caused by dirty contact surfaces. 3) A millivoltmeter with a copper pronged search rod measures the electrode face-to-face voltage below the surface of the electrolyte.

These basic methods of inspection are carried out on a rigid schedule and improperly operating elec-

Four sample cathodes per section are drilled and the drillings sent to assay office for spectrographic analysis.

Table III—Tankhouse Characteristics

Anodes:

Length, width, thickness	36x36x1¼ in.
Weight:	
Commercial	545 lb
Stripper	630 lb
Suspension	Plain cast lugs
Anode spacing	4½ in.
Replacement period	28 days
Scrap	12 to 15 pct

Starting Sheets:

Length, width, thickness	37¼x37⅞x0.025 in.
Weight (without loops)	9½ lb
Suspension	two 4 in. wide loops

Cathodes:

Weight	245 lb
Replacement period	14 days

Deposition Tanks:

Construction	Precast reinforced concrete slabs
Linings	8 lb per sq ft, 6 pct antimonial lead
Length, width, depth	12 ft 6 in. x 3 ft 6 in. x 3 ft 9 in.
Electrodes per tank:	
Commercial	33 anodes 32 cathodes
Stripper	31 anodes 30 blanks
Electrical connection:	Walker multiple contacts Commercial contacts on ⅜ in. triangular bar Stripper contacts on 1⅛ in. triangular bar

Initial Tank House:

Commercial sections, 11 each of 40 tanks—	440
Stripper sections, 25 tanks on sheet production, 15 tanks on commercial cathode—	40
Liberator sections, 2 each of 4 tanks—	8
Total tanks—	488

Deposition Current:

Nominal rate 9,200 amp	
Current density:	
Commercial	14.9 amp per sq ft
Stripper	15.5 amp per sq ft
Current efficiency	95 pct
(Based on 0.0627 lb theoretical copper per ampere-tank-day)	

Voltage and Power:

Voltage per tank	0.205 v
Deposition current:	
kwh per short ton gross cathode	185
lb gross cathode per kwh	10.8
Alternating current:	
Total kwh per short ton gross cathode	245
Circuit voltage	110 v avg

M-G Sets:

Two units each of 1000 kw rating	Synchronous ac motor at 11,000 v and 2,500 kw dc generators each unit
Available	10,000 amp dc at 20 to 120 v
Rectification efficiency	85.4 pct

Busbars:

Tank bar cross-section	20 sq in.
Distribution bars	20 sq in.
Normal current loading	460 amp per sq in.
Busbar drop	4.4 v

Electrolyte:

Temperature	135° to 140°F
Tank circulation	3 gpm
Specific gravity	1.23

Addition Agents:

	Lb per short ton copper deposited	
	Commercial	Stripper
Glue	0.054	0.39
Avitone	0.054	Nil
Salt	0.027	0.054

Production:

Commercial output per deposition tank day	550 lb
Average daily pull commercial cathode	158 tons
Gross cathode per month (75 pct is dispatched as whole and 25 pct as cut cathodes)	3900 tons
Liberator copper per month	60 tons
Sheets per month	37,000
Decoppered slime per month	3000 lb

trodes are marked for prompt follow up and correction of defects.

Starting Sheet Production

Stripper Operation: Of the 40 tanks in Section 10, 25 are used for sheet production. These are worked with 30 oiled hard-rolled copper blanks as cathodes and 31 large stripper anodes per tank. The remaining 15 tanks are on cathode production.

The stripper electrolyte, in a separate circulation, is given heavier additions of glue and salt and no Avitone to ensure a tough starting sheet deposit. The starting sheet is a 24-hr deposit of copper stripped from one side of an oiled copper blank. The edges of the blanks are grooved and fitted with slotted tubular strips of rubber to prevent edge deposits and thereby reduce both scrap return and time required to clean the blanks.

Sheet Preparation: The stripper section produces 1500 sheets per day. About 10 pct of the sheets are cut into 18x4 in. strips on rotary gang slitting machines. Uncut sheets have suspension loops, derived from the strips, punched on to them. Assembled sheets are flung onto steel workbenches at each side of the press and flattened with wooden beating sticks. The sheets are then indented with a diagonal stiffening cross by a sharp blow of the stick and threaded with clean cathode cross-rods. Assembled sheets, suspended from the cross-rods, are loaded by hand into the sheet racks.

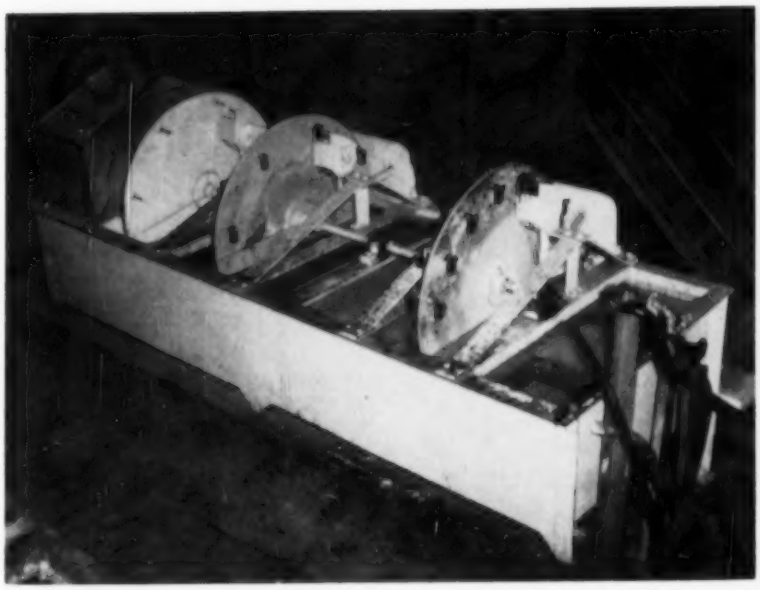

Disk-and-thimble reagent feeders supply addition agents and end compartment of feeder functions as continuous sampler. Electrolyte is bled from main pipeline to this compartment and sample from single cup on disk is collected in feeder body. In use, device has Perspex cover to prevent evaporation loss and contamination.

Mufulira anode copper is exceptionally high grade and throws down little slime. Slime is removed from the tanks at 8-week intervals and 20 tanks are cleaned at a time. The end tank of a section is emptied of electrolyte by rubber syphon hoses, and after scrap has been removed the drain plug is pulled and slime is swept out with a rubber squeegee. The cleaned tank is swilled down with a few gallons of electrolyte blown over from the next tank with a stainless steel steam ejector. The tank plug is replaced and the electrolyte in the next tank, except for the bottom 6 in., is passed over into the clean tank by the steam ejector. This process is repeated down the line of the half section. Setting of new anodes and starting sheets then follows.

Slimes

Slime bearing electrolyte passes through stainless steel screens to a collecting box in the pump aisle. Small float operated pumps convey this air agitated slurry to either of two series of three decanting tanks. Slime settles in these tanks for about 20 hr, that is after the slime from two muddings have been collected and the surplus liquor has been returned to the circuit through filter presses.

The slime slurry is run into two lead-lined steel cylinders equipped with lead-covered stirrers. In these decoppering tanks the slime is given a 48-hr treatment with commercial electrolyte at 160°F and air and steam are blown through the liquor which is stirred for 5 min per hr. Decoppered slime is filtered, washed, and dried with compressed air in the lead plate filter presses. The filter cake is broken up on a steam heated stainless steel pan and dried for at least 24 hr. Dried slime is collected monthly in composite batches, packed into steel drums lined with tarred paper, steel lids are welded on the drums, and the slime is shipped overseas.

Controls

Inspection: In addition to the instruments used in the sections there is a plug and socket voltage board and a record is kept of the hourly readings of all sections. Another board gives the voltage to ground of all sections and this is checked once a week. A weekly survey is also made of the voltage across main insulating pipes in the electrolyte circuit to indicate when it is necessary to remove copper growths which have bridged the insulating breaks.

On the third day of a cathode cycle the sheets which then weigh about 40 lb, are manually lifted in what is called "wet flapping."

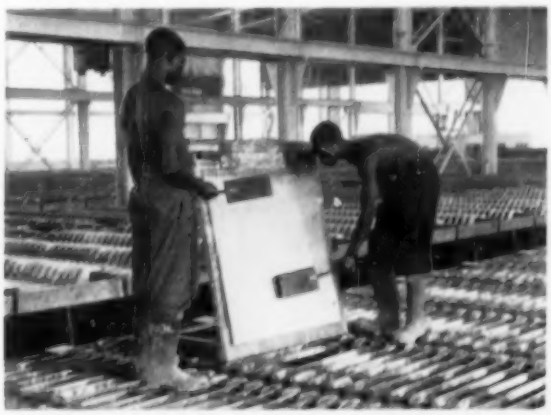

Lifted sheets are flattened with rubber paddles against the copper clad face of a portable bench that is slid along the top of the tanks.

Table IV—Representative Analyses

Anodes (4 week cycle)

Analysis, Pct			
Cu	99.76	Ni	0.007
S	0.002	Co	0.0002
As	0.001	Bi	0.0016
Sb	0.0005	Se	0.0015
Fe	0.0003	Te	Trace
Insoluble	0.003	Pb	0.001
O	0.22		
	Au	0.01 oz per ton	
	Ag	2.50 oz per ton	

Cathodes (2 week cycle)

Analysis, Pct			
Cu	99.97 to 99.99	As	0.0001
S	0.0002 to 0.0006	Fe	0.0001 to 0.0005
	Ag	0.10 oz per ton	

(Sb, Ni, Bi, Se, Te, and Pb, less than 0.0001 pct each)

Commercial Electrolyte:

Analysis, G per L.			
Cu	40 to 45	Ni	1.8
H_2SO_4	200 to 210	Bi	0.18
CaO	0.9	Fe	0.9
MgO	1.0	Cl	0.030

Tankhouse Slimes (8 week cycle)

Analysis			
Raw[a]			
Cu	35 to 43 pct		
Au	22 oz per ton		
Ag	3700 oz per ton		
[a] Yield per short ton of anodes about 1.2 lb.			
Decopperedb			
Cu	8 to 10 pct	Se	5.2 pct
CaO	2.5 pct	Te	0.3 pct
Insoluble	35 pct	Pb	2.5 pct
S	8 pct	Au	35 oz per ton
Bi	0.3 pct	Ag	6000 oz per ton
[b] Yield per short ton of anodes about 0.70 lb.			

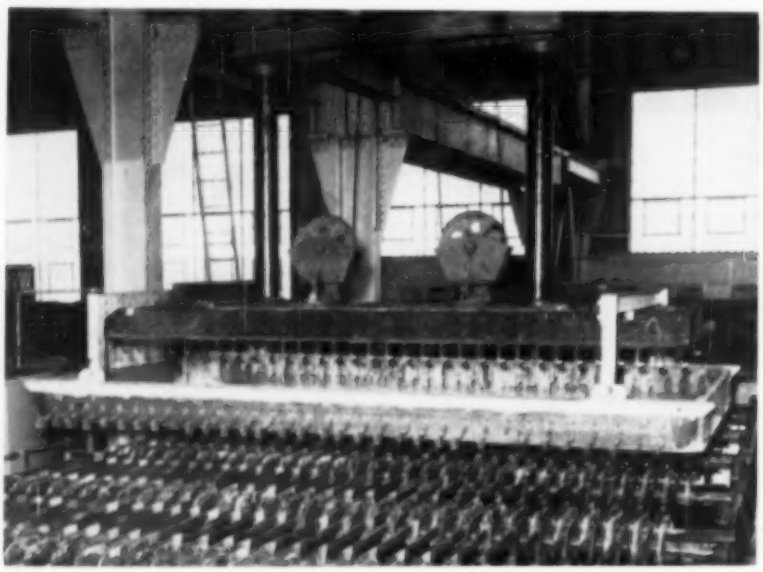

Jumper bar, being lowered into position in this photograph, is used isolate one tank at a time for repair and thus reduce cut out time. Device consists of frame of 1x10-in. copper bus-bar fitted on two long sides with pigtail clips.

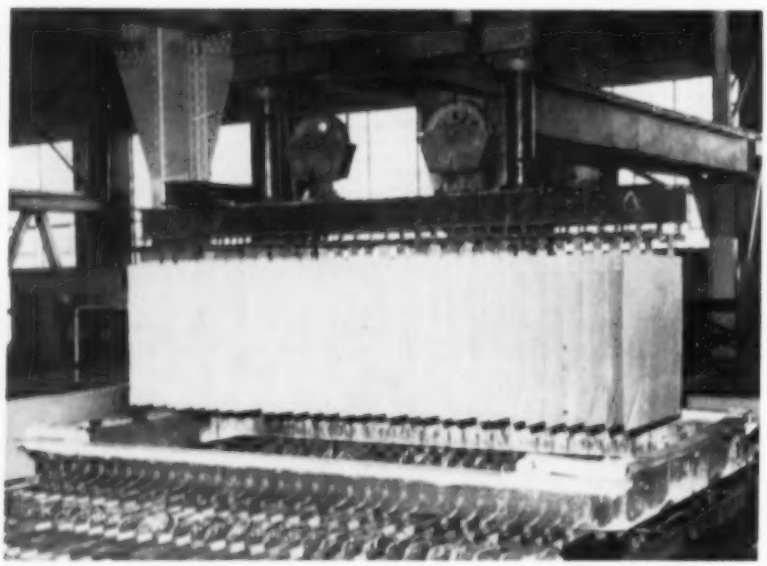

Jumper bar has been positioned over leaking tank, which has been shorted out of circuit together with adjoining tank by attaching clips to cathode cross rods. The other 38 tanks in the section remain in operation.

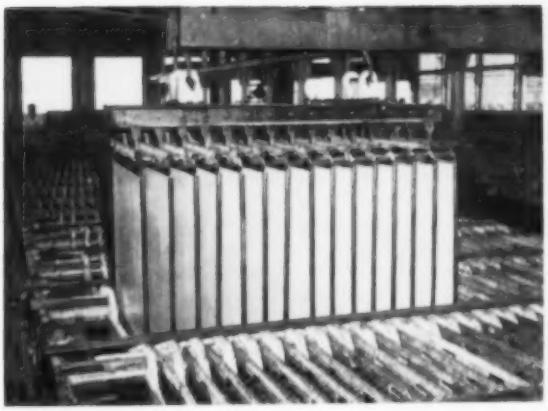

Deposition current remains continuously on the stripper section and only 15 blanks, half a tank load, are removed at a time.

Sheets are stripped daily from blanks while they are suspended from the crane bales on special lead covered racks.

Circulation: The electrolyte head tanks are fitted with high and low level alarms. Condensate from the Karbate heat exchangers is returned as boiler feed water and the boilers are protected against acid contamination of this water, which would arise from a cracked or leaking tube, by modified spark plugs in the condensate pipe circuits. In the case of electrolyte leakage the condensate between the plug electrodes becomes a conductor and operates indicator lights and sirens showing the location of the defect. This system is fitted with three degrees of sensitivity and has proved effective. The temperatures of the stripper and commercial electrolytes are measured at the head tanks by continuous dial recorders.

Substation: The operating amperage is adjusted every 30 min to the nominal rate of 9200 amp and readings prior to adjustment are recorded hourly.

Starting Sheets: A representative load of 32 starting sheets is weighed from the production of sheets every day. The weight allowance for starting sheets, used in calculating deposition efficiency, is readjusted every 14 days on the basis of these weights.

Maintenance

The tankhouse maintenance staff consists of two lead burners, one electrician, and one fitter. Cut-out time for repairs to the lead lining of the tanks is kept to a minimum by use of the tank jumper bars shown below. This device is a rectangular frame of 1x10-in. copper busbar fitted with pigtail clips along the two long sides of the rectangle. It is positioned on top of a leaking tank, which is then shorted out of the circuit, together with one adjoining tank, by attaching the clips to the cathode cross-rods on the adjoining tanks. The leaking tank can then be emptied of copper and electrolyte and repaired while the remaining 38 tanks of the section operate.

Concrete in the tank house is protected generally by at least three layers of bitumastic paint. Overlays of chlorinated rubber base paint are used for all tankhouse steelwork. In the cellar and other vulnerable areas this protection is supplemented daily by copious washing with hot water, and there is also a daily examination of the concrete and steelwork. The acid protective coatings are renewed whenever necessary.

Tank with jumper bar in position has been emptied for repair. Tops of tanks in background have been covered with PVC blanket to conserve process steam. About half the sections are covered with these blankets when inspection work has been completed and throughout the night shift. However, some evaporation loss must be permitted, in order to absorb intake of wash water and spillage.

Electrical Distribution — Boiler Plant — Yard and Transportation —

THE substation is housed in a 58x96-ft building with a basement which is pressurized. Two 1000 kw motor generator sets, one of which is a stand-by, supply dc current to the tank house busbar system. Each motor generator set comprises a salient pole, synchronous motor coupled at each end to a direct shunt-wound generator. The machines are self-ventilating and cool air is drawn from the pressurized basement via ducts incorporated in the concrete foundation, passing through the machine and discharged into the room. The designed rated output from each complete motor generator set is 10,000 amp at voltages from 20 to 100, and 8,330 amp at 120 v. The synchronous motor operates on an electrical supply of 11 kv, the main switchboard being located on the operating floor at the rear of the machines.

A lean-to, between the substation and the tank house building, accommodates the main direct current control switchboard, together with the 550 volt ac switchboard for auxiliary services. A 750 kva transformer, together with rectifier equipment for the 250-v direct current supply, for the tankhouse cranes are accommodated in the basement, access to which is provided via air locks.

The main busbars from the generators to the dc switchboard are designed at a rating of 750 amp per sq in. and the 10x2-in. main positive and negative bars capable of carrying 10,000 amp at 500 amp per sq in. from the dc switchboard go via a tunnel to the tankhouse basement. See Fig. 5. The main positive bars run below the tankhouse operating platforms and the negative bars are carried above

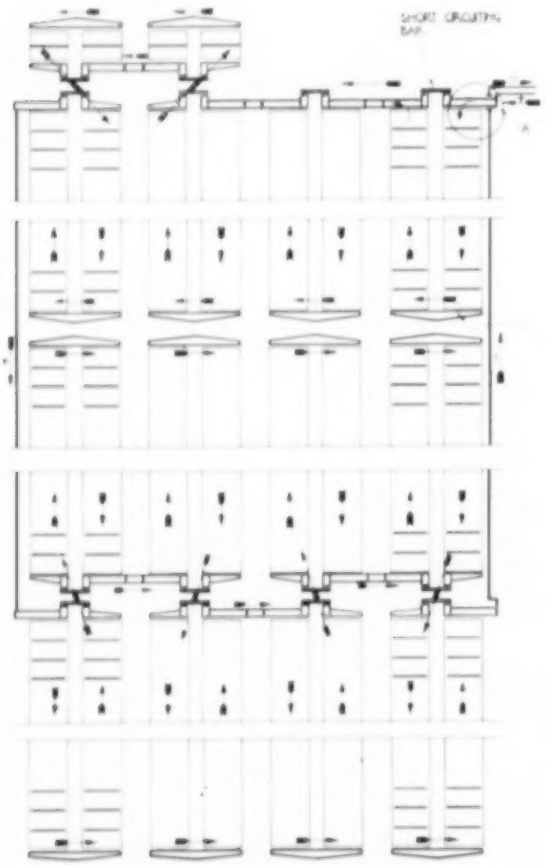

Fig. 5A—Diagram of busbar system. Busbar shape provides reduction in width proportional to current flow.

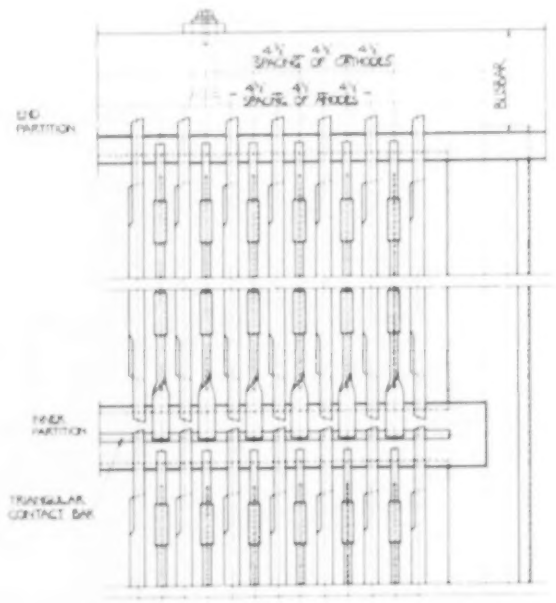

Fig. 5B—Enlarged plan of tank at "A" shows anode spacing and placing of triangular contact bar.

platform level. Subsidiary laminated busbars from the positive main bars are led to the top of the tanks, where they connect to the busbars running throughout the complete tank system. These are supported on top of the concrete slabs forming the tanks and are insulated from the concrete by rubber insulators.

Boiler Plant

The steam requirements for the tankhouse approximate 12,000 lb per hr and until fire-refining furnaces with associated waste heat boilers are installed, steam is supplied from a small boiler installation. The 43x76-ft boiler plant houses three single-drum and one double-drum Babcock & Wilcox boilers.

The installation will become redundant when the refined copper casting plant is commissioned, as the steam from the waste heat boilers following the reverberatory furnaces, together with that generated

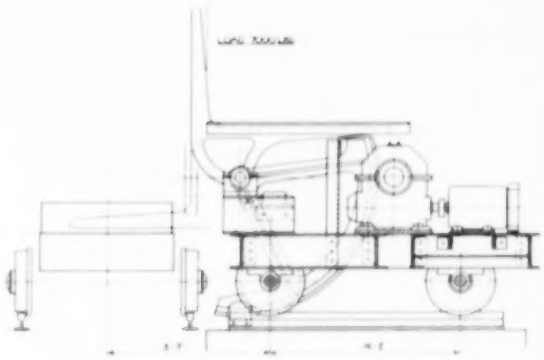

Fig. 6—Cathode unloader car is shown in action in photographs on page 251. Balance weights are located in frame over wheels at right.

Storage Yard Facilities

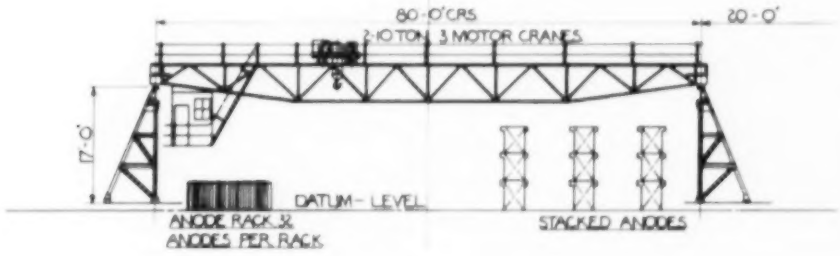

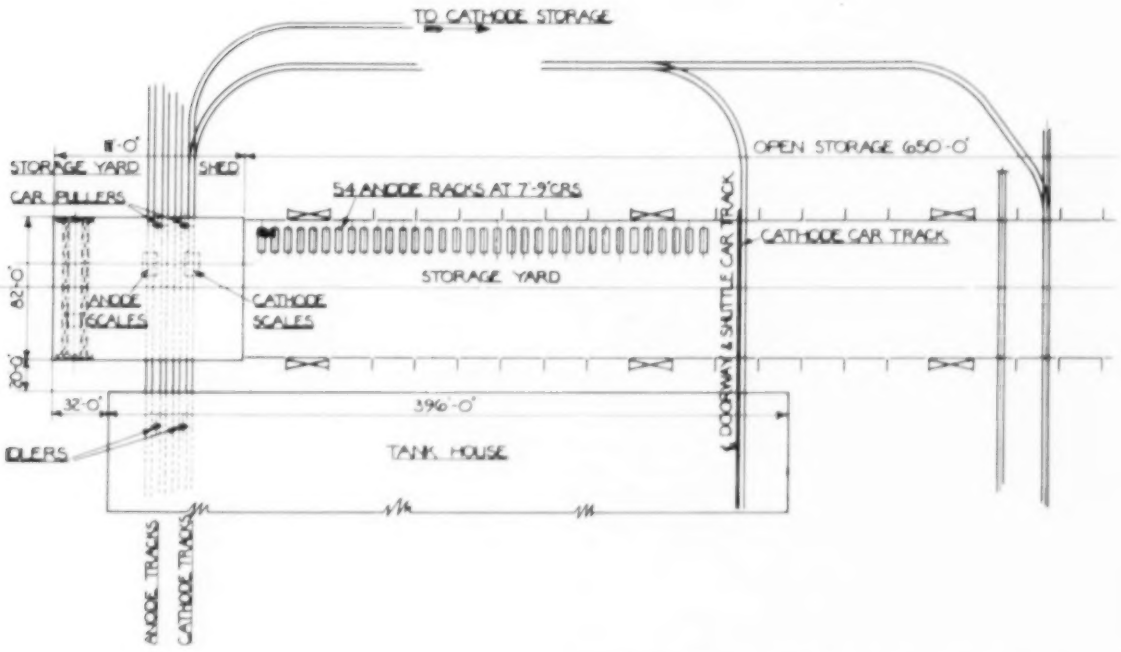

Fig. 7—Plan of anode and cathode storage yard is above, with typical section through yard shown at top. Yard extends to right of plan for future extension and refinery furnace building service.

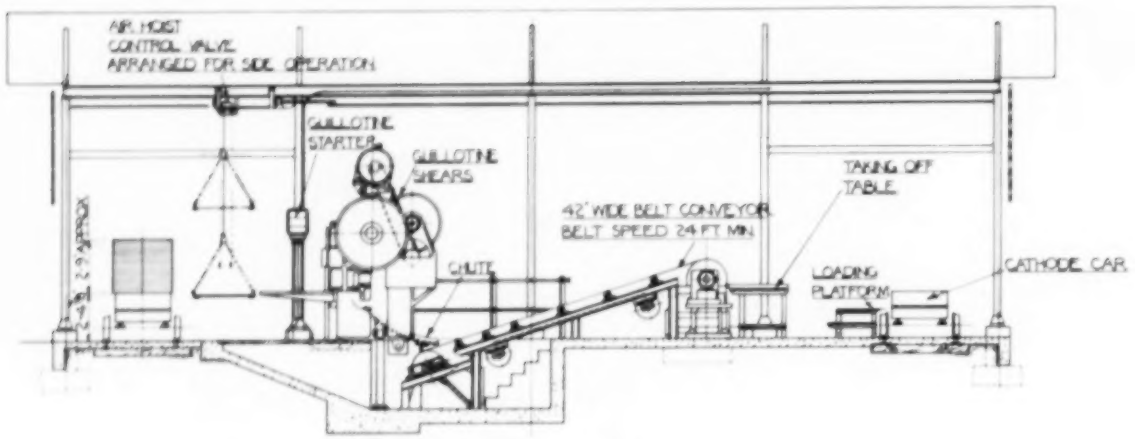

Fig. 8—Longitudinal section cathode cutting shed shows conveyor serving guillotine shears.

in an auxiliary direct-fired boiler, will be delivered via a back pressure turbine exhausting at 15 psi to the tankhouse.

Yard and Transportation System

Anode cars, loaded from the bosh tank by the crane in the casting shed, are hauled by 50 hp Hunslet & Simplex 7½-ton diesel locomotives, to the southern end of the tankhouse. All tracks are 3 ft-6 in. gauge and a turnout and rail system is introduced from the main track to accommodate the storage of 60 cars, with provision made for extending this system to accommodate an ultimate 148 cars. Incoming anode cars pass through the southern end of the storage yard where they are weighed over a 20-ton load capacity railway truck weighbridge with 13-ft capacity, by increments of 5 and 30,000 lb.

The anode cars are hauled by car pullers inside the tankhouse where a fairly elaborate system of switches and turnouts enables a number of cars to be accommodated at any one time.

Washed cathodes are lifted in batches of 32 and transported by the tankhouse cranes to a quadrant arm unloader located in each tank aisle, see Fig. 6. Each unloader is mounted on a turntable having a 90° rotation and the unloader is maneuvered on track and turntable manually. The unloader is equipped with a platform supported by two quadrant arms on to which the tank load of cathodes is automatically stacked from the crane bale by the cross-travel motion of the stiff leg crane. The stack of cathodes are thus transferred on to the flat top cathode cars, the unloader arms being spaced to clear the double-bulb angle supports on which the cathode rest. The unloader car is then retracted manually until the arms are withdrawn clear of the batch of cathodes and the platform is rotated ready for the next operation.

Anode cars have a 20,000-lb carrying capacity, double bogie type fitted with half size Alliance automatic spring couplers and back gear. Cathode cars are four-wheeled type, 14,000 lb capacity, with T-section supports for the cathodes constructed from two 8x3-in. bulb angles welded back to back. Both anode and cathode cars are fitted with Teko-type roller bearing wheels.

The storage yard comprises a series of *A* frames 17 ft from ground level, carrying crane girders at 80-ft centers. Longitudinal centres of the *A* frames are 25 ft, giving an initial total open storage length of 650 ft. Both anodes and cathodes can be readily stored by means of two 10-ton capacity overhead cranes. See Fig. 7.

Fifty-four permanent steel and concrete and steel racks are installed at the southern end of the storage yard which accommodates 1728 anodes, and further storage is provided by stacking anodes on the ground, using a special grab on the crane which enables 12 anodes to be handled at one lift.

The storage aisle is arranged for a future extension at the northern end of 135 ft to enable final electrolytic shapes to be transferred from the inspection aisle of the future fire refinery to one of the storage yard cranes.

Cathodes for direct shipment are transferred singly from the cars by an air-operated hoist running on a central crawl beam to the table of the guillotine shears. Following the cutting operation, the sheared cathodes are delivered via a chute to a 42-in. belt conveyor, Fig. 8.

The conveyor delivers the sheared cathodes to a receiving table and covered ramps from which they go via roller conveyors directly to cathode cars or to railway trucks. Sampling is carried out at an adjacent shed where cathodes are drilled and the sample drillings checked by spectrographic analysis.

Future Expansion

The first extension to the tankhouse increasing the overall rated capacity to a nominal 72,000 long tons of cathode copper per year was completed in 1955.

Construction is now proceeding on the final refined copper casting plant for electrolytic wire bars, cakes, billets, and ingots, with production scheduled for February 1956. This comprises a 342x194-ft steel-frame building housing two 220-ton refining furnaces, two 20,000 lb per hr waste heat boilers and air heaters, two universal casting wheels, and one wheel for vertical casting of billets and bars. Bosh and inspection conveyors, together with auxiliary equipment, are provided.

Kinetic Study of the Oxidation of Sphalerite

The temperature and oxygen concentration dependence on the reaction of sphalerite in oxygen at pressures from 6 to 640 mm Hg have been investigated in the temperature range 700° to 870°C. Sphalerite has been found to oxidize linearly over this entire temperature and pressure range. At higher rates, considerable self-heating was observed. The dependence of the oxidation rate on the oxygen concentration may be expressed by: Rate $= k' \theta$, where k' is the specific rate constant and $\theta = K_1[O_2]/(1 + K_1[O_2])$, where K_1 is the equilibrium rate constant for the adsorption of oxygen on sphalerite. Values of the activation energy and the enthalpy of adsorption were found to be 60.3 and —59.6 kcal per mol, respectively. Data have been presented that indicate conditions under which either a sulphatizing or an oxidizing roast may be obtained.

by John N. Ong, Jr., Milton E. Wadsworth, and W. Martin Fassell, Jr.

ROASTING processes have been employed in the metallurgy of a great number of basic metals in use today. Until recently, however, little attempt has been made to deduce the fundamental mechanism by which oxidation takes place. Structural changes upon oxidation have been investigated[1, 2] and thorough work has been performed with regard to the reaction products and the thermodynamics of the oxidation reactions.[3-6] The objective of this investigation was to determine the rate of oxidation of sphalerite and to apply the absolute reaction rate theory in the theoretical interpretation of the experimental results.[8, 10]

Description of Apparatus

The apparatus contains the following features: 1—a furnace with gas system, 2—an autographic weighing system, and 3—a temperature control system.

Furnace With Gas System—The furnace was mounted by a yoke on each end and was free to travel up and down on steel guide rods, permitting the introduction and removal of samples from the apparatus with minimum difficulty. The furnace was heated by three sections of Kanthal wire wound externally on a zirconia tube and insulated with Fiberfrax. Pure gases or mixtures of gases were introduced into the lower end of the furnace through two flowmeters, a mixing chamber, and a gas-tight sparger, Fig. 1. The gaseous products of the reaction and the unused gases were prevented from escaping to the atmosphere by maintaining a small negative pressure on the system. This procedure permitted air from the outside to enter through the small annulus around the quartz suspension fiber and prevented the escape of the internal gases.

J. N. ONG, JR., Junior Member AIME, M. E. WADSWORTH, Junior Member AIME, and W. M. FASSELL, JR., Member AIME, are Graduate Student, Assistant Professor, and Associate Professor, respectively, Dept. of Metallurgy, University of Utah, Salt Lake City.

Discussion of this paper, TP 4071D, may be sent, 2 copies, to AIME by Apr. 1, 1956. Manuscript, Apr. 14, 1954. Chicago Meeting, February 1955.

This paper is based on a portion of a thesis by J. N. Ong, Jr. submitted, in partial fulfillment of the requirements for the degree of Doctor of Philosophy, to the University of Utah.

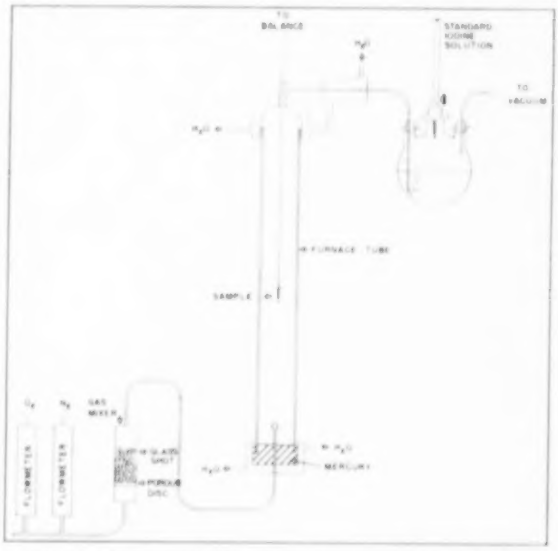

Fig. 1—Gas control and collection system is illustrated schematically. Pure gases or mixtures of gases were introduced into the lower end of the furnace through the two flowmeters (left), the mixing chamber, and the gas-tight sparger.

Autographic Weighing System—The autographic weighing system consisted of an adapted gold balance, a photoelectric circuit, and a weight recorder, Fig. 2. The sample was suspended from one end of the balance beam by means of a platinum chain outside the furnace and a long thin quartz fiber on the inside of the furnace. On the other end of the balance beam, the necessary weights were added to counterbalance the sample. In addition, a calibrated chain was added to the balance which was linked directly to the weight recording unit. Control was effected by means of a photoelectric circuit.[11] A parallel beam of light from a strong source was directed onto a small front-surfaced aluminum mirror mounted in the middle of the balance beam and then to a front-surfaced mirror mounted on the ceiling of the room. The beam was then reflected onto a front-surfaced right prism at a distance of 9 ft from the balance

The Transactions papers appearing in the Journal of Metals during 1956 will subsequently appear in AIME Transactions Volume 206, and may be permanently referenced to that volume.

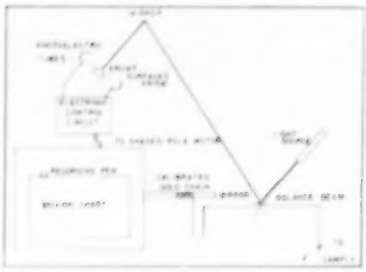

Fig. 2—Autographic weighing system is shown schematically and consists of an adapted gold balance, a photoelectric circuit, and a weight recorder.

beam. The right prism, which splits the light beam, was located in a cabinet next to the balance. The split beams were directed to the two photocells. A slight displacement of the balance beam caused the light to be directed primarily onto one of the two photocells. The impulse thus received was amplified and directed to a shaded-pole motor which drove the recorder pen in the recording unit in the proper direction. At the same time, the motor adjusted the gold chain attached to the balance beam, restoring it to a null position. Displacement of the balance beam in the other direction caused the reverse to happen. In this manner, weighing by swings was effected. The changes in weight of the sample was recorded continuously on a chart moving at constant speed.

The extent of the swing of the balance corresponded to a line on the moving chart of approximately 0.1 in. (1.3 mg). The rate of movement of the chart was ¼ in. per min, setting the lower limit of rate determination at about 3 mg per hr.

Temperature Control System—The furnace temperature was measured by three chromel-alumel thermocouples located in the tube wall of the furnace approximately in the middle of each winding. The furnace temperature was controlled by the thermocouple located directly against the middle winding of the furnace, operating through a Leeds Northrup Micromax Type S temperature controlling recorder, a Micromax Electronic Control Unit, and a motor drive unit. The power input to each of the three windings of the furnace was separately adjusted by means of a powerstat. A direct linkage between the powerstat to the middle winding of the furnace and the motor drive unit controlled the temperature in the reaction zone to within ± 1°C of control setting. Accurate temperature readings were made by switching the thermocouple leads to type 8662 Leeds & Northrup potentiometer.

Experimental Procedure

The sphalerite samples were cut from massive single crystals of the naturally occurring mineral. For this purpose, a jig was constructed on which the sphalerite samples were ground. The samples were ground to shape as nearly as possible along the natural dodecahedral cleavage planes of the sphalerite using a Carborundum wheel. The shape of the samples was rectangular, approximately 0.52 in. long, 0.12 in. wide, and 0.055 in. thick. Platelike samples were used to minimize the change in surface area during oxidation. Samples of these dimensions weighed approximately 0.85 g. A small hole was drilled at one end of the sample for the purpose of suspension on a quartz fiber inside the furnace. Each sample was cleaned with a washing of dilute HCl, two washings of distilled water, and a final wash in alcohol. The sample was then dried and placed on the hook of the quartz fiber and the furnace was slowly lowered over it. Considerable difficulty was experienced in getting the samples into the reaction zone. Since a temperature gradient existed along the furnace tube from the bottom to the reaction zone, thermal stresses were set up in the sample, causing fracture. This resulted in a loss of about three samples in every four. The sample was suspended in pure dry nitrogen while the autographic weighing mechanism was set in operation. The concentration of oxygen was then adjusted to the desired flow rate and a complete rate curve was obtained. The product gases including SO_2 were collected in a three-necked flask and titrated with a standard iodine solution to determine the rate of SO_2 evolution.

The dimensions of the samples were carefully measured beforehand, and the sample area calculated. In order to obtain quantitative data, the rate curves were plotted as weight loss per unit area vs time. Corrections were also made for the reduction in area during oxidation.

Experimental Results

The results to be described are based on the experimental observations of the oxidation of 82 sphalerite samples over the temperature range 700° to 870°C and oxygen partial pressures from 6 to 640 mm Hg. Typical rate curves are presented in Fig. 3. This figure also shows the oxidation rate at 799°C before and after surface area correction.

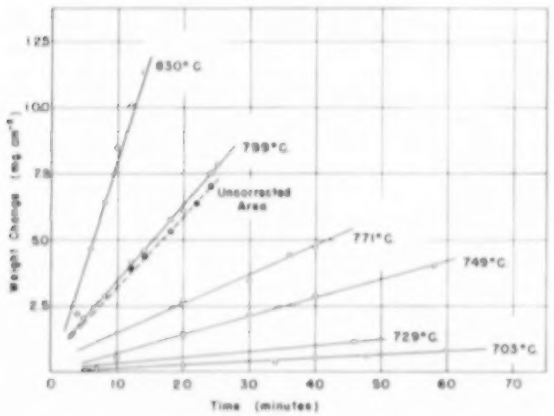

Fig. 3—Curves and data points show the oxidation rates of sphalerite in O_2 at atmospheric pressure.

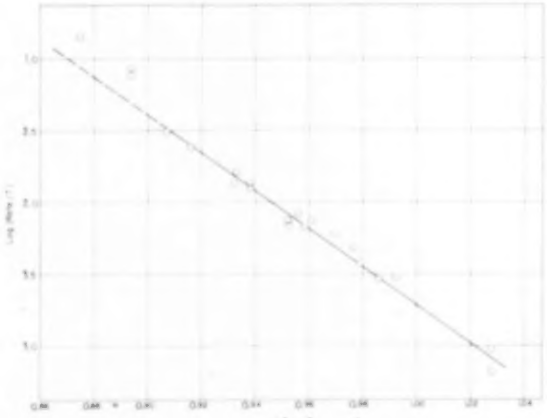

Fig. 4—Arrhenius plot shows the experimental oxidation rates of sphalerite in oxygen at 640 mm Hg pressure.

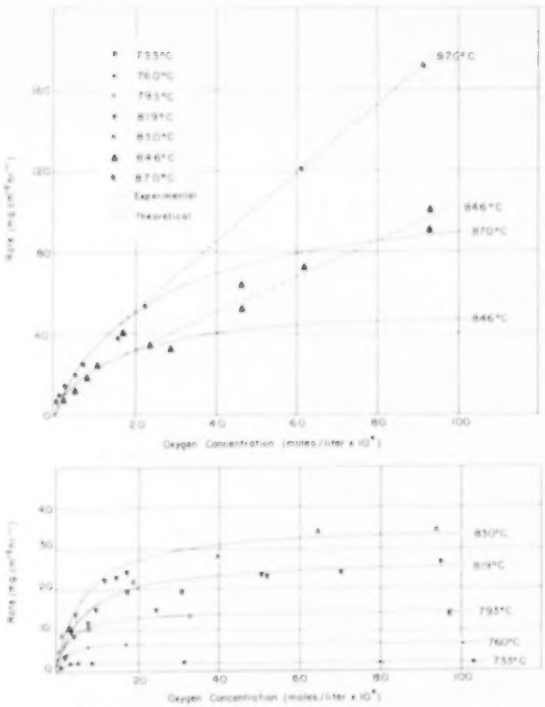

Fig. 5—Oxidation rate of sphalerite vs oxygen concentration is plotted in the two graphs. Legend of the top graph also applies to the bottom one.

While this correction was small, it was often of sufficient magnitude to warrant its use.

This correction was made on the assumption that oxidation occurred evenly at every face on the sample. This was borne out by visual observation of partially oxidized samples. The oxide formed was very porous and the oxidation rate was found to be linear over the entire range of investigation.

The results of 82 separate rate curves are presented in Figs. 4, 5a, and 5b. Fig. 4 is an Arrhenius plot of the rates obtained in pure oxygen at atmospheric pressure (640 mm Hg) vs reciprocal temperature. The deviation from linearity at the higher temperatures can be attributed to self-heating of the sample at the reaction interface.

To determine the effect of oxygen at low partial pressures, seven rate isotherms shown in Figs. 5a and 5b were run. The partial pressure of oxygen was varied by dilution with nitrogen. The five lowest temperature isotherms exhibited the typical behavior of an exothermic surface reaction involving an adsorption process. At higher temperatures and proportionately increased oxidation rates, apparent deviation from the Langmuir-type adsorption isotherm became evident. The rate of evolution of SO_3 was obtained for a number of runs and an Arrhenius plot of these rates gave an activation energy of 58.6 kcal per mol. Difficulty was encountered with the SO_3 balance. Values obtained for rates by the SO_3 determinations as compared with weight change data were consistently low. The SO_3 data, however, are considered unreliable in view of the complex SO_2—SO_3—O_2 equilibrium, the catalytic effect of ZnO, and the possible leaks within the system.

Discussion

The partial pressure effects exhibited by the five lowest temperature isotherms indicate a dependency

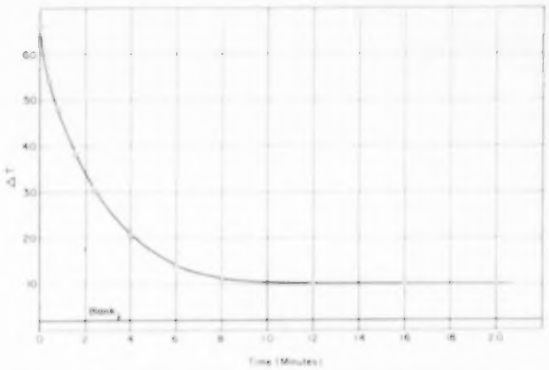

Fig. 6—Curve illustrates the experimental difference between the furnace and sample temperature vs time.

similar to the Langmuir-type adsorption isotherm. This suggests a preliminary adsorption process, followed by decomposition of surface sites. The absolute rate of reaction depends on the concentration of reactive surface sites and becomes constant as the ratio of the number of reactive surface sites covered to the total number of reactive sites available approaches unity. At higher temperatures, however, the disproportionately higher rates observed were found to be due to self-heating of the sample which should occur in some temperature range for all exothermic processes. At first, this effect was masked by the fact that no temperature rise was observed in the recording thermocouple during the course of the experiment. Furthermore, the rate of oxidation was linear at all times, which in general is not expected, since self-heating normally results in an exponentially increasing rate.

A linear rate will obtain, however, if the system is considered to be in a steady state condition, in which the heat generated by the sample is being transferred to the outside through a film of constant thickness at a constant rate.

If the rate of heat generation is proportional to the rate of heat loss through heat transfer, then

$$(\text{Rate})\ (\Delta H_r) = -\frac{J}{X}\ (T_r - T_m) - \sum_i J_i\ (T_{x_i}, X_i, t) \quad [1]$$

where ΔH_r is the heat of reaction in calories per gram, J is the heat transfer coefficient in calories per degree hour-centimeter^2 per centimeter, T_r is the temperature at the reaction zone, T_m is the measured temperature, $\sum_i J_i\ (T_{x_i}, X_i, t)$ is the general heat transfer term including all other forms of heat loss, t is time, X is the thickness of heat transfer film, and T_x is the temperature of the interior of the sample.

Assuming that the rate of heat loss due to heating the sample and radiation and other effects are negligible, Eq. 1 reduces to

$$(\text{Rate})\ (\Delta H_r) = -\frac{J}{X}\ (T_r - T_m)\ . \quad [2]$$

To substantiate that self-heating of the sample did occur, an experiment was run at 900°C, in which a thermocouple was secured against the surface of a sphalerite sample and a series of temperature read-

ings of the sample and the furnace wall was taken over a period of 12 min. The results are shown in Fig. 6. The drop in ΔT with time can be attributed to the recession of the reaction zone from the thermocouple during the course of the reaction. At the highest rate measured (171.8 mg per cm²-hr), the actual rate of heat evolution was about 5.4 cal per min. Because of the large heat capacity of the furnace, this quantity was not large enough to affect the temperature of the furnace or the recording thermocouple.

Theoretical

The linear oxidation of sphalerite may be considered a heterogeneous gas-solid reaction involving an adsorption process on the surface followed by desorption of the products.[9] According to the absolute reaction rate theory,[9, 10] the rate of a reaction may be represented by

$$\text{Rate} = \kappa \frac{kT}{h} \prod_i C_i e^{\Delta F^+/RT} = \prod_i C_i k' \qquad [3]$$

where $\prod_i C_i$ is the product of the concentration of the reactants, ΔF^+ is the free energy of activation, κ is the transmission coefficient (usually taken as unity), k and h are Boltzmann and Planck constants, respectively, and k' is the specific reaction rate constant.

If the rate-determining reaction is the thermal decomposition of a surface site, Eq. 3 becomes

$$\text{Rate} = f(\theta)\, k'$$

where $f(\theta)$ is some function of the fraction of the surface covered.

The rate may then be written as

$$\text{Rate} = \frac{kT}{h} f(\theta)\, k_{ss}\, e^{-\Delta F^+/RT} = \frac{kT}{h} f(\theta)\, k_{ss}\, e^{-\Delta H^+/RT} e^{\Delta S^+/R} \qquad [4]$$

where k_{ss} is a constant which includes a surface-roughness factor and the conversion units necessary to express the fraction of surface coverage in suitable units, ΔH^+ and ΔS^+, are the enthalpy and entropy of activation, respectively. For the mechanism involving single site adsorption of an oxygen molecule on the surface, the reaction appears to be extremely rapid, whereupon it may be considered as an equilibrium process. This may be represented by the equation

$$\text{ZnS (surface)} + \text{O}_2 \rightleftharpoons \text{ZnS} \ldots . \text{O}_2 \text{ (surface)} \qquad [5]$$

from which

$$K_1 = \frac{\theta}{1-\theta} \frac{1}{[\text{O}_2]} = e^{-\Delta F_1/RT} \qquad [6]$$

where θ represents the fraction of the surface covered with adsorbed oxygen, K_1 is the equilibrium constant of the adsorption process, $[\text{O}_2]$ is the concentration of oxygen in the gas phase, and ΔF_1 is the free energy of adsorption. The equilibrium value of ΔF_1 from thermodynamic considerations may be expressed as

$$\frac{-\Delta F_1}{RT} = \ln K_1 - \ln K_1^0 = \ln \frac{\prod_i {}^{\pi}C_p}{\prod_i {}^{\pi}C_R} - \ln \frac{\prod_i {}^{\pi}C^0_p}{\prod_i {}^{\pi}C^0_R} \qquad [7]$$

where C_p and C_R are the concentrations of the products and reactants, respectively. Superscript 0 refers to the standard state. The quantity $\ln \prod_i {}^{\pi}C^0_p / \prod_i {}^{\pi}C^0_R$ is arbitrarily chosen such that it equals zero in the standard state. In the case of the single site mechanism, this quantity is $\ln \{\theta^0/(1-\theta^0)[\text{O}_2^0]\}$. Since the oxygen concentration is expressed in mol per liter, the standard state is defined as $\theta^0 = 0.5$ and $[\text{O}_2^0] = 1$ mol per liter.

Eq. 7 therefore reduces to Eq. 6. Solving Eq. 6 for θ, the following is obtained

$$\theta = \frac{K_1[\text{O}_2]}{1 + K_1[\text{O}_2]} . \qquad [8]$$

Assuming that at constant temperature the quantity $k_{ss} \frac{kT}{h} e^{-\Delta F^+/RT}$ remains constant, Eq. 4 may be written in the form

$$\text{Rate} = K_s \frac{K_1[\text{O}_2]}{1 + K_1[\text{O}_2]} \qquad [9]$$

from which a value of K_1 may be obtained by simultaneous evaluation of two points on each isotherm. The values of K_1 for the four lowest temperature isotherms are given in Table I.

Table I. Values of K_1 for Four Temperature Isotherms

log K_1	T, °K
4.4	1006
4.004	1033
3.580	1066
3.236	1092

Fig. 7 is a plot of log K_1 vs the reciprocal temperature. From this plot, the enthalpy of adsorption, ΔH_1, of O_2 on sphalerite was found to be −59.6 kcal per mol of oxygen with an entropy of adsorption of

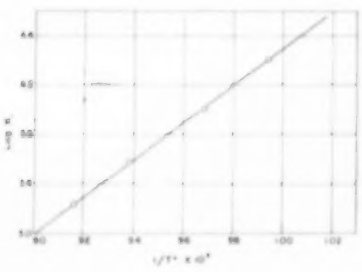

Fig. 7—Line and data points show the relationship of the equilibrium constant of adsorption and the temperature.

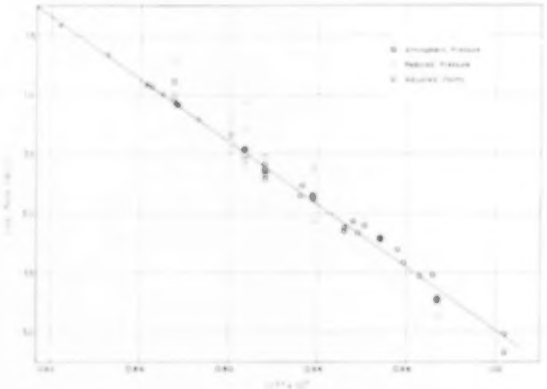

Fig. 8—Total absolute rate of reaction of sphalerite in oxygen is plotted vs the reciprocal temperature.

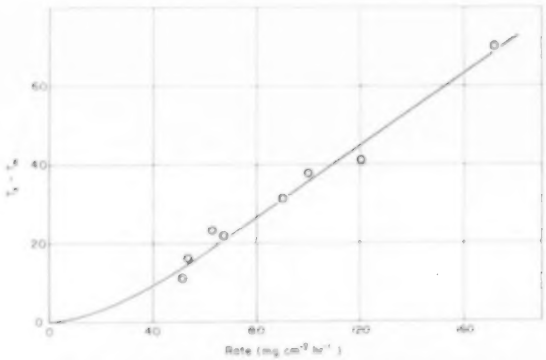

Fig. 9—Curve and data points illustrate the overheating of sphalerite with increases in the rate of oxidation.

−39.2 E.U. The value of ΔH_1, although large, is of the order obtained for chemisorption of gases on solids. The large negative entropy suggests the transition of the oxygen from a disordered gaseous phase to a highly ordered adsorbed phase on the surface. The theoretical curves for the three highest temperature curves (830°, 845°, and 870°C), obtained by evaluating the isotherm using one point at low oxygen concentration and the value of K_1 extrapolated from Fig. 7, are shown in Fig. 5.

The steps by which the reaction of sphalerite proceeds may then be considered to be as follows

$$ZnS + O_2 \rightleftharpoons ZnS \ldots O_2 \text{ (chemisorption)} \quad [5]$$

followed by decomposition of the surface site

$$ZnS \ldots O_2 \rightarrow (\text{activated state})^{+} \rightarrow ZnO + SO \quad [10]$$

and

$$2\,SO + O_2 \rightarrow 2\,SO_2 \quad [11]$$

ultimately resulting in the formation of ZnO and SO_2. The postulate that SO exists as an intermediate product has been suggested before[13-16] and the compound $ZnSO_2$ has been reported.[15] Its presence would be only transitory and it would be immediately removed at the surface by reaction 11. Other possible adsorption mechanisms were tried, such as single and double site adsorption with oxygen-splitting. For these processes, the values of ΔH_1 were of the order of −120 kcal per mol and ΔS_1 of the order of −90 E.U., both of which are abnormally large.

Eq. 4 may be rewritten in the form

$$\frac{\text{Rate}}{(\theta)(T)} = \frac{k}{h} k_{zz}\, e^{\Delta S^{+}/R} e^{-\Delta H^{+}/RT}. \quad [12]$$

It is evident, therefore, that a plot of log {Rate/$(\theta)(T)$} vs reciprocal temperature should yield linear plots. Fig. 8 represents the correlation of 74 experimental rate determinations in the temperature range 700° to 845°C. The experimental heat of activation determined from this plot is 60.3 kcal per mol.

The data from the high temperature isotherms in which the rates exhibit apparent deviation from the Langmuir-type adsorption plot may be corrected to the Arrhenius plot by employing the relationship

$$\text{Rate} = \frac{kT_s}{h} k_{zz}\, \theta_s\, e^{\Delta S^{+}/R} e^{-\Delta H^{+}/RT_s} \quad [13]$$

where T_s is the temperature of the sample due to overheating and θ_s the surface coverage at that temperature calculated from extrapolated values of K_1 obtained from Fig. 7, ΔH^{+} is the value determined for the activation energy at the lower temperatures, and the constant $k_{zz}\frac{k}{h}e^{\Delta S^{+}/R}$ is numerically determined from the low temperature data. That self-heating occurs as the rate of reaction increases is indicated in Fig. 9, in which the rate is plotted vs the difference between the sample temperature (T_s) calculated from Eq. 13 and the measured temperature (T_m).

The form of Eq. 2 suggests that the quantity J/X should remain essentially constant at constant temperature, i.e., the thickness of the film through which heat transfer takes place should remain the same. Furthermore, J/X should also be a function of the temperature. Preliminary calculations show this to be the case, but the accuracy of the extrapolated high temperature data does not warrant arriving at any definite conclusions as to the nature of this function.

A linear oxidation rate as observed in this study and in the study of the oxidation of metals necessitates proposing a mechanism whereby the products of reaction will remove themselves from the surface in order that further reaction may ensue. This problem to date has not yet been adequately explained. Three possibilities present themselves in the case of sphalerite:

1—The activated state will involve a rearrangement of the activated complex (Eq. 10) during the rate-determining step.

2—The freshly formed ZnO molecule may possess sufficient energy to detach itself from the ZnS surface and reattach itself to the ZnO film.

3—Due to the misfit of the ZnO and ZnS lattices, the ZnO will tend to assume its own structure. This can be done only by breaking away from the surface, following which the ZnO diffuses and recrystallizes in the normal ZnO lattice.[16] This step, however, does not appear to be rate-controlling. The rapid removal of ZnO from the sulphide surface is necessitated by the observed linear reaction rates.

If the rate of the reaction is measured in molecules per centimeter^2 —second, k_{zz} of Eq. 4 has the units: molecules per centimeter^2. It is interesting to determine its value in terms of the proposed mechanism. Consistent with the proposed rate-controlling reaction, Eq. 10, ΔS^{+} should be small. Assuming its value to be zero, k_{zz}, determined under the conditions T = 1014°K, Rate = 2.98 mg per cm^2—hr, ΔH^{+} = 60.3 kcal per mol, and θ = 0.995, was found to be 1.47×10^{16} mol per cm^2. There are approximately 4.8×10^{15} surface sites per centimeter^2 along the natural dodecahedral cleavage planes of sphalerite, which gives k_{zz} a value of 30.7. A more reasonable value of the surface roughness of 2 would give a value of ΔS^{+} = 5.4 E.U. Table II gives various ΔS^{+}

Table II. ΔS^{+} Values Obtained for Arbitrarily Chosen Values of the Surface Roughness

ΔS^{+}	Surface Roughness
6.8	1
5.4	2
3.6	5
2.2	10
0.4	25
0.0	30.7

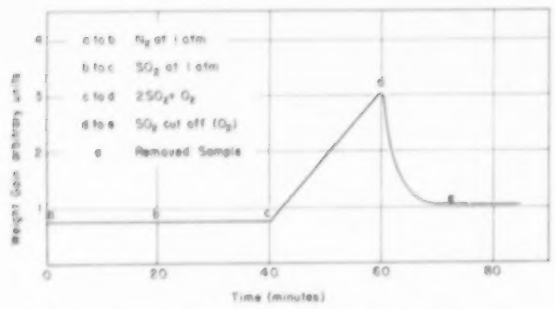

Fig. 10—Rate of $ZnSO_4$ formation from ZnO in various gases is shown at 780°C.

values obtained for arbitrarily chosen values of the surface roughness.

In addition to the mechanisms proposed previously, the authors have considered the following:

1—Vaporization of ZnS occurring within the temperature range investigated.[11] Accordingly, an experiment was performed to determine the rate of vaporization of ZnS. A stream of oxygen-free nitrogen was passed over a sample of sphalerite at 870°C. No detectable weight change was observed over a 2 hr period. It may be concluded, therefore, that the rate of vaporization is not great enough to account for the rates observed.

2—*Sulphate* mechanisms. Experiments to be described in the next section indicate that sulphate formation occurs subsequent to the formation of ZnO and therefore cannot be considered in any preliminary mechanisms.

3—Interaction between ZnS and ZnO

$$ZnS + 2\,ZnO \rightarrow 3\,Zn + SO_2$$

This reaction proceeds at an appreciable rate in the neighborhood of 1400°C.[18] The temperatures of this study are too low to consider that any reaction of this type occurs.

Sulphate Formation

Throughout these studies, it was found that the formation of $ZnSO_4$ was negligible. An experiment was performed in which a plate of pure ZnO was reacted with pure SO_2 and then a mixture of SO_2 and O_2 at a temperature of 780°C. A disk 22 mm diam and 1 mm thick was prepared by pressing analytic grade ZnO in an evacuated die using a 20 ton load. The results are shown in Fig. 10, where weight gain (arbitrary units) is plotted vs time.

The region *a* to *b* shows no detectable weight gain during the time that N_2 was passed over the sample. After 20 min, SO_2 by itself was passed over the sample, *b* to *c*. No weight change occurred in the presence of SO_2 alone. Next, a stoichiometric quantity of O_2 for sulphate formation was added with the SO_2. A rapid weight gain was observed and is shown in Fig. 10, *c* to *d*. At *d*, the SO_2 was shut off and in the presence of O_2 alone the sample lost weight immediately. The $ZnSO_4$ that had formed decomposed very rapidly and at time *e* the sample was removed from the furnace. The sample was extracted before all the $ZnSO_4$ had decomposed. The weight gain of the sample was compared with the amount of sulphate in the sample determined by conventional quantitative analytical techniques and found to correspond closely with the observed weight gain.

Data reported by Maier[5] from the equilibrium data of Wöhler, Plüddemann, and Wöhler[19] showed that the equilibrium SO_3 partial pressure for the $ZnSO_4$—SO_3 system at 775°C is 0.0196 atm. From this, it can be concluded that $ZnSO_4$ should form at partial pressures of SO_3 greater than this. It may be concluded that sulphate formation is subsequent to the formation of ZnO and its formation requires the presence of both SO_2 and O_2.

Preliminary investigations on the rate of formation of zinc sulphate were also carried out. A number of rates were determined at a temperature of 819°C. From Maier,[5] the equilibrium constant K for the reaction $2SO_2 + O_2 \rightleftharpoons 2SO_3$ was calculated to be 0.5 at this temperature. From this, the amount of SO_3 that would be formed under equilibrium conditions for any given SO_2—O_2 composition could be determined (Fig. 11, line 1).

The equilibrium partial pressure of SO_3 in the $ZnSO_4$ — SO_3 system is given[5] as 0.05 atm at 819°C. Under experimental conditions (atmospheric pressure of 640 mm Hg) and assuming complete SO_3—SO_2—O_2 equilibrium, this corresponds to a 6.54 pct SO_2—93.46 pct O_2 mixture. At SO_2 percentages of 6.54 and lower, no measurable weight gain was observed. At increasing SO_2 percentages, the rate of weight gain of the ZnO samples increased until a maximum was reached around 64 pct SO_2 (Fig. 11, line 2). This corresponds closely to the maximum of line 1, Fig. 11. It may be concluded, therefore, that the rate of formation of SO_3 is very fast and that the rate of formation of $ZnSO_4$ is proportional to the amount of SO_3 present in the reacting system. When mixtures of SO_2 and O_2 were passed through the reacting system in which there was no ZnO present, no SO_3 was formed; whereas, in the presence of the oxide, SO_3 was formed in appreciable quantities. This indicates further that zinc oxide behaves as a catalyst, forming the sulphate which in turn decomposes to ZnO and SO_3. Basic zinc sulphate ($3ZnO \cdot 2SO_3$) is formed above 740°C and zinc sulphate ($ZnSO_4$) below 740°C.[20]

Summary

1—The oxidation rate of sphalerite has been found to be linear over the range 700° to 870°C, with an activation energy of 60.3 kcal per mol.

2—Studies of the rate as a function of oxygen concentration have indicated primary single-site adsorption of oxygen on the surface with an enthalpy and entropy of adsorption of −59.6 kcal per mol and −39.3 E.U., respectively.

3—In the light of the experimental evidence presented, the overall reaction $2ZnS + 3O_2 \rightarrow 2ZnO +$

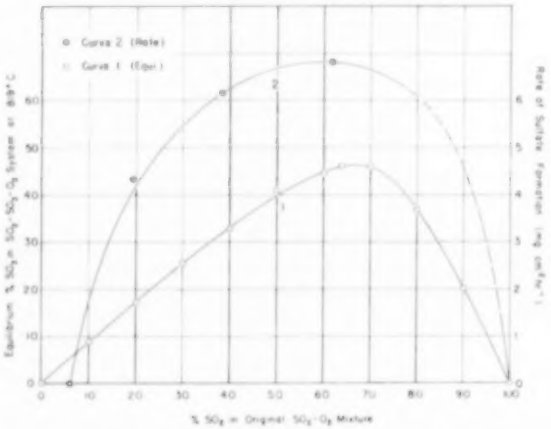

Fig. 11—Rate of $ZnSO_4$ formation from ZnO under varying concentrations of SO_2 and O_2 is shown at 819°C.

$2SO_3$ has been postulated to occur according to the following steps

$$ZnS + O_2 \rightleftharpoons ZnS \cdot \cdot \cdot O_2$$
(Equilibrium chemisorption)

$$ZnS \cdot \cdot \cdot O_2 \rightarrow \text{Activated state} \rightarrow ZnO + SO$$
(Rate-determining step)

$$2\,SO + O_2 \rightarrow SO_2 \qquad \text{(Fast)}.$$

4—At the higher rates of oxidation, appreciable self-heating of the samples occurred.

5—An investigation of the possibility of sulphate formation during the roasting of sphalerite has indicated that, under the experimental conditions of this study, a negligible amount of sulphate was formed.

6—Preliminary rate studies on the sulphatization of zinc oxide in SO_2—O_2 mixtures indicated that the rate of sulphate formation was proportional to the amount of SO_3 that would be present in the system under equilibrium conditions and that zinc oxide acts as a catalyst for the formation of SO_3.

7—Conditions have been proposed under which either a sulphatizing roast or an oxidizing roast may be obtained by maintaining the SO_2 concentration in the roast above a certain specified amount.

Acknowledgments

The authors wish to express their appreciation to the AEC and the University of Utah Research Fund for the funds supplied for this investigation. The project was sponsored by the AEC under Contract No. AT(11-1)-82; the Research Fund provided for the construction of equipment used.

Discussion of this paper, if any, will appear in JOURNAL OF METALS, November 1956, and in AIME Metals Branch *Transactions*, Vol. **206**, 1956.

References

[1] S. Ryochiro: *Journal* Physical Soc., Japan (1951) **6**, pp. 527-528.

[2] G. Aminoff: *International Assn. of Testing Materials Congress* London, Advance Proof (1937) Group A, pp. 80-82.

[3] E. A. Perretti: *Discussions* Faraday Soc. (1948) No. 4, pp. 174-179.

[4] D. M. Chizhikov, G. S. Frents, and Y. B. Tratsevitskaya: *Izvest. Akad. Nauk SSSR*, Otdel Tekh. Nauk, Moscow (1949) pp. 1352-1360.

[5] N. P. Diev and Y. V. Karyakin: *Journal of Applied Chemistry* USSR (1938) **11**, pp. 112-122.

[6] D. M. Chizhikov and G. S. Balikhina: *Tsvetnye Metal* (1937) No. 4, pp. 72-74.

[7] N. P. Diev, Y. V. Karyakin, and A. G. Loshkarev: *Journal of Applied Chemistry* USSR (1938) **11**, pp. 1389-1397.

[8] C. G. Maier: Zinc Smelting From A Chemical and Thermodynamic Viewpoint. *Bulletin No. 324* U. S. Bureau of Mines (1930).

[9] K. J. Laidler: *Chemical Kinetics*. (1950) p. 152. New York. McGraw-Hill Book Co. Inc.

[10] S. Glasstone, K. J. Laidler, and H. Eyring: *The Theory of Rate Processes*. (1941) p. 197. New York. McGraw-Hill Book Co. Inc.

[11] J. A. Lasater, E. L. Nimer, E. L. Quinn, and A. Davidson: Design of a Sensitive Autographic Balance. *Technical Report No. XXXV*. Contract No. NR-032-168, University of Utah (June 1952).

[12] O. V. Deines and G. Elstner: *Ztsch. für Anorg. Allgem. Chemie* (1930) **191**, p. 340.

[13] F. Raschig: *Schwefelund Stickstoffstudien* (1924) p. 324. Leipzig, Verlag G. m.b.H.

[14] M. E. Wadsworth and W. M. Fassell, Jr.: *Trans.* AIME (1953) **197**, pp. 1556-1558; JOURNAL OF METALS (November 1953).

[15] E. Fromm and J. S. Palma: *Berichte Deut. Chemie Gesell* (1906) **39**, pp. 3317.

[16] N. Cabrera and N. F. Mott: Theory of Oxidation of Metals. *Reports on Progress in Physics*. (1948-1949) **XII**, p. 163.

[17] C. L. McCabe: *Trans.* AIME (1954) **200**, p. 969; JOURNAL OF METALS (September 1954).

[18] E. J. Kohlmeyer and G. Goldschmidt: *Ztsch. für Erzbergau und Metallhuttenwesen* (1954) **17**, p. 387.

[19] L. Wöhler, W. Plüddenmann, and R. Wöhler: *Berichte Deut. Chemie Gesell* (1908) **41**, pp. 703.

[20] K. Frederick and A. Blicke: *Metallurgie* (1910) **7**, p. 323.

Technical Note

Filtering Apparatus for Study of Liquid-Solid Equilibria in Alloy Systems

by L. A. Willey

IN 1953, a method for filtering a liquid phase from solid phases while in equilibrium at elevated temperatures was devised at the Alcoa Aluminum Research Laboratories. Since then, it has been applied to the investigation of liquid-solid equilibrium in metallic systems. In application, the method simplifies the centrifuge filtration procedure as developed by Scheil and described by Gebhardt.[1]

Fig. 1 shows a sketch of the filtering apparatus located within a thermal analysis furnace. It consists of a stainless steel filter crucible *A*, into the bottom of which a porous carbon filter disk *B*, 1¾ in. diam by ¼ in. thick, is sealed to the shoulder and rim with carbonaceous cement. The base of the filter crucible, machined to an angle, fits into a tapered seat at the mouth of a stainless steel vacuum chamber C. A connecting tube from the vacuum chamber to a vacuum line also serves as a means for supporting the apparatus from the base of the furnace. An alundum crucible *D* of 25 ml capacity is placed within the vacuum chamber below the filter for collecting the filtrate. Two thermocouples *E*, in stainless steel protection tubes, which extend from 1/16 to ⅛ in. above the center of the filter, are mounted on the rim of the filter crucible. One thermocouple is used in differential connection with the furnace control thermocouple to regulate rates of heating and cooling. The other serves as a means for recording the temperature of the alloy prior to filtering.

A suitable mold coating is used on exposed surfaces of stainless steel parts to guard against attack upon these parts as well as to avoid contamination of the alloy samples. A mold wash prepared from precipitated $CaCO_3$ is suitable for aluminum alloys.

The porous carbon for the filter disks and the carbonaceous cement, grade 200 (graphite base), were obtained from the National Carbon Co. Porous carbon, grade Nos. 10 to 60, has been employed. Grade No. 40, however, appeared to give the optimum advantages in operation.

In operation, an alloy sample is remelted and heated to about 50°C above its liquidus temperature. At the same time, the filter apparatus is preheated to about the same temperature. The alloy then is cast into the filter crucible.

L. A. WILLEY, Member AIME, is Senior Scientist, Alcoa Aluminum Research Laboratories, Aluminum Co. of America, New Kensington, Pa.

TN 286E. Manuscript, May 19, 1955.

By switching from direct to differential control, as indicated in Fig. 1, and adjusting the furnace controller, cooling of the sample at a predetermined rate, such as would be used in thermal analysis, is accomplished. During cooling and any subsequent heating of the sample, time-temperature curves are automatically recorded. The cooling or heating may be arrested and the sample held at any constant temperature by readjustment of the controller setting and by reverting to direct control.

Frequently it is desirable to obtain complete cooling or heating curves and then reheat or recool to a temperature at which equilibrium between liquid and solid is desired. After holding at this temperature for a sufficient period to assure a close approach to equilibrium, a stopcock in the vacuum line is opened. Pressure differential forces the liquid phase from spaces between the solid dendrites or crystals of the solid phases, through the porous carbon, and into the collecting crucible. The furnace then is removed from its base and the filtrate and residue, within the filtering apparatus, are permitted to cool in air at room temperature.

A chemical analysis of the filtrate gives the composition of the liquid phase in equilibrium with solid at the temperature of filtering. Since all the liquid phase cannot be drawn from the liquid-solid mixture, the residues are not "clean." In limited cases, however, crystals of the solid phases may be separated from the residues by mechanical, chemical, or electrolytic means and identified by determination of their composition and crystal structure.

For proper operation, the liquid portion of the alloy at equilibrium usually should be greater than 50 pct. This will vary appreciably, however, and will be dependent for the most part upon the characteristics of the dendrite or crystal formations.

The apparatus has been operated in the range 185° to 800°C and probably could be operated in its present form at temperatures exceeding 1000°C. Obviously, with filter disks and crucibles made of other refractory materials which would not be "wet" or attacked by alloys under investigation, the apparatus could be extended to wider ranges of operation. Also, by some simple alterations, operation in inert atmospheres could be accomplished.

The method, employing the apparatus described previously, has been used to establish liquidus curves

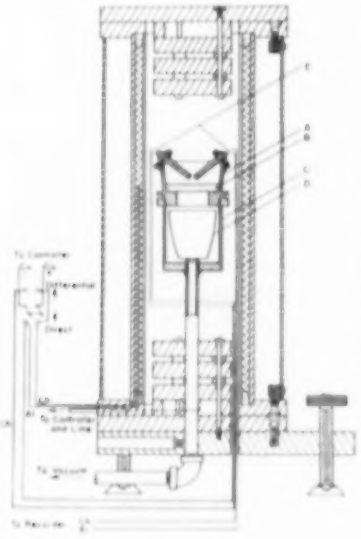

Fig. 1—Elevated temperature filtering apparatus as located within a thermal analysis furnace. Letters on the diagram represent: *A*, stainless steel filter crucible; *B*, porous carbon filter disk; *C*, stainless steel vacuum chamber; *D*, alundum crucible; and *E*, two thermocouples.

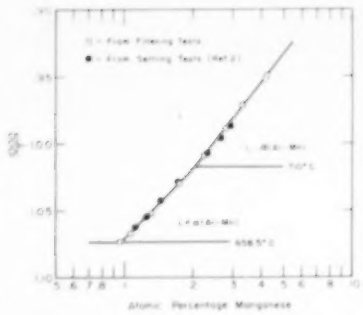

Fig. 2—Liquidus curves in the Al-Mn system are given as a comparison between results determined in the filtering tests and a previous settling experiment.

in several high purity aluminum-rich alloy systems. As an example, the results of tests in the determination of a portion of the aluminum-rich Al-Mn hypereutectic liquidus are shown in Fig. 2 in comparison with previous results determined in a settling experiment.[2]

By filtering at temperatures below the secondary thermal arrest in ternary alloys, points along the eutectic valley of a system may be readily established. Relatively few alloys are required, thereby considerably reducing the work of investigation.

The method is particularly useful for the determination of eutectic concentrations in systems with any number of components. These concentrations are precisely established from filtrates obtained during the invariant reaction either upon melting or solidification. Positive checks upon results are obtained by comparing analyses of filtrates from both hypoeutectic and hypereutectic alloys.

A redetermination of the eutectic concentration in the Al-Si system may be cited as an example. From the many investigations of this concentration, values ranging from 10.0 to 13.8 wt pct Si have been reported. The generally accepted value has been 11.6 pct Si.[3] Filtrates, collected during the eutectic melting at 578°C of two high purity hypoeutectic alloys containing 8.93 and 11.57 pct Si and two high purity hypereutectic alloys containing 13.94 and 19.02 pct Si, were found to contain 12.61, 12.40, 12.62, and 12.57 pct Si, respectively. These give an average value of 12.55 pct for the eutectic concentration which is in good agreement with the value of 12.5 pct Si as most recently determined by Craighead et al.[4]

Accuracy, in the three types of determinations, appears to be high. In a total of 125 determinations, standard deviations from average percentage values for points and curves were found to be 0.03, 0.10, and 0.14 for the concentration ranges 0.2 to 1.0, 1 to 10, and 10 to 50 pct, respectively.

Acknowledgment

The author expresses appreciation to William L. Wesoloski for performing the filtering tests and to other members of the staff of the Alcoa Aluminum Research Laboratories for valuable assistance.

References

[1] E. Gebhardt: Untersuchungen im Dreistoffsystem Aluminium-Eisen-Zink. *Ztsch. für Metallkunde* (1953) **44**, pp. 206, 211.

[2] E. H. Dix, Jr., W. L. Fink, and L. A. Willey: Equilibrium Relations in Aluminum-Manganese Alloys of High Purity, II. *Trans.* AIME (1933) **104**, p. 335.

[3] *Metals Handbook*. (1948) p. 1166. Cleveland, ASM.

[4] C. M. Craighead, E. W. Cawthorne, and R. I. Jaffee: Solution Rate of Solid Aluminum in Molten Al-Si Alloy. *Trans.* AIME (1955) **203**, p. 81; JOURNAL OF METALS (January 1955).

Intermediate Phases in Binary Systems of Certain Transition Elements

Thirty binary systems of vanadium and chromium group transition elements with second and third long period transition elements were explored in regard to the intermediate phases formed. It was found that the phases predominating in these systems are σ, A_3B type with ordered β-tungsten or C8 structure, close-packed-hexagonal with small unit cell dimensions and, finally, phases isomorphous with α-manganese.

by Peter Greenfield and Paul A. Beck

IN recent years, considerable information has become available concerning the intermediate phases in binary systems of the transition elements. Thus, the σ phase has been found to occur in most of the binary systems of vanadium, chromium, and molybdenum with the group of elements manganese, iron, cobalt, and nickel.[1] It was observed that, while the σ phases formed by chromium with manganese, iron, or cobalt possess a considerable temperature range of stability, particularly in the Cr-Co system, the corresponding σ phases with molybdenum are limited to a temperature range of less than 400° above about 1200°C. Goldschmidt[2] reported σ phases of tungsten with iron and cobalt, and these are apparently stable only at (and above?) 1400°C.[3] Exploratory work in this laboratory with Fe-W and Co-W alloys of approximately 60 atomic pct W annealed at 1300°C did not produce X-ray patterns suggesting the presence of σ phase. It appears then that the σ phases of iron and cobalt with the chromium group elements decrease in stability as the two components are chosen from long periods further removed from each other.

From the available information, it might be concluded that the controlling factor is the increasing difference in atomic radii between the components. In contrast to the σ phase, the μ phases formed by iron and cobalt with chromium group elements[4] are stable only when the latter have large atomic radii (molybdenum and tungsten); the corresponding μ phases with chromium do not occur. When the difference in atomic size becomes still larger (r_x/r_a approaching the ideal value of 1.225), the σ and μ phases are replaced by Laves phases (AB_2), as in the alloys of iron and cobalt with columbium,[5] tantalum,[5] and titanium.[6,*]

However, atomic size certainly cannot be the sole determining factor, since, for instance, in contrast to the very stable (Mo, Co)μ phase, no such phase occurs in the Mo-Ni system even though the atomic diameters of cobalt and nickel are nearly the same. Similarly, chromium and cobalt form a σ phase in a wide temperature range,[7] but the corresponding σ phase in the Cr-Ni system is missing. It has been shown that the composition of the σ phase in various binary and ternary systems of transition elements in the first long period may be correlated in a fairly quantitative manner with the number of electron vacancies.[7-10] The influence of electronic structure is probably present also in binary and ternary μ phases[4] and to some extent, apparently, even in Laves phases.[11,12] Although the absence of σ phases in the Cr-Ni and Mo-Ni systems has not as yet been explained on the basis of electronic structure, it appears reasonable to suspect a connection.

One of the great difficulties in arriving at well founded rules in regard to the alloying behavior of transition elements lies in the lack of reliable information concerning the details of their electronic structure in the metallic and alloy form. The theoretical penetration of this field appears to be beset by very considerable difficulties, even when the complications due to alloy formation are disregarded. Another great source of uncertainty is the scarcity of phase diagram information even for binary systems of the transition elements so that only a very limited basis is provided for generalizations as to the occurrence of intermediate phases. For instance, very few binary phase diagrams of second and third long period transition element systems have so far been published. The present work was undertaken in order to survey the various types of intermediate phases occurring in 30 binary systems of elements of the group vanadium, columbium, tantalum, chromium, molybdenum, and tungsten with the elements rhenium, ruthenium, rhodium, palladium, and platinum. For most of these binary systems phase diagrams are very incompletely or not at all known, as will be further reviewed.[5]

P. GREENFIELD and P. A. BECK, Member AIME, are former Research Associate and Research Professor of Physical Metallurgy, respectively, College of Engineering, University of Illinois, Urbana, Ill.

Discussion of this paper, TP 4097E, may be sent, 2 copies, to AIME by May 1, 1956. Manuscript, Mar. 9, 1955. New York Meeting, February 1956.

* After the present investigation was partially completed, a paper by Raub[13] was published on binary systems with molybdenum. That paper includes four of the five molybdenum systems dealt with in the present paper. A paper by Raub and Mahler[14] on the Pd-Cr system appeared after the completion of the present work. After the present paper was written and accepted for publication, a new paper by Raub and Mahler[15] appeared on three other of the five chromium systems dealt with here.

Experimental Procedure

Quantities (1 g) of the alloys were prepared by melting in an arc furnace, using helium atmosphere.

Table I. Typical Impurities in Weight Percentages in the Metals Used

	V	Cb	Ta	Cr	Mo	W	Re	Ru	Rh	Pd	Pt
Al							0.02				
Ca							0.02				
Mg							0.035				
Si		0.01			0.01		0.03				
Fe		0.01	0.015	0.06	0.01		0.08				
Ni					0.005						
Mn							0.007				
Cu				Trace			0.001				
Sn							0.002				
Ti		0.03	0.05								
Cb			0.02								
Ta		0.2									
W					0.01						
Pb				0.001							
S				0.012							
O_2	0.063			0.51		0.04					
N_2	0.077			0.10							
H_2	0.01			0.045							
Alkali					0.01						
SiO_2						0.02					
Fe_2O_3						0.005					
CaO						0.005					
KCl						0.07					
C	0.08	0.5	0.01	0.01	0.002						
Total			0.1 maximum	0.1 maximum				0.15	0.15	0.1	0.1

In order to achieve a reasonable degree of homogeneity, each alloy sample was remelted twice. Typical impurities in weight percent in the metals used are shown in Table I.

Due to large differences in the melting points and in the vapor pressures of the components, for some of the alloys the actual analyses may have deviated considerably from the intended compositions. In view of the very small quantities of samples available for analysis, even the analyzed compositions cannot claim a very high degree of accuracy.

The alloy specimens were annealed at 1000° or 1200°C for 72 to 120 hr in an atmosphere of He + 8 pct H_2 and quenched in cold water. After polishing, the specimens were etched using one of the following etchants: 1—20 pct H_2SO_4 used electrolytically, 2—10 pct HCl in alcohol used electrolytically, or 3—concentrated HNO_3 with a few drops of HF.

After microscopic examination, the same samples were used for the preparation of X-ray powder specimens, which were annealed in evacuated and sealed quartz tubes at the same temperature at which the preceding bulk anneal took place. The powder specimens were quenched in cold water. Powders of the brittle phases σ, β-tungsten, and α-manganese type were not annealed. X-ray diffraction patterns were made with unfiltered CrK radiation, using a back-reflection focusing-type camera of asymmetrical design.

Experimental Results

The alloys prepared for each binary system and the structures observed by means of X-ray diffraction and microscopic examination of the polished and etched sections are given in Table II. The intended composition is given for each alloy, except for those marked with asterisks which were obtained by chemical analysis. The phases designated in the table by a single chemical symbol are terminal solid solutions based on the element concerned.

In the alloy systems examined, a number of σ phases were identified, which are listed together with their X-ray data in Table III. In this table, the values of $\sin^2\theta$ for the new σ structures are compared with those for the (Fe, Cr)σ phase, after appropriate factors for the elimination of the effect of changes in the unit cell dimensions were used, in accordance with the practice followed by Pearson and Christian.[14] σ has a space group of D_{4h}^{14}—$P4/mnm$. The structure with 30 atoms in the tetragonal unit cell is now known.[15, 16]

Four so-called *β-tungsten-type* phases (composition A_3B) were identified. It is now known that *β-tungsten* does not actually exist and that the structure originally attributed to it (now considered to be associated with W_2O) is not ordered,[17] while the corresponding phases identified in the present investigation are ordered. The following designation *ordered β-tungsten-type* will be used. This designation is also used in Table II. The positions of the eight atoms in the unit cell (space group is O_h^8—$Pm3n$) are as follows:

2 atoms B: 0, 0, 0; ½, ½, ½
6 atoms A: ¼, 0, ½; ½, ¼, 0; 0, ½, ¼;
¾, 0, ½; ½, ¾, 0; 0, ½, ¾.

Each has two nearest A atom neighbors; the A/A atoms form three mutually perpendicular sets of chains parallel to the cubic crystal axes. The six structures of this type found, together with their X-ray data, are listed in Table IV.

Four intermediate phases with simple close-packed-hexagonal structure were found, and the corresponding X-ray data are given in Table V. In the course of the present investigation, four phases were found with the well known body-centered-cubic complex α-manganese structure (space group T_d^3 with 58 atoms in the unit cell). The X-ray data are given in Table VI. Phases with this structure are designated in Table II as α-manganese. The X-ray data in Table VI did not lead to the conclusion that these structures are ordered as reported by Kasper[18] for the (Fe,Cr,Mo)χ phase, which is otherwise similar to α-manganese.

In the following section, a brief description is given of the phases present in each binary system investigated:

Re-V System—Nothing was found in the literature concerning the equilibria in this system. Four alloys were annealed at 1200°C (Table II). No intermediate phases were found. The solid solution limit

Table II. X-Ray Diffraction and Microscopic Study of Alloys

Alloy System	Atomic Pct		Temperature, °C	Phases Present
Re-V	66	V	1200	V
	55	V	1200	V + Re
	41	V	1200	V + Re
	40	V	1200	Re
Re-Cb	65	Cb	1200	Cb
	57	Cb	1200	Cb + α-Mn
	46	Cb	1200	Cb + α-Mn
	37	Cb	1200	α-Mn
	50	Cb	1000	Cb
	53	Cb*	1000	Cb + 40 pct σ
	45.3	Cb*	1000	σ + 30 pct α-Mn
	18	Cb	1000	α-Mn
Re-Ta	52	Ta	1200	Ta
	46	Ta	1200	Ta + σ
	43	Ta	1200	Ta + σ
	41.7	Ta	1200	Ta + σ
	41.3	Ta*	1200	σ + 3 pct Ta
	39.2	Ta*	1200	α-Mn + 30 pct σ
	36.2	Ta	1200	α-Mn
	33	Ta	1200	α-Mn
	25	Ta	1200	α-Mn
Re-Cr	60	Cr	1200	Cr + σ
	53	Cr	1200	Cr + σ
	36.8	Cr*	1200	σ
	49	Cr	1200	Re + σ
	45	Cr	1200	Re + σ
	28	Cr	1200	Re + σ
	20	Cr	1200	Re + σ
Re-Mo	55	Mo	1200	σ + other phase
	50	Mo	1200	σ
	46.5	Mo	1200	σ
	45	Mo	1200	σ
	35.9	Mo*	1200	σ
	30.7	Mo*	1200	σ + α-Mn
	22.5	Mo	1200	σ + α-Mn
	20	Mo	1200	α-Mn
Re-W	63	W	1200	σ + other phase
	60	W	1200	σ + other phase
	59.6	W*	1200	σ + other phase
	58	W	1200	σ
	53	W	1200	σ
	48	W	1200	σ
	43	W	1200	σ
	40	W	1200	σ
	34	W*	1200	σ + little α-Mn
	30	W	1200	σ + α-Mn
	25	W	1200	α-Mn
Ru-V	64	V	1200	CsCl-type ordered
	50	V	1200	Tetragonal
	29	V	1200	Ru + unidentified phase
	18	V	1200	Ru + unidentified phase
Ru-Cb	68	Cb	1200	Cb (may be CsCl)
	52	Cb	1200	Tetragonal
	31	Cb	1200	Tetragonal
	42	Cb	1200	Unidentified phases
	32	Cb	1200	Unidentified phases
	22	Cb	1200	Ru + other phase
Ru-Ta	62	Ta	1200	CsCl-type ordered
	50	Ta	1200	Tetragonal
	45	Ta	1200	Tetragonal
	36	Ta	1200	Unknown phase + Ru
	27	Ta	1200	Unknown phase + Ru
Ru-Cr	74	Cr	1200	Cr + 8 pct σ
	70.7	Cr*	1200	Cr + σ
	66	Cr	1200	σ
	64.4	Cr*	1200	Ru + σ
	50	Cr	1200	Ru
Ru-Mo	76	Mo	1200	σ + Mo
	64.2	Mo	1200	σ + 2 pct Mo
	61.4	Mo	1200	σ + Mo
	59.4	Mo	1200	σ + Ru
	50.7	Mo	1200	σ + Ru
Ru-W	50	W	1200	Ru + W
Rh-V	75	V	1200	β-W
	58	V	1200	β-W + c.p.h.†
	50	V	1200	β-W + c.p.h.†
	40	V	1200	C.p.h.†
Rh-Cb	78	Cb	1000	β-W
	72	Cb	1000	β-W + σ
	65	Cb	1000	β-W + σ
	63	Cb*	1000	σ + 3 to 5 pct Cb
	60	Cb	1000	σ
	58	Cb*	1000	σ + 5 to 10 pct Rh
	52	Cb	1000	σ + Rh
Rh-Ta	83.6	Ta	1000	σ + Ta
	70	Ta	1000	σ + Ta
	64	Ta	1000	σ + other phase
	60.2	Ta	1000	σ + trace of other phase
	57	Ta	1000	σ + Rh
	48	Ta	1000	σ + Rh
	27.5	Ta	1000	Rh + other phase
	19	Ta	1000	Rh + other phase
Rh-Cr	75	Cr	1200	β-W
	70	Cr	1200	β-W + c.p.h.†
	65	Cr	1200	C.p.h.†
	60	Cr	1200	C.p.h.†
	50	Cr	1200	C.p.h.†
	25	Cr	1200	Rh
Rh-Mo	75	Mo	1200	Mo + c.p.h.†
	64	Mo	1200	Mo + c.p.h.†
	50	Mo	1200	C.p.h.†
	27	Mo	1200	C.p.h.† + Rh
Rh-W	75	W	1200	W + c.p.h.†
	53	W	1200	W + c.p.h.†
	19.2	W	1200	C.p.h.†
Pd-V	76	V	1200	V + other phase
	72	V	1200	V + other phase
	64	V	1200	Pd + other phase
	60	V	1200	Pd + other phase
	50	V	1200	Pd
Pd-Cb	68	Cb	1000	Cb + σ
	59	Cb	1000	Cb + σ
	57	Cb	1000	Cb + σ
	55	Cb	1000	Cb + σ
	53.3	Cb*	1000	Cb + σ
	56.6	Cb*	1000	Pd + σ
	48	Cb	1000	Pd + σ
Pd-Ta	75	Ta	1000	Ta + Pd
	62	Ta	1000	Ta + Pd
	50	Ta	1000	Ta + Pd
Pd-Cr	60	Cr	1200	Pd + Cr
	50	Cr	1200	Pd
Pd-Mo	75	Mo	1200	Mo
	50	Mo	1200	Mo + Pd
Pd-W	37	W	1200	Pd + W
Pt-V	75	V	1200	β-W
	65	V	1200	β-W + other phase
	49	V	1200	Pt + other phase
	40	V	1200	Pt
Pt-Cb	78	Cb	1000	β-W
	67	Cb	1000	β-W + σ
	63.3	Cb*	1000	σ + 15 to 20 pct β-W
	61.8	Cb*	1000	σ + trace Pt
	58.3	Cb	1000	σ + 10 pct Pt
	53	Cb	1000	σ + Pt
	43	Cb	1000	Pt
Pt-Ta	83.5	Ta	1000	σ + Ta
	81.5	Ta*	1000	σ
	75	Ta	1000	σ
	69.5	Ta	1000	σ
	65.8	Ta	1000	σ + other phase
	62	Ta	1000	σ + other phase
	57	Ta	1000	σ + other phase
Pt-Cr	75	Cr	1000	β-W
	63	Cr	1000	Probably ordered AuCu₃ type
	50	Cr	1000	Pt
Pt-Mo	71.7	Mo	1200	C.p.h.† + Mo
	57.6	Mo	1200	C.p.h.†
	47.2	Mo	1200	Pt + c.p.h.†
	35.9	Mo	1200	Pt
Pt-W	70	W	1200	Pt + W

* Starred values were derived from chemical analyses.
† C.p.h. stands for close-packed-hexagonal phase.

of rhenium in vanadium is about 38 atomic pct Re, while the solution limit of vanadium in rhenium is approximately 40 atomic pct V.

Re-Cb System—Nothing was found in the literature concerning the intermediate phases in this system, but Duwez[10] mentioned in oral discussion the existence of a σ phase at the composition ReCb. The alloys listed in Table II showed that no σ phase exists at 1200°C. An alloy containing 37 atomic pct Cb, however, was found to have a structure of the α-manganese type, Table VI. Alloys in this system were also annealed at 1000°C, at which temperature a σ phase enters into equilibrium between the α-manganese-type phase and the body-centered-cubic columbium-base solid solution. The σ phase appears to have a very narrow range of composition at about 50 atomic pct Cb, Table III, in agreement with Duwez. The α-manganese structure is stable

from about 40 atomic pct Cb down to at least 18 atomic pct Cb. The solid solution of rhenium in columbium is about 40 atomic pct Re.

Re-Ta System—There is nothing in the literature concerning the equilibria in this system, but Duwez mentioned[17] in oral discussion the existence of a σ phase at the composition Re_2Ta_3. The alloys listed in Table II were annealed at 1200°C. The same two intermediate phases were found in this system as in the Re-Cb system, namely, a σ phase, Table III, and an α-manganese type, Table VI. The σ phase field appears to be narrow, at about 41 atomic pct Ta, Table II. A very narrow two phase field lies between the σ phase and the α-manganese type. The latter has a wide composition range, from about 37 to at least 25 atomic pct Ta. The solid solution limit of rhenium in tantalum is between 48 and 54 atomic pct Re.

Re-Cr System—Nothing was found in the literature concerning the equilibrium conditions in this system. Great difficulty was encountered in preparing the alloys, since apparently considerable losses in chromium occurred. The intended compositions probably differ markedly from the true values. One intermediate phase was found and this has the σ structure, Table III. X-ray diffraction data showed that it is in equilibrium with both terminal solid solutions at 1200°C. An alloy chemically analyzed as containing 63.2 atomic pct Re and 36.8 atomic pct Cr consisted entirely of the σ phase. The difficulty in obtaining a single phase σ alloy with no second phase present suggests that the σ phase has a narrow composition range.

Re-Mo System—According to Duwez,[17] a σ phase exists in this system at ReMo. A face-centered-cubic phase with a parameter of $a = 3.70$Å has also been reported at 85 atomic pct Mo.[20] The alloys listed in Table II were annealed at 1200°C. Two intermediate phases were found. One of these, between limits of approximately 33 to 52 atomic pct Mo, was found to have the σ structure, Table III. The other intermediate phase, which extends from approximately 21 atomic pct Mo toward the rhenium end of the system, has the α-manganese structure. Agreement between the observed and calculated X-ray intensities is good, Table VI, except that some of the very low intensity low angle reflections are missing.

Re-W System—Becker and Moers[21] determined the liquidus curve, which showed a sharp maximum at 62 atomic pct Re. This is strongly indicative of an intermediate phase melting at 3010°C. Duwez mentioned in oral discussion[17] that this phase has the σ structure. The alloys listed in Table II were annealed at 1200°C. Two intermediate phases were found at this temperature. These phases have the same crystal structures as those in the Re-Mo system, namely, a σ phase, Table III, and an α-manganese-type phase, Table VI. The σ phase has a composition range from approximately 37 to 58 atomic pct W. The α-manganese-type structure exists from about 27 atomic pct to an undetermined lower tungsten value.

Ru-V System—Nothing was found in the literature concerning the equilibria in this system. The alloys listed in Table II were annealed at 1200°C. An intermediate phase was found at approximately 50 atomic pct V, having a slightly tetragonal lattice, Table VII, with unit cell dimensions similar to those of the vanadium-base body-centered-cubic solid solutions. Whether this tetragonal phase is present at 1200°C or is a result of transformation on cooling to room temperature is not known. An alloy with approximately 64 atomic pct V was found to have an ordered CsCl-type structure, with unit cell dimensions very similar to those of the vanadium-base body-centered-cubic solid solutions. Again, it is not certain whether ordering is present at 1200°C or develops during cooling. The solubility limit of vanadium in ruthenium is less than 18 atomic pct V.

Ru-Cb System—Nothing was found in the literature concerning the equilibria in this system. The alloys listed in Table II were annealed at 1200°C. An intermediate phase at about 52 and 51 atomic pct Cb was tentatively assigned a tetragonal lattice, Table VII. The X-ray diffraction patterns for the 42 and 32 atomic pct Cb alloys were not interpreted; one or two additional intermediate phases of unidentified structure are apparently present in this

Table III. New σ Phases Compared with (Fe, Cr) σ

Alloy System	Fe-Cr	Re-Cb	Re-Ta	Re-Cr	Re-Mo	Re-W	Ru-Cr	Ru-Mo	Rh-Cb	Rh-Ta	Pd-Cb	Pt-Cb	Pt-Ta
a		9.72	9.72	9.23	9.58 9.54	9.55	9.007 9.03	9.54	9.774	9.754	9.89	9.89	9.95
c		5.07	5.07	4.80	4.96 4.95	4.98	4.663 4.67	4.95	5.084	5.058	5.11	5.11	5.16
c/a		0.53	0.52	0.52	0.52 0.52	0.52	0.518 0.52	0.52	0.517	0.518	0.52	0.52	0.52
Multiplying factor:	1.0	1.223	1.231	1.097	1.179	1.178	1.049	1.174	1.231	1.233	1.257	1.257	1.274
Line							$\sin^2\theta$ Values						
311	0.2318	0.2315	0.2314	0.2314	0.2324	0.2313	0.2330	0.2313	0.2324	0.2320	0.2310	0.2317	0.2313
002	0.2528	0.2507	0.2494	0.2499	0.2509	0.2495	0.2530	0.2518	0.2527	0.2528	0.2520	0.2525	0.2505
410 112	0.2866	0.2884	0.2877	0.2860	0.2887	0.2880	0.2882	0.2875	0.2871	0.2894	0.2883	0.2863	0.2878
330	0.3034	0.3054	0.3046	0.3043	0.3033	0.3045	0.3051	0.3028	0.3040	0.3058	0.3044	0.3040	0.3040
202	0.3203	0.3177	0.3181	0.3178	0.3178	0.3172	0.3198	0.3194	0.3205	0.3211	0.3184	0.3203	0.3177
213 420	0.3371	0.3342	0.3341	0.3341	0.3345	0.3345	0.3368	0.3370	0.3364	0.3362	0.3357	0.3376	0.3347
411	0.3498	0.3510	0.3502	0.3496	0.3494	0.3513	0.3508	0.3504	0.3496	0.3509	0.3506	0.3494	0.3496
331	0.3666	0.3675	0.3667	0.3663	0.3656	0.3668	0.3673	0.3667	0.3665	0.3683	0.3667	0.3667	0.3658
222	0.3877	0.3847	0.3847	0.3847	0.3840	0.3851	0.3867	0.3868	0.3859	0.3867	0.3888	0.3872	0.3856
430 312 500	0.4214	0.4178	0.4178	0.4210	0.4181	0.4184	0.4211	0.4210	0.4200	0.4196	0.4191	0.4206	0.4180
322	0.4720	0.4709	0.4693	0.4730	0.4686	0.4690	0.4740	0.4705	0.4713	0.4710	0.4715	0.4716	0.4697
501 431	0.4846	0.4863	0.4841	0.4826	0.4833	0.4847	0.4861	0.4826	0.4830	0.4835	0.4840	0.4843	0.4841
511	0.5015	0.5022	0.5006	0.5010	0.4993	0.5017	0.5014	0.5009	0.5004	0.5012	0.5009	0.5033	0.5000
402	0.5225	0.5210	0.5238	0.5226	0.5210	0.5528	0.5230	0.5223	0.5215	0.5230	0.5235	0.5226	0.5224

Table IV. (A_3B), β-Tungsten Type Phases—CrKα Diffraction Lines

	$\sin^2\theta$		Intensity		$\sin^2\theta$		Intensity		$\sin^2\theta$		Intensity	
$h\,k\,l$	Observed	Calculated	Observed*	Calculated	Observed	Calculated	Observed*	Calculated	Observed	Calculated	Observed*	Calculated
	V_3Rh, a_0 = 4.767A				Cb_3Rh, a_0 = 5.115A				Cr_3Rh, a_0 = 4.656A			
110	0.1176	0.1152	S	—	—	—	M	—	—	—	Absent	—
200	0.2327	0.2304	S	278	0.2030	0.2004	M	376	0.2419	0.2416		367
210	0.2901	0.2880	S	374	0.2528	0.2505	S	1000	0.3019	0.3020	S	510
211	0.3480	0.3456	VS	633	0.3038	0.3006	S	833	0.3625	0.3624	S	813
220	0.4625	0.4608	W	23	—	0.4008	Absent	0.5	0.4829	0.4832	VW	28
$310\alpha_1$	0.5765	0.5760	M	41	—	0.5010	Absent	0.9	0.6042	0.6040	VW	49
$310\alpha_2$	0.5780											
222	—	0.6912	Absent	20	0.6020	0.6012	—	114	—	0.7248	Absent	33
$320\alpha_1$	0.7475	0.7488	M	208	0.6514	0.6513	M	391	0.7818	0.7852	W	216
$320\alpha_2$	0.7495								0.7846			108
$321\alpha_1$	0.8048	0.8064	VS	1000	0.7007	0.7014	S	903	0.8427	0.8456	S	1000
$321\alpha_2$	0.8075								0.8452			505
400	—	—	—	—	0.7991	0.8016	M	508	—	—	—	—
	V_3Pt, a_0 = 4.808A				Cb_3Pt, a_0 = 5.11A				Cr_3Pt, a_0 = 4.706A			
110	0.1142	0.1134	VS	712	0.1013	0.1000	MW	201	0.1178	0.1184	S	480
200	0.2271	0.2268	S	462	0.2006	0.2000	M	422	0.2367	0.2368	S	290
210	0.2835	0.2835	MS	271	0.2500	0.2500	S	577	0.2959	0.2960	S	248
211	0.3408	0.3402	VS	1000	0.2998	0.3000	VS	934	0.3553	0.3552	VS	868
$220\alpha_1$	0.4545	0.4536	MW	107	0.3992	0.4000	W	31	0.4731	0.4736	M	58
$220\alpha_2$									0.4743		MW	28
$310\alpha_1$	0.5668	0.5670	MW	121	0.4990	0.5000	W	48	0.5906	0.5920	M	102
$310\alpha_2$	0.5681		MW	60					0.5930		M	50
222	0.6801	0.6804	VW	1.7	0.5963	0.6000	VW	22	—	0.7104	Absent	0.7
$320\alpha_1$	0.7365	0.7371	W	142	0.6476	0.6500	M	223	0.7681	0.7696	M	98
$320\alpha_2$									0.7703		M	48
$321\alpha_1$	0.7928	0.7938	VS	994	0.6986	0.7000	VS	1000	0.8272	0.8288	VS	1000
$321\alpha_2$	0.7956		VS	497					0.8302		VS	505
400	—	—	—	—	—	—	—	—	—	—	—	—

* *VW* stands for very weak; *MW*, medium weak; *W*, weak; *M*, medium; *S*, strong; *MS*, medium strong; and *VS*, very strong.

composition range. The solubility limit of columbium in ruthenium is less than 22 atomic pct Cb. An alloy with approximately 68 atomic pct Cb was found to have either body-centered-cubic or CsCl-type structure. The lack of observable superstructure lines in this case does not decide this choice, since the difference in scattering power between ruthenium and columbium atoms for CrK radiation is insufficient.

Ru-Ta System—Nothing was found in the literature concerning this system. The alloys listed in Table II were annealed at 1200°C. The alloy with about 50 atomic pct Ta is apparently tetragonal, Table VII. There is also a second intermediate phase between 36 and 45 atomic pct Ta with unknown structure. The X-ray diffraction pattern taken at room temperature of the 1200°C annealed and quenched alloy with approximately 62 atomic pct Ta indicates that this structure is also of the CsCl type, i.e., an ordered solid solution, such as was found to occur in the Ru-V system. The solubility limit of tantalum in ruthenium is less than 27 atomic pct Ta.

Ru-Cr System—Nothing was found in the literature concerning the equilibrium conditions in this system. The five alloys listed in Table II were examined at 1200°C. Only one intermediate phase was found and this has the σ structure, Table III. This phase has a narrow range of composition, probably about 2 pct wide, about 66 atomic pct Cr. The solid solubility limit of chromium in ruthenium exceeds 50 atomic pct, while the solid solubility limit of ruthenium in chromium is less than 26 atomic pct.**

** Raub and Mahler[18] published data concerning this system after the present paper was accepted for publication. They also found only one intermediate phase at 900° to 1300°C at the same composition, but they did not identify it as a σ phase. These authors also found Cr_2Ru and $CrRu$ at temperatures below 900°C.

Ru-Mo System—Recently, Raub[16] reported the occurrence of an intermediate phase of unknown structure in this system at the composition Ru_3Mo_5. The alloys listed in Table II were annealed at 1200°C. In accordance with Raub, only one intermediate phase was found, and this has now been identified as a σ phase, Table III, existing over a very narrow range of composition of the order of 1 pct at 60 atomic pct Mo. The X-ray diffraction data are in good agreement with those reported by Raub for Ru_3Mo_5.†

† After the completion of the present paper, a publication by D. S. Bloom[29] appeared, which identifies Ru_3Mo_5 as a σ phase, in agreement with the present work.

Ru-W System—According to Raub and Walter,[30] there are no intermediate phases in this system; the solid solution limit of tungsten in ruthenium

Table V. Phases with Close-Packed-Hexagonal Structure, Unfiltered Chromium Radiation

	Rh-Cr, 50 Atomic Pct Rh, 50 Atomic Pct Cr*		Rh-Mo, 73 Atomic Pct Rh, 27 Atomic Pct Mo†		Rh-W, 80.8 Atomic Pct Rh, 19.2 Atomic Pct W‡		Pt-Mo, 42.4 Atomic Pct Pt, 57.6 Atomic Pct Mo§	
	$\sin^2\theta$		$\sin^2\theta$		$\sin^2\theta$		$\sin^2\theta$	
$h\,k\,l$	Observed	Calculated	Observed	Calculated	Observed	Calculated	Observed	Calculated
100β	0.2047	0.2033			0.1992	0.1992	0.1878	0.1873
002β	0.2410	0.2408	0.2322	0.2308	0.2333	0.2320	0.2189	0.2168
100α	0.2476	0.2456	0.2380	0.2371	0.2390	0.2384	0.2263	0.2259
101β	0.2651	0.2635	0.2545	0.2532	0.2564	0.2572	0.2416	0.2415
002α	0.2905	0.2904	0.2795	0.2784	0.2813	0.2809	0.2634	0.2616
101α	0.3208	0.3182	0.3070	0.3070	0.3087	0.3084	0.2917	0.2913
102β	0.4458	0.4441	0.4265	0.4263	0.4293	0.4312	0.4048	0.4041
102α	0.5363	0.5360	0.5142	0.5155	0.5162	0.5184	0.4873	0.4875
$110\alpha_1$	0.7369	0.7368	0.7111	0.7113	0.7145	0.7152	0.6743	0.6777
$110\alpha_2$	0.7390							
103β	0.7426	0.7451						
112β	0.8487	0.8507					0.7741	0.7787
201β	0.8734	0.8734	0.8368	0.8397				
$103\alpha_1$	0.8941	0.8990	0.8577	0.8635	0.8610	0.8684	0.8134	0.8145
$103\alpha_2$	0.8973							
004α							0.8674	0.8672

* a_0 = 2.668A, c_0 = 4.249A, and c/a = 1.592.
† a_0 = 2.715A, c_0 = 4.340A, and c/a = 1.598.
‡ a_0 = 2.708A, c_0 = 4.328A, and c/a = 1.598.
§ a_0 = 2.782A, c_0 = 4.477A, and c/a = 1.609.

Table VI. Phases with α-Manganese Structure, CrKα Diffraction Lines

	Sin² θ		Intensity		Sin² θ		Intensity	
h k l	Observed	Calculated	Observed*	Calculated	Observed	Calculated	Observed*	Calculated
		Re-Cb, a_o = 9.670A				Re-Ta, a_o = 9.711A		
220	0.1131	0.1122	VW	0.70	—	—	Absent	0.70
310	—	0.1402	Absent	0.10	—	—	Absent	0.10
222	0.1680	0.1682	VW	0.58	0.1667	0.1668	VW	0.58
321	—	0.1962	Absent	0.53	0.1946	0.1946	Absent	0.53
400	0.2254	0.2243	W	3.78	0.2226	0.2224	W	3.78
411 / 330	0.2538	0.2524	VW	89.4	0.2509	0.2502	VS	89.4
420	—	0.2804	Absent	0.40	—	—	Absent	0.40
332	0.3093	0.3084	S	27.6	0.3060	0.3058	S	27.6
422	0.3375	0.3365	M	9.4	0.3339	0.3335	M	9.4
510 / 431	0.3657	0.3645	S	13.9	0.3620	0.3614	S	13.9
521	0.4208	0.4206	VW	1.10	0.4163	0.4170	VW	1.10
440	—	0.4486	Absent	0.25	—	—	Absent	0.25
433 / 530	0.4775	0.4766	VW	1.14	0.4733	0.4726	VW	1.14
600 / 442	—	0.5046	Absent	1.38	—	—	Absent	1.38
532 / 611	0.5320	0.5326	VW	2.32	0.5282	0.5282	VW	2.32
620	—	0.5606	Absent	0.37	—	—	Absent	0.37
622	0.6171	0.6169	W	3.4	0.6122	0.6116	W	3.4
444	0.6736	0.6730	W	8.6	0.6670	0.6672	W	8.6
550 / 710 / 543	0.7008	0.7010	M	11.6	0.6954	0.6950	M	11.6
640	—	0.7290	Absent	0.01	—	—	Absent	0.01
721 / 633 / 552	0.7568	0.7570	S	47.9	0.7510	0.7506	S	47.9
642	0.7848	0.7851	M	7.5	0.7784	0.7784	M	7.5
730	0.8118	0.8131	M	5.4	0.8061	0.8062	M	5.4
		Re-Mo, a_o = 9.55A				Re-W, a_o = 9.588A		
220	0.1160	0.1150	VW	0.70	0.1139	0.1141	Absent	0.70
310	—	0.1437	Absent	0.10	—	0.1426	Absent	0.10
222	0.1730	0.1724	VW	0.58	—	0.1711	Absent	0.58
321	—	0.2012	Absent	0.53	—	0.1996	Absent	0.53
400	0.2322	0.2300	W	3.78	0.2285	0.2282	W	3.78
411 / 330	0.2610	0.2587	VS	89.4	0.2574	0.2567	VS	89.4
420	—	0.2874	Absent	0.40	—	0.2852	Absent	0.40
332	0.3179	0.3161	S	27.6	0.3140	0.3137	S	27.6
422	0.3469	0.3449	M	9.4	0.3425	0.3422	M	9.4
510 / 431	0.3750	0.3736	S	13.9	0.3711	0.3708	S	13.9
521	0.4321	0.4311	VW	1.10	0.4287	0.4278	VW	1.10
440	—	0.4600	Absent	0.25	—	0.4564	Absent	0.25
433 / 530	0.4872	0.4886	VW	1.14	—	0.4849	VW	1.14
600 / 442	—	0.5174	Absent	1.38	—	0.5134	Absent	1.38
532 / 611	0.5490	0.5461	VW	2.32	0.5430	0.5419	VW	2.32
620	—	0.5748	Absent	0.37	—	0.5704	Absent	0.37
622	0.6314	0.6322	W	3.4	0.6265	0.6274	W	3.4
444	0.6889	0.6898	W	8.6	0.6846	0.6845	W	8.6
550 / 710 / 543	0.7174	0.7185	M	11.6	0.7132	0.7130	M	11.6
640	—	0.7472	Absent	0.01	—	0.7416	Absent	0.01
721 / 633 / 552	0.7736	0.7760	S	47.9	0.7699	0.7700	S	47.9
642	0.8023	0.8047	M	7.5	0.7985	0.7986	M	7.5
730	0.8315	0.8334	M	5.4	0.8267	0.8271	M	5.4

* VW stands for very weak; W, weak; M, medium; S, strong; and VS, very strong.

is 36.5 atomic pct W and the limit of solution of ruthenium in tungsten is 15 atomic pct Ru. Only one alloy was examined in this system (annealed at 1200°C) and this confirmed the absence of intermediate phases. This alloy, containing 50 atomic pct W, was found to consist of the body-centered-cubic tungsten-rich solid solution in equilibrium with the close-packed-hexagonal ruthenium-rich solid solution.

Rh-V System—Nothing was found in the literature concerning the equilibria in this system. Four alloys were annealed at 1200°C and these are listed in Table II. Two intermediate phases were found. One of these, V_3Rh, possesses the ordered β-tungsten structure, Table IV. An alloy containing 40 atomic pct V consists of a second intermediate phase with a close-packed-hexagonal crystal structure, Table V.

Rh-Cb System—Nothing was found in the literature concerning the equilibria in this system. Seven alloys, listed in Table II, were annealed at 1000°C. Two intermediate phases were found. Cb_3Rh was found to have the ordered β-tungsten structure, Table IV. Another intermediate phase was found over a range of about 1 pct at approximately 60 atomic pct Cb. Direct comparison of X-ray films showed that this phase is isomorphous with σ, Table III. The rhodium-rich phase in equilibrium with σ may be either another compound or the rhodium-rich solid solution. No data were obtained on this point.

Rh-Ta System—No work has been reported in the literature on this system. The eight alloys listed in Table II were annealed at 1000°C. Only one intermediate phase was found, the σ phase, Table III, which exists over a narrow range at approximately 60 atomic pct Ta.

Rh-Cr System—Nothing was found in the literature concerning this system. The six alloys listed in Table II were annealed at 1200°C, and two intermediate phases were found. Cr_3Rh is of the ordered

Table VII. X-Ray Diffraction Data for Four Intermediate Phases, CrK_α Radiation

$\sin^2\theta$ Observed	Intensity Observed#	$\sin^2\theta$ Calculated	Tentative Indices	$\sin^2\theta$ Observed	Intensity Observed#	$\sin^2\theta$ Calculated	Tentative Indices
63 Atomic Pct Cr + 37 Atomic Pct Pt*				50 Atomic Pct V + 50 Atomic Pct Ru†			
0.1830	M	0.1820	110	0.1476	W	0.1495	100
0.2749	S	0.2730	111	0.2858	S	0.2865	101
0.3650	MS	0.3640	200	0.2985	M	0.2990	110
0.4554	W	0.4550	210	0.4356	M	0.4360	111
0.5460	VW	0.5460	211	0.5991	W	0.5980	200
0.7262	S	0.7280	220	0.7350	M	0.7350	201
0.8180	W	0.8190	221	0.7490	W	0.7475	210
				0.8456	M	0.8470	112
				0.8853	S	0.8845	211
52 Atomic Pct Cb + 48 Atomic Pct Ru‡				50 Atomic Pct Ta + 50 Atomic Pct Ru‡			
0.2624	S	0.2606	101	0.2605	S	0.2595	101
0.2674	W	—	?	0.2881	M	0.2880	110
0.2925	W	0.2912	110	0.4619	VW	—	?
0.5812	W	0.5824	200	0.5753	W	0.5760	200
0.7485	VW	0.7512	112	0.7482	VW	0.7500	112
0.7721	S	—	?	0.8338	S	0.8325	211
0.8442	M	0.8430	211				

* Cubic ordered $AuCu_3$ type structure, $a = 3.775$Å.
† Tetragonal, $a = 2.96$Å, $c = 3.09$Å, $c/a = 1.04$.
‡ Tetragonal, $a = 3.00$Å, $c = 3.38$Å, $c/a = 1.13$.
§ Tetragonal, $a = 3.02$Å, $c = 3.37$Å, $c/a = 1.11$.

W stands for weak; *VW*, very weak; *M*, medium; *S*, strong; and *MS*, medium strong.

β-tungsten type, Table IV. A second intermediate phase with close-packed-hexagonal crystal structure was found between approximately 50 and 65 atomic pct Cr. The solid solution of chromium in rhodium exceeds 25 atomic pct.††

†† Raub and Mahler[28] published data on this system after the present paper was accepted for publication. They identified the same two intermediate phases as described here, but some differences exist as to the exact location of certain phase boundaries.

Rh-Mo System—Raub[12] reported the presence of a close-packed-hexagonal phase in this system in the composition range between 15 and 52.5 pct Mo at about 800° to 1400°C. The four alloys listed in Table II were examined at 1200°C. Only one intermediate phase was found and this has, in accordance with Raub, a close-packed-hexagonal crystal structure, Table V, with a composition range from approximately 27 to over 50 atomic pct Mo.

Rh-W System—According to Raub and Walter,[20] the only intermediate phase in this system at 1600° to 1650°C has a close-packed-hexagonal crystal structure. An alloy containing 14.3 atomic pct W when annealed at 1000°C and quenched consists of the face-centered-cubic rhodium solid solution only; but with 17.2 atomic pct W at 1300°C, the face-centered-cubic solid solution coexists with a close-packed-hexagonal phase. Alloys containing 19.3 and 46.7 atomic pct W at 1600°C consist of the close-packed-hexagonal intermediate phase only and an alloy containing 56.6 atomic pct W at 1600°C has, in addition to the hexagonal compound, the body-centered-cubic tungsten-rich terminal solid solution. The three alloys listed in Table II were annealed at 1200°C, and they agree with the results of Raub and Walter. X-ray diffraction data for the close-packed-hexagonal phase are shown in Table V.

Pd-V System—Nothing was found in the literature concerning the equilibrium conditions in this system. The five alloys annealed at 1200°C are listed in Table II. It is probable that there is at least one intermediate phase of unknown structure, although the data obtained are not decisive. The solution of vanadium in palladium is approximately 50 atomic pct V, but the solution of palladium in vanadium is less than 20 atomic pct.

Pd-Cb System—Nothing was found in the literature concerning the phase relationships in this system. Difficulty was encountered in melting these alloys without excessive loss in weight of the charge. However, analysis results showed that the intended composition agrees within about 10 atomic pct with the true composition. The alloys, which were annealed at 1000°C, are tabulated in Table II. Only one intermediate phase was found. This has the σ structure, Table III, and exists over a very narrow range of composition at 60 atomic pct Cb.

Pd-Ta System—There was nothing in the literature concerning the equilibrium conditions in this system. The three alloys listed in Table II were annealed at 1000°C and these show that no intermediate phase exists at this temperature.

Pd-Cr System—Only one intermediate phase was reported[24] in this system, namely, Pd_3Cr_5, which has a face-centered-cubic structure with a parameter of $a = 3.838$Å. Only two alloys were annealed at 1200°C and these are listed in Table II. These neither confirm nor disallow the presence of the Pd_3Cr_5 phase, as the reported parameter of the latter is very similar to that of the face-centered-cubic palladium-rich solid solution. It is apparent, however, that no other intermediate phase exists at 1200°C, as the face-centered-cubic structure coexists with the body-centered-cubic chromium-rich solid solution.‡

‡ After the completion of this paper, the authors became aware of a recent publication by Raub and Mahler[28] which, in agreement with the foregoing conclusion, shows no Pd_3Cr_5 phase.

Pd-Mo System—Raub[12] reported no intermediate phase in this system in the temperature range of 800° to 1200°C. Two alloys were annealed at 1200°C, Table II, and these confirm that the face-centered-cubic and body-centered-cubic solid solutions exist together in equilibrium. The solid solution of palladium in molybdenum appears to be greater than 25 atomic pct Pd, although an alloy with 28 atomic pct Pd was reported by Raub[12] to consist of two phases.

Pd-W System—According to Raub and Walter,[20] an alloy containing 19.9 atomic pct W consists of the face-centered-cubic palladium-rich solid solution at 1100°C. An alloy containing 36.7 atomic pct W at 1000°C consists of the face-centered-cubic palladium-rich solid solution plus the body-centered-cubic tungsten-rich solid solution. In the

present work, one alloy, containing 37 atomic pct W, was annealed at 1200°C. It was found to consist of the face-centered-cubic and body-centered-cubic solid solutions, thus confirming the absence of intermediate phases at 1200°C.

Pt-V System—Nothing was found in the literature relating to this system. The four alloys listed in Table II were annealed at 1200°C. Only one intermediate phase was found, V_2Pt of the ordered β-tungsten type, Table IV. The solid solution of vanadium in platinum exceeds 40 atomic pct V. It appears probable that between V_2Pt and the platinum-rich solid solution another intermediate phase occurs, but this has not been definitely established.

Pt-Cb System—Wallbaum[29] examined this system for the presence of Laves phases, but found none. He apparently did not investigate for other phases. Seven alloys were annealed at 1000°C, and these are listed in Table II. Two intermediate phases were found. Cb_2Pt has the ordered β-tungsten structure, Table IV.* A second intermediate phase exists in this system over a range of less than 1 pct at about 62.5 atomic pct Cb. X-ray diffraction evidence, shown in Table III, indicates that this phase has the σ structure.

* After this paper was submitted for publication, the authors have become aware of a recent paper by Geller, Matthias, and Goldstein[47] in which the existence of this phase was already described.

Pt-Ta System—Nothing was found in the literature relating to this system. The seven alloys which were annealed at 1000°C are listed in Table II. The only intermediate phase found is σ, Table III, with limits between 65.8 and 69.5 atomic pct Ta at the platinum-rich end and between 81.5 and 83.5 atomic pct Ta at the tantalum-rich end.

Pt-Cr System—According to Gebhardt and Koster,[27] up to 50 pct Cr goes into solution in platinum at the solidus temperature. Compounds of unknown composition form below 1150°C. On the basis of a hardness survey, Nemilov[28] concluded that the compounds are the following: Cr_2Pt, PtCr, and $PtCr_2$. The three alloys listed in Table II were annealed at 1000°C. An intermediate phase, corresponding to Cr_2Pt, was found to have the ordered β-tungsten structure. Another intermediate phase, present at about 63 atomic pct Cr, has been tentatively identified, Table VII, as an $AuCu_3$-type ordered structure, derived from the face-centered-cubic platinum-rich solid solutions. Its unit cell dimension of $a_o = 3.775$A is in line with that for the face-centered-cubic phase, if the contraction of the platinum lattice by the addition of chromium in solid solution is taken into account. For platinum, the unit cell dimension is $a_o = 3.916$A, and for the face-centered-cubic alloy with 50 atomic pct Cr, $a_o = 3.802$A. The ordered phase apparently either coexists with Cr_2Pt at 1000°C or it forms on cooling to room temperature from the face-centered-cubic disordered solid solution that may coexist with Cr_2Pt at 1000°C.‡‡

‡‡ Raub and Mahler[48] published data concerning this system after the present paper was accepted for publication. They, too, found Cr_2Pt, with ordered β-tungsten structure, and an ordered face-centered-cubic solid solution in the composition range 23.3 to 60.5 atomic pct Cr.

Pt-Mo System—Nemilov[28] investigated alloys containing up to 42 pct Mo without exceeding the face-centered-cubic platinum-rich solid solution limit. Hultgren and Jaffee[30] found that at least 50 atomic pct Mo is soluble in platinum at 1000° and 800°C. Raub[10] recently found a close-packed-hexagonal intermediate phase at 1200°C. Four alloys were annealed at 1200°C, and these are listed in Table II. Only one intermediate phase was found at this temperature, which is close-packed-hexagonal, Table V, in agreement with Raub.

Pt-W System—Jaffee and Nielson[31] found no intermediate phases in this system. They report that platinum dissolves about 60 to 65 pct W, and tungsten dissolves approximately 4 to 6 pct Pt at 2460°C. Only one alloy was examined, containing 70 atomic pct W, annealed at 1200°C. It consisted of the body-centered-cubic and face-centered-cubic terminal solid solutions, in agreement with Jaffee and Nielson.

Discussion of Results

That the composition of the σ phases formed by the elements manganese, iron, cobalt, and nickel with vanadium and chromium may be correlated with the hybride $3d + 4s$ electron shell vacancy numbers taken from Pauling's theory[21] was noted earlier.[1, 10, 32] The σ alloys formed by molybdenum with iron and cobalt also conform fairly well with this scheme.[1] The alignment of ternary σ and μ phase fields with lines of constant electron vacancy numbers has been established in several systems.[8, 10] However, the recently discovered σ phase in the Mn-Mo system[33] occurs at approximately 40 atomic pct Mo, in contrast to the σ phases formed by manganese with chromium and vanadium where the mean chromium and vanadium content is in the neighborhood of 20 atomic pct. Thus, although the description based on electron vacancy numbers is quite self-consistent for the σ phases formed by first long period transition elements,[1] it was found to break down in the case of at least one σ phase with a second long period element. Examination of the data for σ phases investigated in the present work indicated that they, too, are not in quantitative agreement with predictions that might be made on the basis of assuming hybride $4d + 5s$ and $5d + 6s$ shell electron vacancy numbers for these elements in accordance with the $3d + 4s$ shell electron vacancy numbers for the corresponding first long period transition elements. Thus, the mean compositions of rhenium σ phases range from about 37 to 50 atomic pct of the other element. These compositions correspond much more closely to the manganese σ with molybdenum than to the manganese σ alloys with first long period elements.

Even if the electron vacancy numbers for the second and third long period transition elements are not the same as those of the corresponding first long period transition elements, it is worth considering whether or not a self-consistent scheme, based on a set of empirical *electron vacancy numbers* for the second and third long period transition elements, could be developed. That no such scheme may be quantitatively based on the assumption of a characteristic electron vacancy number for each element (independently of the choice of its partner for σ) is evident from the data, Table VIII. For instance, the σ phases formed by rhodium with columbium and tantalum have about the same composition, which would lead to the assignment of the same characteristic number for columbium and for tantalum; however, the σ phases formed by platinum with columbium and tantalum have distinctly different compositions. As a result, no set of characteristic numbers can be assigned so as to be self-consistent. As mentioned previously, a similar inconsistency is revealed by comparing the manganese, iron, and

cobalt σ phases formed with chromium and those formed with molybdenum.

Nevertheless, there are at least qualitative relations between the positions of the second and third long period transition elements in the periodic table and the corresponding σ compositions, which are analogous to those found in the first long period, Table VIII. For two pairs of σ phases—the pair formed by columbium with rhenium and platinum and the pair formed by tantalum with rhenium and platinum—the composition shifts in the same direction as in the case of the corresponding first long period σ phases (vanadium with manganese and nickel). The third such comparison that can be made on the basis of the present data does not indicate a shift: the composition of the σ phases formed by columbium with rhodium and palladium is approximately the same. (However, it may be noted that the composition of (Cb,Rh)σ given in Table VIII is not based on chemical analysis.) No data for other pairs of σ phases formed by two elements in the same (second or third) long period with the same third element are now available.

If the compositions of the chromium or molybdenum σ phases with rhenium in the third long period and with ruthenium in the second long period are compared, it is found that the shift is again in the right direction. Similarly, the composition of the tantalum σ phase with rhodium (second long period) falls between those of the tantalum phases with the third long period elements rhenium and platinum, as it should. A similar shift also appears in the case of the σ phases of columbium with rhenium, rhodium, and platinum. It may therefore be concluded that, at least qualitatively, the shift in σ phase compositions with the position of one component in the periodic table, investigated in some detail for the first long period σ phases,[1] is effective also for the second and third long period systems.

It is interesting to note in view of the present work that the face-centered-cubic metals nickel, palladium, platinum, and rhodium do form several σ phases with the vanadium group elements, Table VIII, but none with the chromium group elements.§

§ The present data obtained for one or two temperatures only are not, of course, really adequate to prove the absence of an intermediate phase in any binary system. However, the absence of a certain phase at 1000° or 1200°C indicates at least that, if at all present, the phase in question must have a rather limited temperature range of existence. The following comments should be interpreted with this limitation in mind.

On the other hand, the close-packed-hexagonal transition elements ruthenium and rhenium do form σ phases with the chromium group elements and at least ruthenium does not form σ phases with the vanadium group elements. Rhenium does form σ phases also with the vanadium group elements, but even here the σ forming tendency appears to be definitely weaker than in the corresponding alloys with the chromium group elements. Thus, (Re,Mo)σ and (Re,W)σ are 20 and 23 atomic pct wide, respectively, while (Re,Cb)σ and (Re,Ta)σ are much narrower (4 and 1 pct wide, respectively).

An Os-Mo intermediate phase was reported by Raub[12] to be isomorphous with Ru_3Mo_2, which is shown in the present work to be a σ phase. Presumably, therefore, Os_3Mo_2 is also a σ phase and, as such, fits into the foregoing pattern. Cobalt, which is in the same group of the periodic table as face-centered-cubic rhodium, nevertheless does form a σ phase with chromium; it is interesting that, in accordance with its alloying behavior, cobalt is close-packed-hexagonal at least at lower temperatures. The physical basis of the foregoing relationships is not clear, but it is likely to be connected with the electronic structure of the various atoms in their alloys.

In all σ phases previously known, except those formed by manganese with chromium and vanadium, the component with the larger electron vacancy number also has the larger atomic radius, Table VIII. For the (Cr,Mn)σ, this relationship is reversed; and in the case of (V,Mn)σ, the Goldschmidt atomic radii of the components are the same. (Cr,Re)σ and (Cr,Ru)σ, found in the present investigation, provide additional examples of σ phases with the reversed atomic size relationship. It may be significant that almost all known σ phases are formed by two elements from the same long

Table VIII. Composition of Binary σ Phases in Atomic Percentages at Temperatures Indicated

	First Long Period				Second Long Period				Third Long Period			
	Mn, 1.35Å*	Fe, 1.28Å*	Co, 1.25Å*	Ni, 1.24Å*	Te, 1.36Å*	Ru, 1.34Å*	Rh, 1.34Å*	Pd, 1.37Å*	Re, 1.37Å*	Os, 1.37Å*	Ir, 1.35Å*	Pt, 1.38Å*
V, 1.35Å*	1000°C 13.4 to 24.5 pct V	1000°C 33.5 to 56 pct V	1200°C 43.5 to 68.0 pct V	1200°C 54.5 to 71.0 pct V	†	1200°C None	1200°C None	1200°C None	1200°C None	†	†	1200°C None
Cb, 1.47Å*	†	1200°C None	1200°C None	1200°C None	†	1200°C None	1000°C 60 pct Cb‡	1000°C 60 pct Cb	1200°C 50 pct Cb	†	†	1000°C 62.5 pct Cb
Ta, 1.47Å*	†	1200°C None	1200°C None	1200°C None	†	1200°C None	1000°C 60 pct Ta‡	1000°C None	1200°C 41 pct Ta	†	†	1000°C 68 to 82 pct Ta
Cr, 1.28Å*	1000°C 16 to 24 pct Cr	600°C 43 to 49 pct Cr	1200°C 58 to 63 pct Cr	None	†	1200°C 66 pct Cr	1200°C None	1200°C None	1200°C 36.8 pct Cr	†	900° to 1300°C None	1000°C None
Mo, 1.40Å*	1125°C 40 pct Mo	1300°C 50 pct Mo	1300°C 60.5 pct Mo	None	†	1200°C 60 pct Mo‡	1200°C None	1200°C None	1200°C 33 to 52 pct Mo	1200°C 62.5 pct Mo	1200°C None	1200°C None
W, 1.41Å*	†	1400°C approximately 60 pct W	1400°C approximately 50 pct W	None	†	1200°C None	1200°C None	1200°C None	1200°C 37 to 58 pct W	#	1400° to 1600°C None	1200°C None

* Goldschmidt atomic radii.
† Occurrence of σ phase is unknown for this system.
‡ No chemical analysis is available for this composition.

Raub and Walter[28] reported an intermediate phase at 70.9 to 80.5 atomic pct W, which was not identified by them but which, from their data, may possibly be σ.

period or from long periods adjacent to each other. (Cr,Re)σ and the σ phases apparently formed by tungsten with iron and cobalt[7] are the only ones now known in which the two components are from long periods twice removed from each other. As mentioned earlier in this paper, on the basis of previously known data it was possible to ascribe this tendency to intolerance of the σ phase for partners with too great difference in atomic size. However, the following examples, resulting from the present investigation, indicate that this view is probably wrong, at least when the difference in the atomic radii is less than about 12.8 pct (σ phase with tungsten and cobalt). Palladium forms a σ phase with columbium (in the same long period) but not with tantalum, although the Goldschmidt atomic radii of columbium and tantalum are identical. Furthermore, palladium and rhenium do form σ phases with columbium, but not with vanadium, although vanadium has a Goldschmidt atomic radius much closer to the formers' than columbium does. Columbium and tantalum, both of which form σ phases with rhodium, have atomic radii approximately 9.7 pct larger than that element; while vanadium, in the same group of the periodic table, does not form a σ phase with rhodium although it has an atomic radius less than 1 pct larger than that of rhodium. That, on the other hand, near equality of the partners' size does not prevent the formation of the σ phase is shown by the (V,Mn)σ, mentioned previously, which has a rather wide composition and temperature range of stability. The present work provides an additional example where the difference of the atomic radii of the components is fairly small —about 2 pct in the case of the σ phase formed by rhenium with molybdenum.

A relationship with the location of the components in the periodic table, somewhat similar to that described for the σ phase, appears to hold also for the close-packed-hexagonal intermediate phases described in the present paper. It may be significant that rhodium, a face-centered-cubic metal immediately to the right in the periodic table from the close-packed-hexagonal transition elements, forms close-packed-hexagonal intermediate phases with the body-centered-cubic chromium group elements which are placed immediately to the left of the close-packed-hexagonal transition elements, but that it does not form such phases with the vanadium group transition elements one column further to the left of the chromium group.* The only close-packed-hexagonal intermediate phases known to be formed by transition elements of the nickel group (nickel and platinum) are also with an element in the chromium group (molybdenum).

* Additional close-packed-hexagonal intermediate phases, also conforming to this observation, were recently found by Raub and Mahler[16] in the Ir-Cr system (24.4 to 60 atomic pct Cr), by Raub[15] in the Ir-Mo system (33.5 to 57.3 atomic pct Mo) and by Raub and Walter[16] in the Ir-W system (25.4 to 51.2 atomic pct W).

It is interesting to note that a composition shift with varying location of a component in the periodic table, similar to that described previously for the σ phase, appears to occur also in the case of the close-packed-hexagonal intermediate phases. The composition range of the rhodium and iridium[15] phases with molybdenum is roughly 20 to 55 atomic pct Mo, while that of the Pt-Mo phase is about 50 to 65 atomic pct Mo. In view of the large size difference between chromium and tungsten, both forming close-packed-hexagonal phases with rhodium, atomic size does not appear to be critical in the selection of partners to form this phase.

A suggestion of the influence of electronic structure is also apparent in the formation of the α-manganese-type intermediate phases described in the present work. It may be significant that, apparently, the only element forming such phases with vanadium and chromium group elements is rhenium, which is in the same group of the periodic table as manganese itself. Judging by the composition of the σ phases formed by chromium with manganese (approximately 20 atomic pct Cr) and with rhenium (approximately 36.8 atomic pct Cr), it may be said that rhenium behaves in these alloys as if it had a lower $5d + 6s$ band electron vacancy number than the corresponding $3d + 4s$ electron vacancy number of manganese. If the α-manganese structure is assumed to correspond to an electron vacancy number characteristic of manganese, it would then be appropriate to find an intermediate phase of this structure in the alloys of rhenium with elements that are capable of raising the average number of electron vacancies in the alloy, i.e., with vanadium and chromium group transition elements.

The fact that vanadium and chromium themselves do not form α-manganese phases with rhenium, but columbium, tantalum, molybdenum, and tungsten do, may perhaps be rationalized on the basis that the Goldschmidt atomic radii of vanadium and chromium are too small. Since, in these structures, rhenium may be considered as if it were located to the right of manganese in the periodic table, it is of interest that the ternary χ phase,[14] which has an ordered α-manganese structure,[15] is formed by the elements iron (directly to the right of manganese in the periodic table) with chromium and molybdenum (both directly to the left of manganese). If the average electron vacancy number is calculated for the χ phase, using the representative composition of this phase and the electron vacancy numbers of the component elements, such as are used for similar purposes in connection with the σ phase, it is found that this electron vacancy number is practically identical with that attributed to manganese. Although the analogous relationships for the α-manganese phases formed by rhenium would be difficult to check accurately because of the wide composition range of these phases, the composition relationships described certainly suggest, at least qualitatively, that the occurrence of the α-manganese phase is strongly influenced by the electron vacancy conditions, in a way similar to that in the case of the σ phase.

CsCl-type ordering was observed to occur in the body-centered-cubic terminal solid solutions of vanadium and tantalum with ruthenium. Presumably, such ordering also takes place in the Cb-Ru alloys, although X-ray evidence is lacking because of the small difference in the scattering factor of these two metals. In the body-centered-cubic terminal solid solutions of the chromium group metals with ruthenium, no evidence of ordering was detected in the quenched alloys. Similarly, Tagaya, Nenno, and Nishiyama[17] found no CsCl-type ordering in the body-centered-cubic solid solutions in the Cr-Fe system, and Raub[15] did not report such ordering in the Mo-Os system.

It would appear that the relative attraction between the atoms of vanadium group elements and of iron group elements is greater than that between the atoms of chromium group elements and of iron

group elements. Thus, ordering may also be expected to occur in the alloys of iron and osmium with vanadium group elements. On the contrary, as already discussed, ruthenium is not known to form σ phases with the vanadium group elements, but σ phases do occur in the alloys of ruthenium with the chromium group elements and in the Mo-Os system.

The ordered β-tungsten structure, discussed previously, has been known to occur in the alloys of vanadium with cobalt and nickel.[36, 37] The phases with this structure, described in the present paper, are formed by the cobalt and nickel group elements rhodium and platinum with vanadium and chromium group elements. The β-tungsten phase recently reported by Raub[38] in the Ir-Mo system also falls in this category. (However, Raub also found a β-tungsten structure in the Os-Mo system, although the ruthenium and iron systems with molybdenum and chromium apparently do not have a similar phase.)

All phases of the β-tungsten structure appear to have a very narrow composition range at the stoichiometric composition of A_3B. In these ordered structures, the A atoms are arranged in *chains* (coordination number is 2) in the three mutually perpendicular directions of the cubic axes. The spacing of the A atoms in the chain corresponds to one-half of the edge length of the unit cell. Table IX gives a list of the known structures of this type, including those described in the present paper (marked with an asterisk) and those recently reported by Raub[38] and by Matthias, Gieballe, Geller, and Corenzwit.[39]

As seen in the table, in all such phases so far known, the A element is one from the titanium, vanadium, or chromium groups in the periodic table, while the B elements may be in the cobalt, nickel, copper, zinc, or germanium groups, including silicon from the second short period.§§ The highly selective choice of the A atom on the one hand and the rather wide range of electronic structures acceptable in the B atoms on the other hand is rather interesting. As seen in Table IX, there is a fairly consistent correlation between the Goldschmidt radius of the A atom and the $\frac{1}{4}$ a_o (which corresponds to one-half the distance of neighboring A atoms in the chains). In the various phases with β-tungsten structure, the atomic radius of the A atom in the chains is approximately 8 to 14 pct smaller than the accepted value[40] of the Goldschmidt atomic radius of the same element, as may be expected in view of the difference in the respective coordination numbers (2 vs 12). It appears then that the close-packed chains of A atoms essentially determine the unit cell dimensions of the structure. On the other hand, the radii of the B atoms may vary from approximately 10 pct smaller than that of the A atom (as in V_3Ni) to at least approximately 7.5 pct larger (Cr_3Pt).

These variations in the size of the B atoms appear to have only a minor effect on the lattice constant; the lack of selectivity in regard to electronic structure for the atoms in the B position is matched by a lack of selectivity in regard to their atomic size. The conditions described make the ordered β-tungsten-type phases a rather intriguing object of study. It would be interesting to study the nature of the binding forces in these structures. It has been recently reported[39] that at least some of the silicon and tin-containing structures of this type become superconductive at temperatures as high as 17° to 18°K.

§§ W_3O has not been included in the table, since its structure is not ordered.[41] Mo_3Zr was omitted because its existence is now in doubt.[42]

Table IX. Collected Data for (A_3B) Ordered β-Tungsten Phases

A_3B	Reference	a_o	r_A	r_B	$\frac{a_o}{4r_A}$
V_3Si	42	4.71	1.35	~1.33	0.87
V_3Ge	43	4.759	1.35	1.39	0.88
V_3Sn	47	4.94	1.35	~1.58	0.92
V_3Ni	37	4.70	1.35	1.24	0.87
V_3Co	36	4.675	1.35	1.25	0.86
V_3Rh	*	4.767	1.35	1.34	0.88
V_3Pt	*	4.805	1.35	1.38	0.89
Cr_3Si	44	4.555	1.28	~1.33	0.89
Cr_3Ge	45	4.616	1.28	1.39	0.90
Cr_3Ru	46	4.674	1.28	1.34	0.92
Cr_3Rh	*	4.656	1.28	1.34	0.91
Cr_3Ir	46	4.669	1.28	1.35	0.92
Cr_3Pt	*	4.709	1.28	1.38	0.92
Nb_3Sn	38	~5.3	1.47	~1.58	0.90
Nb_3Rh	*	5.115	1.47	1.38	0.87
Nb_3Os	47	5.121	1.47	1.37	0.87
Nb_3Ir	47	5.131	1.47	1.35	0.87
Nb_3Pt	47*	5.11	1.47	1.34	0.87
Ta_3Sn	38	~5.3	1.47	~1.58	0.90
Mo_3Si	45	4.890	1.40	~1.33	0.87
Mo_3Os	13	4.963	1.40	1.37	0.91
Mo_3Ir	13	4.96	1.40	1.35	0.92
Ti_3Pt	40	5.033	1.46	1.36	0.86
Ti_3Au	40	5.096	1.46	1.44	0.87
Ti_3Hg	41	5.189	1.46	1.55	0.87
Zr_3Hg	41	5.558	1.60	1.55	0.87

* Data are taken from this investigation.

Summary

Thirty binary systems of vanadium and chromium group transition elements with second and third long period transition elements were explored in regard to the intermediate phases formed. It was found that the phases predominating in these systems are σ, A_3B type with ordered β-tungsten structure, close-packed-hexagonal phases with small unit cell dimensions, and finally phases isomorphous with α-manganese. Correlations between the occurrence and the composition of the various phases with electronic structure and atomic size of the components have been discussed.

Acknowledgments

This work was supported by the Office of Ordnance Research, U. S. Army, Contract No. DA-11-022-ORD-1175. The authors are greatly indebted to E. Wise and to the International Nickel Co. for the grant of 1 oz quantities of the precious elements ruthenium, rhodium, palladium, and platinum. H. P. Croft and the Chase Brass and Copper Co. have kindly contributed 5 oz of rhenium, for which the authors are deeply grateful. Thanks are also due to M. Hansen and to H. Kessler, both formerly of Armour Research Foundation of Illinois Institute of Technology, for making available the design of the arc furnace and for advice in connection with its construction and use. One of the authors is pleased to acknowledge the stimulating discussions he has enjoyed with F. Laves.

Discussion of this paper, if any, will appear in JOURNAL OF METALS, November 1956, and in AIME Metals Branch *Transactions*, Vol. **206**, 1956.

References

[1] P. Greenfield and P. A. Beck: The Sigma Phase in Binary Alloys. *Trans.* AIME (1954) **200**, p. 253; JOURNAL OF METALS (February 1954).

[2] H. J. Goldschmidt: A Further High Temperature σ-Phase and a Note on σ-ζ Relations. *Research* (1951) **4**, p. 343.

[3] H. J. Goldschmidt: Private communication.
[4] D. K. Das, S. P. Rideout, and P. A. Beck: Intermediate Phases in the Mo-Fe-Co, Mo-Fe-Ni and Mo-Ni-Co Ternary Systems. *Trans.* AIME (1952) **194**, p. 1071; JOURNAL OF METALS (October 1952).
[5] H. J. Wallbaum: Ergebnisse der rontgenographischen Strukturuntersuchung von Legierungen der Zusammensetzung AB_2 der Eisenmetalle mit Titan, Zirkon, Niob und Tantal (I). *Ztsch. Kryst. Min. Petrogr.* (1941) **A103**, p. 391.
[6] H. Witte and H. J. Wallbaum: Thermische und rontgenographische Untersuchung im System Eisen-Titan. *Ztsch. für Metallkunde* (1938) **30**, p. 100.
[7] H. J. Wallbaum and H. Witte: Die Kristallstrukturen des $TiCo_2$. *Ztsch. für Metallkunde* (1939) **31**, p. 185.
[8] P. Duwez and J. L. Taylor: The Structure of Intermediate Phases in Alloys of Titanium with Iron, Cobalt and Nickel. *Trans.* AIME (1950) **188**, p. 1175; JOURNAL OF METALS (September 1950).
[9] A. R. Elsea, A. B. Westerman, and G. K. Manning: The Cobalt-chromium Binary System. *Trans.* AIME (1949) **180**, p. 579; METALS TECHNOLOGY (June 1948).
[10] S. Rideout, W. D. Manly, E. L. Kamen, B. S. Lement, and P. A. Beck: Intermediate Phases in Ternary Alloy Systems of Transition Elements. *Trans.* AIME (1951) **191**, p. 872; JOURNAL OF METALS (October 1951).
[11] K. Kuo: The Formation of η Carbides. *Acta Metallurgica* (1953) **1**, p. 301.
[12] K. Kuo: Ternary Laves and Sigma Phases of Transition Metals. *Acta Metallurgica* (1953) **1**, p. 720.
[13] E. Raub: Die Legierungen der Platinmetalle mit Molybdan. *Ztsch. für Metallkunde* (1954) **45**, p. 23.
[14] W. B. Pearson and J. W. Christian: The structure of the Sigma Phase in Vanadium-Nickel Alloys. *Acta Crystallographica* (1952) **5**, p. 157.
[15] G. Bergman and D. P. Shoemaker: The Space Group of the σ-FeCr Crystal Structure. *Journal of Chemical Physics* (1951) **19**, p. 515.
[16] G. Bergman and D. P. Shoemaker: The Determination of the Crystal Structure of the Sigma Phase in the Iron-Chromium and Iron Molybdenum Systems. *Acta Crystallographica* (1954) **7**, p. 857.
[17] G. Hagg and N. Schonberg: "β-Tungsten" as a Tungsten Oxide. *Acta Crystallographica* (1954) **7**, p. 351.
[18] J. S. Kasper: The Ordering of Atoms in the Chi-Phase of the Iron-Chromium-Molybdenum System. *Acta Metallurgica* (1954) **2**, p. 456.
[19] P. Duwez: Oral discussion of the constitution of transitional metal alloys. The Institute of Metals (March 1952); also, private communication.
[20] C. J. McHargue and H. W. Maynor: Notes on a Molybdenum-Rhenium Alloy. *Trans.* AIME (1953) **197**, p. 1382; JOURNAL OF METALS (October 1953).
[21] K. Becker and K. Moers: *Metallwirtschaft* (1930) **9**, p. 1063.
[22] D. S. Bloom: Sigma Phases in the Mo-Ru System. *Trans.* AIME (1955) **203**, p. 420; JOURNAL OF METALS (February 1955).
[23] E. Raub and P. Walter: Alloys of the Platinum-Group Metals with Tungsten. *Heraeus Festschrift* (1951) p. 124.
[24] *Gmelin's Handbuch der Anorganischen Chemie* (1951) **68A**, p. 594.
[25] E. Raub and W. Mahler: Die Palladium-Chrom Legierungen. *Ztsch. für Metallkunde* (1954) **45**, p. 648.
[26] H. J. Wallbaum: Zur Legierungschemie der Übergangsmetalle. *Naturwissenschaften* (1943) **31**, p. 91.
[27] E. Gebhardt and W. Koster: Beitrag uber den Aufbau des Systems Platin-Chrom. *Ztsch. für Metallkunde* (1940) **32**, p. 262.
[28] W. A. Nemilov: Uber die Legierungen des Platins mit Chrom. *Ztsch. für Anorg. Allgem. Chemie* (1934) **218**, p. 33.
[29] R. Hultgren and R. I. Jaffee: A Preliminary X-Ray Study of Binary Alloys of Platinum with Cobalt, Molybdenum and Tungsten. *Journal of Applied Physics* (1941) **12**, p. 501.
[30] R. I. Jaffee and H. P. Nielson: Platinum-Tungsten Alloys. *Trans.* AIME (1949) **180**, p. 603; METALS TECHNOLOGY (August 1948).
[31] L. Pauling: The Nature of the Interatomic Forces in Metals. *Physical Review* (1938) **54**, p. 899; G. V. Raynor: Summary report. *Progress in Metal Physics.* (1949) Ed. by Bruce Chalmers. **1**, p. 48. London. Butterworth Scientific Publications.
[32] A. H. Sully: The Sigma Phase in Binary Alloys of the Transition Elements. *Journal* Institute of Metals (1951-1952) **80**, p. 173.
[33] B. F. Decker, R. M. Waterstrat, and J. S. Kasper: Formation of Sigma Phase in the Mn-Mo System. *Trans.* AIME (1953) **197**, p. 1476; JOURNAL OF METALS (November 1953).
[34] J. G. McMullin, S. F. Reiter, and D. G. Eberling: Equilibrium Structures in Fe-Cr-Mo Alloys. *Trans.* ASM (1954) **46**, p. 799.
[35] M. Tagaya, S. Nenno, and Z. Nishiyama: On the Fe-Cr Superlattice. *Memoirs* Institute of Scientific and Industrial Research, Japan (1952) **9**, p. 76.
[36] P. Duwez: The Crystal Structure of V_3Co. *Trans.* AIME (1951) **191**, p. 564; JOURNAL OF METALS (July 1951).
[37] W. Rostoker and A. Yamamoto: A Survey of the Vanadium Binary Systems. *Trans.* ASM (1954) **46**, p. 1136.
[38] B. T. Matthias, T. H. Gieballe, S. Geller, and E. Corenzwit: Superconductivity of Nb_3Sn. *Physical Review* (1954) **95**, No. 6, p. 1435.
[39] W. Hume-Rothery and B. R. Coles: The Transition Metals and Their Alloys. *Advances in Physics* (1954) **3**, p. 149.
[40] P. Duwez and C. B. Jordan: The Crystal Structure of Ti_3Au and Ti_3Pt. *Acta Crystallographica* (1952) **5**, p. 213.
[41] P. Pietrokowsky: Cursory Investigation of Intermediate Phases in the Systems Ti-Zn, Ti-Hg, Zr-Zn, Zr-Cd, and Zr-Hg by X-Ray Powder Diffraction Methods. *Trans.* AIME (1954) **200**, p. 219; JOURNAL OF METALS (February 1954).
[42] H. J. Wallbaum: Uber das Vanadiumsilizid V_3Si. *Ztsch. für Metallkunde* (1939) **31**, p. 362.
[43] H. J. Wallbaum: Uber Intermetallische Germaniumverbindungen. *Naturwissenschaften* (1944) **32**, p. 76.
[44] B. Boren: Rontgenuntersuchung der Legierungen von Silicium mit Chrom, Mangan, Kobalt und Nickel. *Arkiv Kemi Min. Geol.* (1933) **11A**, No. 10.
[45] D. H. Templeton and C. H. Dauben: The Crystal Structure of Mo_3Si. *Acta Crystallographica* (1950) **3**, p. 261.
[46] E. Raub and W. Mahler: Die Legierungen des Chroms mit Platin, Iridium, Rhodium und Ruthenium. *Ztsch. für Metallkunde* (1955) **46**, p. 210.
[47] S. Geller, B. T. Matthias, and R. Goldstein: Some new Intermetallic Compounds with "β-Wolfram" Structure. *Journal* Amer. Chemical Soc. (1955) **77**, p. 210.

Influence of Holes and Electrons on the Solubility Of Lithium in Boron-Doped Silicon

A theoretical and experimental study has been made of those interactions between holes and electrons which influence the solubilities of donors and acceptors in semiconductors. The major portion of the work concerns the solubility of lithium in silicon doped to varying degrees with boron. This solubility increases with increasing boron content in a manner predicted by theory and exhibits the expected temperature dependence. A *qualitative* experiment in germanium is described which demonstrates, in accordance with theory, that doping with a donor decreases the solubility of another donor.

by Howard Reiss and C. S. Fuller

SEVERAL authors have discussed the possibility that holes and electrons behave like chemical entities and influence the solubilities of ionized impurities. Wagner was the first to invoke this concept in connection with his studies[1, 2] on nonstoichiometric oxides. He used it again in explaining the solubility of hydrogen in molten binary alloys.[3]

In a theoretical paper,[4] Reiss drew attention to the fact that solutions of impurities in semiconductors

H. REISS and C. S. FULLER are associated with Bell Telephone Laboratories Inc., Murray Hill, N. J.

Discussion of this paper, TP 4115E, may be sent, 2 copies, to AIME by May 1, 1956. Manuscript, Apr. 6, 1955. New York Meeting, February 1956.

like germanium and silicon constitute a far reaching analogy with aqueous solutions. The key to the analogy consists of permitting holes to play the part of hydrogen ions and electrons the part of hydroxyl ions. Under this system, ionizable donors must be regarded as bases and acceptors as acids. The semiconductor itself assumes the role of water, the thermal generation of hole-electron pairs being likened to the dissociation of water into hydrogen and hydroxyl ions. In the same paper, statistical-mechanical arguments were advanced to demonstrate that equilibria involving donors, acceptors, holes, and electrons could be treated quantitatively by the simple mass action approach, even when they involved heterogeneous stages.

In a recent paper, Kröger and Vink[5] considered theoretically the equilbria in oxides and sulphides involving not only electrons and holes but vacancies as well. Because of the low temperature to which the present experiments are limited, the authors have not found it necessary to introduce vacancies.

The authors performed a quantitative experimental study of some of the predictions regarding solubility which can be made by adopting the aqueous solution analogy. More specifically, they studied the solubility of lithium as a mobile donor in silicon under various conditions of acceptor (boron) doping and temperature. A preliminary report[6] of this work appeared recently as a letter in *Physical Review*. The balance of the present paper will be devoted to an elaboration of this letter and, besides developing the theory, newer more accurate and more extensive data will be given.

Mass Action Theory

Although the authors had a general theory in mind, they chose to illustrate it empirically with the system Li-B-Si. Consequently, it will be convenient to describe the various equilibria involved in terms of these substances. Mathematical expressions, however, will be cast in general notation, applicable to any singly ionized donor or acceptor.

Consider an equilibrium in which lithium is distributed between a molten Li-Si phase (in which the concentration of lithium may be quite high) and solid (single crystal) silicon in which the lithium represents a trace (not more than 10^{15} atoms per cu cm). Actually, the first phase need not be lithium in silicon but any phase in which the activity of lithium can be maintained constant. For the sake of generality, it will be referred to as the *lithium alloy* phase.

Imagine that the silicon crystal has been doped with boron and that the temperature is sufficiently low so that the boron (by virtue of its small diffusivity) is immobile and, therefore, not involved in any heterogeneous process. Under these conditions, the following set of equilibria arise

$$\begin{array}{l} \text{Li (alloy)} \rightleftarrows \text{Li (silicon)} \rightleftarrows \text{Li}^+ + e^- \\ \qquad\qquad\qquad\qquad\qquad\qquad\quad + \\ \text{B (silicon)} \rightleftarrows \text{B}^- + e^+ \\ \qquad\qquad\qquad\qquad\qquad\qquad\quad \Updownarrow \\ \qquad\qquad\qquad\qquad\qquad\qquad\quad e^+e^- \end{array} \qquad [1]$$

Here the symbol e^+ has been used to represent a hole and e^+e^- to denote a recombined hole-electron pair.

According to Eq. 1, the formation of the weakly dissociated e^+e^- exhausts the solution of electrons and shifts the set of lithium equilibria to the right. The solubility of lithium in silicon is therefore increased by the presence of boron. It should be noted that the efficiency of the process depends upon e^+e^- being weakly dissociated. At high temperatures when the semiconductor becomes intrinsic, this may not be the case and the solubility of lithium will then be less sensitive to the presence of boron. In terms of the aqueous solution analogue, Eq. 1 represents the neutralization of a base by an acid.

It is obvious that, if boron were replaced in Eq. 1 by an immobile donor, the solubility of lithium would be decreased. Analogously, the solubility of a mobile acceptor in equilibrium with an external phase would be increased by an immobile donor and decreased by an immobile acceptor. Likewise, the arguments can be readily extended to the case where both types of impurities are mobile.

Quantitative expressions for the dependence of solubility on doping are fairly easy to derive, especially when the law of mass action is applicable. It is shown in ref. 4 that the latter procedure ceases to be valid with the onset of degeneracy but that even so the solubility relations can still be derived by judicious application of Fermi-Dirac statistics. In this work, degenerate situations have been avoided explicitly so that the derivations may be based on the law of mass action.

Suppose that the constant activity of lithium in the lithium alloy phase is given by α and that the un-ionized lithium (donor) in silicon is sufficiently sparse so that its activity can be represented by its concentration, D. Then it follows

$$D = \gamma\alpha \qquad [2]$$

where γ is a constant which may depend on temperature but not on composition. For the homogeneous equilibrium corresponding to the ionization of the donor

$$(D^+)n/D = \Gamma \qquad [3]$$

may be written, where Γ is again independent of composition but depends exponentially on temperature with an activation energy equal to the ionization energy of lithium in silicon. Γ is roughly equal to the effective density of states in the conduction band (for a detailed discussion, see ref. 4). D^+ and n stand, respectively, for the concentrations of ionized lithium and conduction electrons.

Throughout the major portion of the considerations, D/D^+ will be a very small number (lithium is almost completely ionized) so that D^+ may be used as a convenient and accurate approximation to $D^+ + D$, the total amount of dissolved lithium. The same approximation may be applied to the acceptor ionization process, although, in what follows, a bit more caution may be required than in the donor case, especially for acceptor dopings in excess of 10^{19} cm^{-3}.

As is more or less customary in semiconductor physics, the equilibrium involving hole-electron pairs may be expressed by the relation

$$np = n_i^2 = C \qquad [4]$$

where C is a constant at a given temperature, p is the concentration of holes, and n_i is the concentration of electrons in an intrinsic sample.

The set of necessary equations is completed by the addition of the charge balance equation

$$D^+ + p = A^- + n \qquad [5]$$

where A^- is the concentration of acceptor ions, as-

sumed equal to the total concentration of acceptors which can be regarded as completely ionized in most cases of interest.

In order to determine the dependence of D^- upon A^-, the authors begin the manipulation of Eqs. 2 through 5 by inserting Eq. 2 into 3 to obtain

$$(D^-)n = \gamma\Gamma\alpha = K \qquad [6]$$

in which K by virtue of the defined constancy of α is a constant at any given temperature. Eqs. 6, 4, and 5, when properly combined, yield the following quadratic equation

$$(D^-)^2 - [KA^-/(K+n_i^2)]D^- - K^2/(K+n_i^2) = 0 . \qquad [7]$$

An interesting and useful quantity is the value of D^- achieved when A^- is 0 (i.e., in an undoped sample). If this quantity is called D_o^-, it follows from Eq. 7 that

$$(D_o^-)^2 = K^2/(K+n_i^2) . \qquad [8]$$

This equation can be solved for K

$$K = (D_o^-)^2/2 + [(D_o^-)^4/4 + n_i^2(D^-)^2]^{1/2} . \qquad [9]$$

Thus a knowledge of D_o^- and n_i^2 suffices to determine K.

After replacing K in Eq. 7 by its value in Eq. 9, the former equation can be solved for D^-

$$D^- = A^-/\{1 + [1 + (2n_i/D_o^-)^2]^{1/2}\} + [(A^-/\{1 + [1 + (2n_i/D_o^-)^2]^{1/2}\})^2 + (D_o^-)^2]^{1/2} . \qquad [10]$$

This last expression admits of some useful rule of thumb interpretations. These interpretations will be listed in order:

1—When A^- is sufficiently large so that $(D_o^-)^2$ may be neglected in comparison with $(A^-/[1 + [1 + (2n_i/D_o^-)^2]^{1/2}])^2$, Eq. 10 reduces to that of straight line with slope

$$(D^-/A^-) = 2/\{1 + [1 + (2n_i/D_o^-)^2]^{1/2}\} . \qquad [11]$$

Knowledge of this slope, together with knowledge of n_i, is equivalent to knowledge of D_o^-.

2—When the condition enunciated in the preceding paragraph has been realized, the temperature dependence of the solubility D^- enters only through the ratio $(n_i/D_o^-)^2$. If this ratio is very small, then

$$D^- \sim A^- \qquad [12]$$

and the solubility is independent of temperature.

3—Even when $(n_i/D_o^-)^2$ cannot be neglected, the solubility D^- can still exhibit eccentric dependence upon temperature, provided that the straight line portion of the D^- vs A^- curve is involved. Thus, D_o^- may be an increasing function of temperature so that an undoped semiconductor saturated with lithium, for example, at some high temperature, will precipitate its lithium at a lower temperature. On the other hand, if $(n_i/D_o^-)^2$ is also an increasing function of temperature (despite the fact that D_o^- itself increases with temperature) then, according to Eq. 11, D^- will increase with *decreasing* temperature. Under this condition, the *boron-doped* semiconductor saturated with lithium at a high temperature will not exhibit the precipitation phenomenon at a lower temperature, i.e., boron doping changes the sign of the temperature coefficient of solubility.

4—If A^- is large enough so that D_o^- in Eq. 10 is small compared to the term in A^-, the square root function can be developed so that it contains a term linear in A^- as well as one in $1/A^-$. Furthermore, if

$$(n_i/D_o^-)^2 \leq 1/3 \qquad [13]$$

the square root functions containing $(2n_i/D_o^-)^2$ can be developed to yield

$$1 + 2(n_i/D_o^-)^2 . \qquad [14]$$

The net result is a formula for D^-/A^-

$$D^-/A^- = 1 - (n_i^2/(D_o^-)^2) + [(D_o^-)^2 + n_i^2]/(A^-)^2 . \qquad [15]$$

This shows that, when n_i/D_o^- is small so that Eq. 12 holds, D^-/A^- can be either less or greater than unity, depending on whether the second or third term on the right of Eq. 15 has the larger absolute value.

5—The rules enunciated previously depend upon the condition that $A^-/(1 + [1 + (2n_i/D_o^-)^2]^{1/2})$ in Eq. 10 exceeds D_o^- by a sizable amount. On the other hand, as a rough measure of when this condition appears, the point at which the term in A^- just mentioned equals D_o^- only may be located.

Consider the case

$$(2n_i/D_o^-)^2 >> 1 . \qquad [16]$$

Then the term in A^- becomes $D_o^- A^-/2n_i$ and equals D_o^- provided that

$$A^- = 2n_i . \qquad [17]$$

Next, take the case

$$2n_i/D_o^- = 1 . \qquad [18]$$

Then the term in A becomes $A/2.4$, and this equals D_o^- when

$$A = 2.4\, D_o^- = 4.8\, n_i . \qquad [19]$$

Finally, for the case

$$2n_i/D_o^- << 1 \qquad [20]$$

the term in A is $A/2$ which equals D_o when

$$A^- = 2D_o^- . \qquad [21]$$

The entire situation may be summed up compactly by the statement that the straight line portion of the D^- vs A^- curve begins to appear whenever

$$A^- > 5(D_o^-, \text{or } n_i) \qquad [22]$$

D_o^- being used when $2n_i$ is less than D_o^-, n_i being used when $2n_i$ is greater than D_o^-, and either D_o^- or n_i being applicable when $2n_i$ and D_o^- are of the same order of magnitude.

Experimental

The experiments were performed on specimens cut from single crystal silicon, both undoped and doped with varying amounts of boron. The undoped material was p-type and ranged in resistivity between 15 and 18 ohm-cm. The doped silicon samples had resistivities in the ranges 2 to 4, 0.8 to 1.0, 0.4 to 0.5, 0.2 to 0.1, and 0.04 to 0.05 ohm-cm. Both the doped and undoped crystals were grown from the same raw silicon. All were grown without rotation to minimize the effects of heat treatment.[7] Tests at various temperatures showed that, although small heat effects were still present at some temperatures, the changes corresponded at most to 10^{14} Li per cm^3 and could be ignored in the calculations.

The specimens measured 1.0x0.4x0.03 cm and were carefully prepared by lapping the surface plane parallel on a Bond lapping device[8] employing No. 600 silicon carbide abrasive in water. For determination of resistivities, dimensions were measured to 0.001 mm. Approximately 0.002 mm was removed from all surfaces before each resistivity

measurement to insure absence of surface effects. Resistivities were determined by measuring the potential differences between two loaded (100 g) tungsten probes spaced 0.375 cm apart when a current of 0.00100 amp was passed longitudinally down the specimen. Measurements were taken at three locations on either face of each specimen and the average taken as the best value. Deviations from the average were less than 5 pct. Boron and lithium ion concentrations in the low concentration range were calculated from electron and hole mobilities determined by Prince.[9] At higher concentrations, the mobilities were taken from a curve based on Hall mobility measurements.[10] The effect on the results of errors in these mobilities is discussed subsequently. All measurements were made at 25±2°C.

The apparatus employed is shown in Fig. 1. Fig. 1a shows the Pyrex tube (with side arm) which serves to hold the lithium alloy bath. The specimen holder is shown in Fig. 1b and consists of a *U*-shaped quartz rod grooved to receive six specimens, one undoped and five boron-doped to provide resistivities in the ranges given previously. During equilibration the specimens in the holder are immersed in the alloy maintained at a fixed temperature (within ±1°C) by means of a surrounding steel block comprising the inner tube of a muffle furnace. Equilibration temperatures ranged between 250° and 500°C and the equilibration times between 4 and 100 hr. The latter were calculated to be well in excess of the times of saturation from the known diffusion constants of lithium in silicon.[11]

Two alloys systems were investigated. Both were prepared by adding lithium (99.9 pct) to pure tin (99.98 pct) to give concentrations of 0.18 wt pct Li and 0.61 wt pct Li.[12] The same two alloys were used throughout the entire temperature range. Two sets of specimens were used, one set for each alloy bath. After the final temperature runs, the weaker alloy analyzed 0.17 pct Li and showed no visible changes. The stronger alloy analyzed 0.57 pct Li at the end of the runs and showed visible darkening.

The procedure in a given run was as follows: The specimens were lapped and measured as described. After measurement, they were cleaned in concentrated HNO_3, rinsed in pure water, immersed in concentrated HF, rinsed in pure water, and dried at 100°C. They were loaded into the quartz holder which was in turn placed in the Pyrex tube, Fig. 1. The ground glass stopper with stop cock (silicone-greased) was put in place and the tube and contents pumped out with gentle warming to about 0.01 mm pressure. Dry helium gas was admitted to about one-half atmospheric pressure and the system repumped. This was repeated several times to remove air and water. The lithium alloy contained in the side arm was melted down around the specimens, and the tube and contents were inserted into the furnace tube at the run temperature. After equilibration, the tube was removed and quickly tipped so as to run the molten alloy back into the side arm. This operation required only about 2 to 3 sec so that no significant effect on the equilibration occurred. After cooling, the tube was opened, the holder removed, and immersed in warm HF until the residue of the alloy was dissolved away. The specimens were then lapped and measured as already described.

The lithium contents of the saturated specimens were determined by taking into account the fact that the impurity concentration did not correspond to the carrier concentration because of the high degree of compensation. This could be accomplished in a fairly straightforward, if tedious, manner by guessing at the lithium concentration. Then, because the boron concentration was known, the total impurity concentration could be estimated and a tentative mobility made available by reference to the data mentioned previously. With this tentative mobility and the estimated carrier concentration (also estimated by virtue of the guess concerning the lithium content), the resistivity could be computed and compared with the experimental value. If it did not agree, other guesses at the lithium content were made until the correct value of resistivity was obtained. This method assumes that the mobility depends upon ionized impurity concentration in the same way, independent of whether the carrier content is or is not equal to the impurity content.

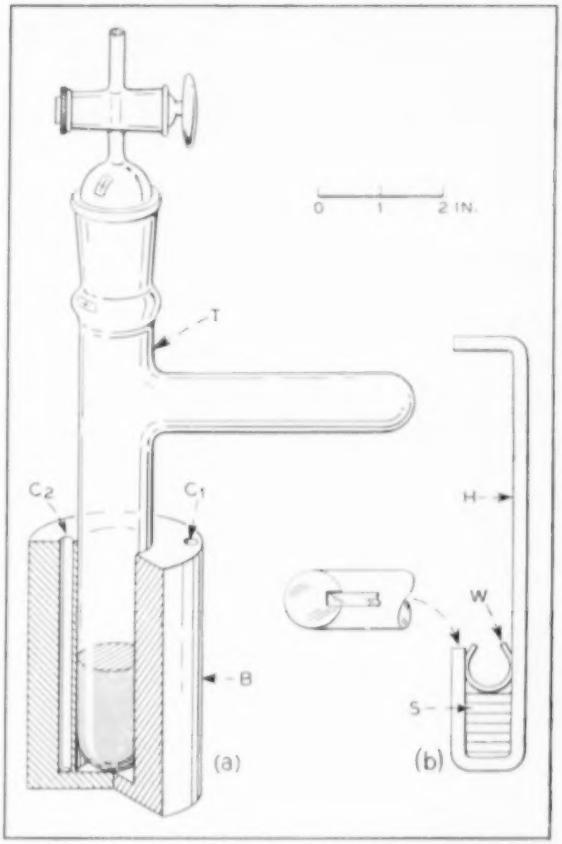

Fig. 1—Apparatus shown was used for determining the solubility of lithium in silicon, doped with varying amounts of boron. Section *a* shows the Pyrex tube which contained the Li-Sn alloy used and section *b* is a diagram of the specimen holder with its retaining spring and specimens in place. Letters on the diagrams indicate: *T*, Pyrex tube; C_1, hole in which a control couple was placed; C_2, hole in which a measuring couple was placed; *B*, metal cylinder with hole positions shown; *H*, cylinder holder; *W*, retaining spring; and *S*, the specimens.

Results and Discussion

Preliminary results, some of which have been reported,[8] have confirmed the theory outlined under "Mass Action Theory" in a semiquantitative way up to temperatures as high as 506°C and for boron dopings up to 5×10^{18} per cm.[3] These early results were, however, carried out with different techniques

Table I. Data Obtained on Boron-Doped Silicon Specimens Equilibrated in 0.18 Pct Li-Sn Alloy

0.18 pct Li-Sn Alloy	Initial Resistivity, Ohm-Cm, 25°C	Boron Content, A^-, Cm^{-3}	Final Resistivity*, Ohm-Cm, 25°C	Lithium Content Observed, D^+, Cm^{-3}	Ratio D^+/A^-	Lithium Content Calculated, Cm^{-3}
Temperature, 249°C	16.7	7.95×10^{14}	113.0*N*	8.50×10^{14}	1.07	7.96×10^{14}
$n_i = 6.16\times10^{14}$	2.44	6.00×10^{15}	5.79*P*	3.40×10^{15}	0.567	3.38×10^{15}
$D_0^+ = 5.27\times10^{15}$	0.718	2.24×10^{16}	1.74*P*	1.27×10^{16}	0.567	1.26×10^{16}
	0.432	3.93×10^{16}	1.03*P*	2.19×10^{16}	0.558	2.21×10^{16}
	0.114	1.95×10^{17}	0.290*P*	1.10×10^{17}	0.563	1.10×10^{17}
	0.0468	6.93×10^{17}	0.108*P*	3.49×10^{17}	0.503	3.91×10^{17}
Temperature, 280°C	16.3	8.20×10^{14}	15.4*N*	1.16×10^{15}	1.41	1.19×10^{15}
$n_i = 1.43\times10^{15}$	2.44	6.00×10^{15}	5.54*P*	3.33×10^{15}	0.555	3.22×10^{15}
$D_0^+ = 9.72\times10^{15}$	0.718	2.24×10^{16}	1.53*P*	1.15×10^{16}	0.513	1.10×10^{16}
	0.432	3.93×10^{16}	0.893*P*	1.93×10^{16}	0.491	1.91×10^{16}
	0.114	1.95×10^{17}	0.242*P*	9.40×10^{16}	0.482	9.49×10^{16}
	0.0468	6.93×10^{17}	0.0905*P*	2.89×10^{17}	0.417	3.36×10^{17}
Temperature, 310°C	16.3	8.20×10^{14}	5.53*N*	1.77×10^{15}	2.16	1.88×10^{15}
$n_i = 2.86\times10^{15}$	2.44	6.00×10^{15}	6.08*P*	3.52×10^{15}	0.587	3.46×10^{15}
$D_0^+ = 1.69\times10^{16}$	0.718	2.24×10^{16}	1.41*P*	1.06×10^{16}	0.473	1.02×10^{16}
	0.432	3.93×10^{16}	0.820*P*	1.77×10^{16}	0.450	1.73×10^{16}
	0.114	1.95×10^{17}	0.218*P*	8.40×10^{16}	0.430	8.59×10^{16}
	0.0468	6.93×10^{17}	0.0845*P*	2.67×10^{17}	0.385	3.05×10^{17}
Temperature, 339°C	16.3	8.20×10^{14}	2.64*N*	2.62×10^{15}	3.44	3.05×10^{15}
$n_i = 5.96\times10^{15}$	2.44	6.00×10^{15}	7.59*P*	4.00×10^{15}	0.666	4.25×10^{15}
$D_0^+ = 2.88\times10^{16}$	0.718	2.24×10^{16}	1.33*P*	0.96×10^{16}	0.428	0.991×10^{16}
	0.432	3.93×10^{16}	0.754*P*	1.53×10^{16}	0.389	1.55×10^{16}
	0.114	1.95×10^{17}	0.198*P*	7.40×10^{16}	0.379	7.42×10^{16}
	0.0468	6.93×10^{17}	0.0765*P*	2.34×10^{17}	0.338	2.64×10^{17}
Temperature, 374°C	16.3	8.20×10^{14}	1.45*N*	4.60×10^{15}	5.62	4.67×10^{15}
$n_i = 1.08\times10^{16}$	2.44	6.00×10^{15}	30.6*P*	5.50×10^{15}	0.917	5.69×10^{15}
$D_0^+ = 4.53\times10^{16}$	0.718	2.24×10^{16}	1.36*P*	1.02×10^{16}	0.455	0.98×10^{16}
	0.432	3.93×10^{16}	0.735*P*	1.53×10^{16}	0.389	1.39×10^{16}
	0.114	1.95×10^{17}	0.186*P*	6.70×10^{16}	0.344	6.70×10^{16}
	0.0468	6.93×10^{17}	0.0728*P*	2.10×10^{17}	0.303	2.38×10^{17}
Temperature, 404°C	16.3	8.20×10^{14}	0.901*N*	7.11×10^{15}	8.67	8.13×10^{15}
$n_i = 2.06\times10^{16}$	2.44	6.00×10^{15}	2.86*N*	8.10×10^{15}	1.35	8.12×10^{15}
$D_0^+ = 8.0\times10^{16}$	0.718	2.24×10^{16}	1.66*P*	1.23×10^{16}	0.548	1.24×10^{16}
	0.432	3.93×10^{16}	0.758*P*	1.60×10^{16}	0.407	1.65×10^{16}
	0.114	1.95×10^{17}	0.179*P*	6.30×10^{16}	0.323	6.34×10^{16}
	0.0468	6.93×10^{17}	0.0674*P*	1.77×10^{17}	0.255	2.22×10^{17}

* In this column, *N* and *P* indicate n-type and p-type, respectively.

and with silicon crystals which were known to be subject to rather large heat treatment changes. The errors inherent in this previous work have been largely overcome in the results reported here. These are summarized in Tables I and II, corresponding to the weaker and the stronger lithium alloy baths, respectively. Fig. 2 shows the corresponding plots for the weaker alloy from which some of the runs have been omitted for the sake of clarity. The open circles are experimental points, while the drawn curves have been computed from theory.

The data on impurity contents summarized in Tables I and II are based on a combination of resistivity measurements and the best mobility data that could be found. Since the absolute accuracy of this

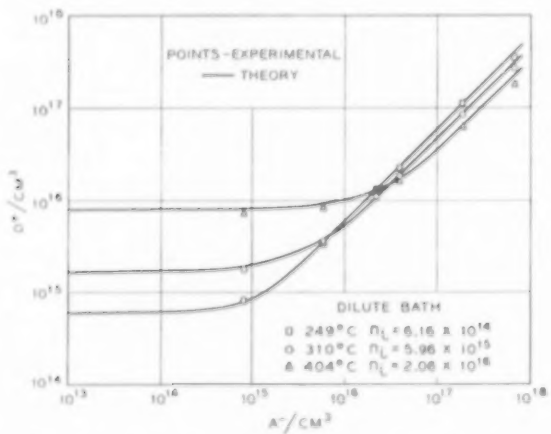

Fig. 2—Graph for the weaker lithium alloy shows the solubilities of lithium (ordinate) in silicon for three temperatures as a function of boron concentration (abscissa). The experimental results are compared with the theory.

mobility data may correspond to a range of ±20 pct (especially at high impurity levels), it is evident that the number of significant figures retained in columns 2 and 4 of the tables is not justifiable on any sort of an absolute basis. However, Eq. 11 demonstrates that for large acceptor dopings agreement of experiment with theory can only be tested through the ratio D^+/A^-. This, in turn, eliminates any strong dependence on the absolute value of mobility, since the impurity contents at which both D^+ and A^- are measured, being in the ratio of only 2:1, correspond to about the same mobility. If the mobilities were exactly the same, D^+/A^- would be obtained from a ratio of resistivities and mobility would not even be a factor. As it is, the slight *relative* difference in the two mobilities can be accurately gauged from the mobility data at hand independent of its absolute accuracy, so that for all practical purposes D^+/A^- is known as accurately as resistivity can be measured. This explains the retention of so many significant figures in Tables I and II.

In this connection, it is seen that the measurement D^+/A^- to the accuracy possible for resistivity measurements in the range where Eq. 11 applies amounts to a measurement of n_i/D_0^+ to the same accuracy by application of the theory.

Tables I and II are divided into six parts, one for each of the four temperatures mentioned previously. At the left of each part the temperature is listed together with the value of n_i corresponding to that temperature and taken from the data of Morin and Maita.[15] The value of D_0^+ computed from the measurements appearing in the tables is also listed. The first column gives the initial resistivities of the specimens and the second, the boron concentration computed from these. The third column lists the resistivities after saturation and the fourth, the

Table II. Data Obtained on Boron-Doped Silicon Specimens Equilibrated in 0.61 Pct Li-Sn Alloy

0.61 Pct Li-Sn Alloy	Initial Resistivity, Ohm-Cm, 25°C	Boron Content, A^-, Cm^{-3}	Final Resistivity,* Ohm-Cm, 25°C	Lithium Content Observed, D^+, Cm^{-3}	Ratio D^+/A^-	Lithium Content Calculated, Cm^{-3}
Temperature, 252°C	16.8	7.95x10^{15}	3.46N	2.32x10^{15}	2.92	1.30x10^{15}
n_i = 6.16x10^{13}	2.40	6.10x10^{15}	9.65P	5.94x10^{15}	0.974	4.81x10^{15}
D_{Li^+} = 9.50x10^{14}	0.718	2.25x10^{16}	7.73P	2.03x10^{16}	0.903	1.71x10^{16}
	0.463	3.65x10^{16}	1.99P	2.74x10^{16}	0.750	2.76x10^{16}
	0.112	1.98x10^{17}	0.620P	1.56x10^{17}	0.788	1.50x10^{17}
	0.0462	7.00x10^{17}	0.210P	5.14x10^{17}	0.735	5.30x10^{17}
Temperature, 280°C	16.8	7.95x10^{15}	2.84N	2.67x10^{15}	3.36	2.55x10^{15}
n_i = 1.43x10^{14}	2.40	6.10x10^{15}	31.7P	5.72x10^{15}	0.937	5.55x10^{15}
D_{Li^+} = 2.22x10^{15}	0.714	2.25x10^{16}	3.80P	1.79x10^{16}	0.794	1.74x10^{16}
	0.463	3.65x10^{16}	1.98P	2.74x10^{16}	0.751	2.76x10^{16}
	0.112	1.98x10^{17}	0.557P	1.52x10^{17}	0.767	1.51x10^{17}
	0.0462	7.00x10^{17}	0.185P	4.90x10^{17}	0.700	5.31x10^{17}
Temperature, 311°C	16.8	7.95x10^{15}	1.52N	4.39x10^{15}	5.52	4.29x10^{15}
n_i = 2.86x10^{14}	2.40	6.10x10^{15}	10.1N	6.70x10^{15}	1.10	6.66x10^{15}
D_{Li^+} = 3.98x10^{15}	0.714	2.25x10^{16}	3.38P	1.75x10^{16}	0.778	1.73x10^{16}
	0.463	3.65x10^{16}	1.82P	2.66x10^{16}	0.729	2.65x10^{16}
	0.112	1.98x10^{17}	0.458P	1.43x10^{17}	0.723	1.44x10^{17}
	0.0462	7.00x10^{17}	0.166P	4.68x10^{17}	0.678	5.09x10^{17}
Temperature, 339°C	16.8	7.95x10^{15}	0.907N	7.10x10^{15}	8.93	7.5x10^{15}
n_i = 5.96x10^{14}	2.40	6.10x10^{15}	2.22N	8.86x10^{15}	1.45	9.60x10^{15}
D_{Li^+} = 7.20x10^{15}	0.714	2.25x10^{16}	3.65P	1.77x10^{16}	0.786	1.82x10^{16}
	0.463	3.65x10^{16}	1.72P	2.60x10^{16}	0.712	2.69x10^{16}
	0.112	1.98x10^{17}	0.400P	1.35x10^{17}	0.682	1.35x10^{17}
	0.0462	7.00x10^{17}	0.143P	4.32x10^{17}	0.617	4.77x10^{17}
Temperature, 386°C	16.8	7.95x10^{15}	0.361N	1.86x10^{16}	23.4	1.52x10^{16}
n_i = 1.71x10^{15}	2.40	6.10x10^{15}	0.498N	1.90x10^{16}	3.18	1.69x10^{16}
D_{Li^+} = 1.50x10^{16}	0.714	2.25x10^{16}	67.0P	2.22x10^{16}	0.986	2.32x10^{16}
	0.463	3.65x10^{16}	2.83P	3.02x10^{16}	0.825	2.93x10^{16}
	0.112	1.98x10^{17}	0.326P	1.21x10^{17}	0.611	1.20x10^{17}
	0.0462	7.00x10^{17}	0.118P	3.79x10^{17}	0.541	4.16x10^{17}

* In this column, N and P indicate n-type and p-type, respectively.

lithium content obtained by combining the information in the second and third columns. The fifth column gives the ratios D^+/A^-, i.e., the ratios of the figures contained in the fourth to those in the second column. The constancy of these ratios for specimens of high boron content confirms the prediction embodied in Eq. 11. In fact, use of this constant ratio in Eq. 11 together with the appropriate value of n_i permits the calculation of D^+_{Li} which appears at the head of each part of the tables. With the knowledge of n and D^+_{Li} at each temperature D^+ can be calculated by the use of Eq. 10. This has been done, and the results appear in the sixth column of the tables.

The close agreement with the theory given under "Mass Action Theory" is gratifying, especially the results obtained with the more dilute lithium alloy (Table I and Fig. 2). The agreement for the more concentrated lithium alloy is not as good but quite satisfactory. The rather poor agreement for the 250°C data in the latter in particular appears to be partly attributable to the nearness to the liquidus and the possibility of some solid phases being present. The closeness of the experimental points to the theoretical predictions also supports the validity of the mobility data and the intrinsic carrier data.

Fig. 2 shows clearly the reversal in temperature dependence of solubility upon going to the high degrees of boron doping. Thus, the higher temperature curves cross over the lower temperature curves as the concentration of boron increases.

Finally, the figure demonstrates effectively the occurrence of the bend at each temperature at the range of boron concentration where the concentration of intrinsic electrons, n_i, approximates the acceptor concentration, A^-.

In this connection, the following experiment with germanium is interesting because lithium previously has been found to precipitate spontaneously from germanium at room temperature:[7] Two specimens of p-type germanium, one of 0.0030 ohm-cm (gallium-doped) and the other pure germanium of 45.0 ohm-cm resistivity at room temperature, were essentially saturated by heating in contact with pure lithium at 350°C for 71 hr. Table III shows the changes which occurred in the resistivities of these two specimens on standing at room temperature after quenching from 350°C.

It is seen that, in spite of the fact that the low resistivity specimen took up an estimated 5x10^{16} atoms Li per cm^3 as compared with only 1.5x10^{16} for the high resistivity specimen, the former shows no precipitation within the experimental error of measurement whereas in the latter over 90 pct Li has precipitated. This result illustrates in striking fashion the point made previously, that the presence of acceptor impurities is able to reverse the solubility-temperature relationship of mobile donor impurities.

Table III. Effect of Gallium Doping in Preventing Precipitation of Lithium in Germanium

Original Resistivity,* Ohm-Cm†	Resistivity* After Saturation, Ohm-Cm†	Resistivity* After Standing at Room Temperature†	
		4 Days	25 Days
45.0N	0.14N	0.24N	1.52N
0.0030P	0.0055P	0.0053P	0.0054P

* In the table, N and P indicate n-type and p-type, respectively.
† Resistivity measurements were made at 25°C.

It is clear from the presentation under "Mass Action Theory" that the mass action relations could have been developed in the same manner for equilibria involving a mobile acceptor in place of a mobile donor, such as has been employed in the present work. Likewise, it is clear that *permanent* donors in silicon, providing as they do an excess of electrons, would be expected on the basis of the

Technical Note

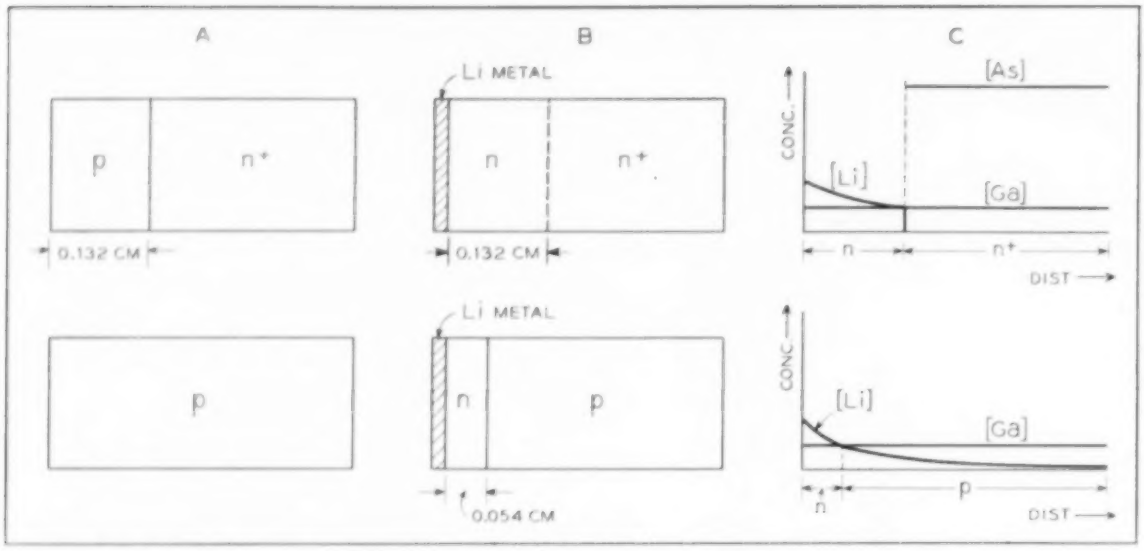

Fig. 3—Tests on two germanium specimens, one consisting of a high resistivity *p*-type section (0.2 ohm-cm by gallium-doping) grown adjacent to a low resistivity *n*-type section (0.003 by arsenic-doping), the other of the high resistivity *p*-type section alone, demonstrate the effect—predicted by the equations presented under "Mass Action Theory"—that *permanent* donors in silicon decrease the solubility of a mobile donor.

A—This section shows the initial distribution of impurities in two germanium crystals used in the same experiment. The level of *p*-doping with gallium is the same in both crystals. In the first crystal, the doping became n^+ at a depth of 0.132 cm due to the introduction of arsenic.

B—Diagram shows the condition of the crystals after the introduction of lithium by diffusion. In the first crystal, lithium at the *p*-doping level or greater has penetrated to the original p-n^+ junction leading to an n-n^+ distribution. In the second crystal, lithium at the *p*-doping level or greater has only penetrated to a depth of 0.054 cm, as is evidenced by the formation of a *p*-*n* junction. Low solubility in the n^+ section causes the *p*-region occupying the first 0.132 cm of the first crystal to fill up more rapidly than the same region of the second crystal.

C—This section is a schematic representation of the doping profiles in the diffused germanium crystals used in the experiment. The concentrations of all the impurities in the two crystals are illustrated.

arguments to decrease the solubility of a mobile donor.

The authors have been able to demonstrate this latter effect qualitatively in the following way: A germanium specimen in the form of a rectangular prism and consisting of a high resistivity p-type section (0.2 ohm-cm by gallium-doping) grown adjacent to a low resistivity *n*-type section (0.003 by arsenic-doping), was diffused unilaterally with lithium placed on the outer surface of the *p*-type section. A control specimen consisting of only the *p*-type section was diffused similarly. The time was 50 hr and the temperature 375°C in each case. Afterward, the two specimens were centrally sectioned parallel to the diffusion direction (i.e., parallel to the long axis of the specimens as well as to a broad surface) and tested for *p*-*n* junctions by means of a rectifying probe. The results are shown in Fig. 3 where the low resistivity *n*-section is labelled n^+. Fig. 3A shows the situation before the lithium diffusion, Fig. 3B after 50 hr. Fig. 3C indicates schematically the concentrations of all impurities in the two specimens. It is seen that, whereas the diffusion distance in the uniformly p-type specimen is only 0.054 cm, in the specimen containing the low resistivity *n*-type section it is 0.132 cm, which is the width of the entire *p*-type section in the original specimen. This result indicates that the n^+ layer acts as a barrier to the lithium ions because of their reduced solubility in this layer. This results in an increase in lithium concentration in the adjacent *p*-type section, thus converting it entirely to *n*-type.

In a previous publication,[8] the authors advanced an explanation of the peculiar trend of the solid solubility of pure metallic lithium in silicon[11] as a function of temperature. Further experimental work has shown that the higher temperature results are in error and therefore in disagreement with the theory as presented in this and in the previous publication. The authors are re-examining this problem at the present time and expect to publish shortly the corrected solubilities as well as a discussion of the present theory in regard to it.

Acknowledgments

The authors wish to thank A. J. Pietruszkiewicz, Jr. and J. A. Ditzenberger for assistance with the experiments and E. Buehler and R. Landgren for furnishing the silicon and germanium crystals.

Discussion of this paper, if any, will appear in JOURNAL OF METALS, November 1956, and in AIME Metals Branch *Transactions*, Vol. **206**, 1956.

References

[1] C. Wagner and K. Grünewald: *Ztsch. für Physikalische Chemie* (1938) **B40**, p. 455.
[2] C. Wagner: *Journal of Chemical Physics* (1950) **18**, p. 62.
[3] C. Wagner: *Journal of Chemical Physics* (1951) **19**, p. 626.
[4] H. Reiss: *Journal of Chemical Physics* (1953) **21**, p. 1209.
[5] F. A. Kröger and H. J. Vink: *Physica* (1954) **20**, p. 950.
[6] H. Reiss and C. S. Fuller: *Physical Review* (1955) **97**, p. 559.
[7] C. S. Fuller, J. A. Ditzenberger, N. B. Hannay, and E. Buehler: *Acta Metallurgica* (1955) No. 1, p. 97.
[8] *Quartz Crystals for Electrical Circuits*, (1946) R. A. Heising, Ed., Chap. IX, p. 290. New York: D. Van Nostrand & Co.
[9] M. B. Prince: *Physical Review* (1954) **93**, p. 1204.
[10] F. J. Morin and J. P. Maita: *Physical Review* (1954) **96**, p. 28.
[11] C. S. Fuller and J. A. Ditzenberger: *Physical Review* (1953) **91**, p. 193.
[12] M. Hansen: *Zwiestoffegierungen*, (1943) p. 856. Berlin: J. Springer.

Technical Note

Effect of Stress on the Martensitic Transformation in the Cu-Zn System

by E. J. Suoninen, R. M. Genevray, and M. B. Bever

THE martensitic transformation in the β-phase of the Cu-Zn system has been the subject of several investigations.[1-4] The transformation is known to be reversible and to be affected by stress. Its temperature range has been determined as a function of composition. In the investigation reported here, the effect of tensile stresses on the transformation was investigated quantitatively. Some information was also obtained on the thermoelastic behavior of the martensite formed in the first stages of the transformation.

Most of the experiments were done with alloy *E* of an earlier investigation;[4] this alloy analyzed 60.49 pct Cu and 39.51 pct Zn by weight. The methods of shaping and heat treatment were also essentially the same as those previously used. The stress was applied to the specimen immersed in a cooling liquid. The transformation was followed by measuring the electrical resistance with a Kelvin bridge and the elongation with a cathetometer.

Fig. 1 shows the M_s temperature as a function of stress. Resistance and strain measurements gave essentially identical values. The results suggest a roughly linear relation between M_s and σ in the range investigated, up to 12 kg mm^{-2}. At higher stresses, plastic deformation begins to interfere seriously with this relationship.

The increase of M_s with stress is consistent with published work on the effect of stress on the martensitic transformation.[5-8] The slope of the curve, 4°C per kg mm^{-2}, is of the same order of magnitude as the corresponding value calculated for steel.[7]

Fig. 1 also shows the difference, ΔM, between the temperature of 50 pct transformation on cooling, as measured by changes in length, and that of 50 pct reverse transformation on heating. This difference, which may be considered a measure of the hysteresis, increases with stress; the decrease at highest stresses is probably associated with plastic deformation.

Preliminary work using only resistance measurements was done with an alloy containing 60.15 pct Cu and 39.79 pct Zn by weight. The results indicated higher values of M_s in agreement with the known variation of M_s with composition.[4] The effect of stress on M_s (2°C per kg mm^{-2}) was of the same order of magnitude as that shown in Fig. 1 for composition *E*. An increase in hysteresis with stress was also found.

The following experiment was made in order to investigate a partially transformed structure. A specimen of alloy *E* was cooled to −85°C under a stress of 4.7 kg mm^{-2}. Under these conditions, the martensitic transformation started but did not go to completion. The stress was then released and the specimen cooled to −105°C. Fig. 2 shows the measured elongation ϵ. The first change in the slope of the curve indicates the beginning of the transformation under stress. Removing the load at −85°C caused a decrease in length to the value corresponding to the elastic elongation of the parent phase resulting from the applied stress. Hence, the martensite formed in the first part of the experiment apparently disappears completely and without hysteresis upon the release of the stress. The increase in length on further cooling indicates renewed formation of martensite. These conclusions are consistent with the concept of "thermoelastic" martensite,[9] which has been confirmed by test.[8]

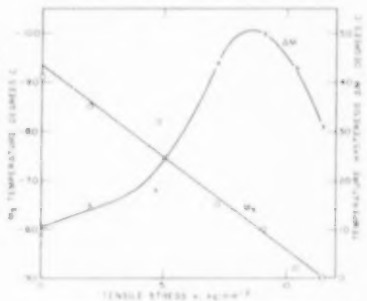

Fig. 1—The starting temperature M_s and the temperature hysteresis ΔM of the martensitic transformation are shown as functions of stress in an alloy containing 60.49 pct Cu and 39.51 pct Zn by weight.

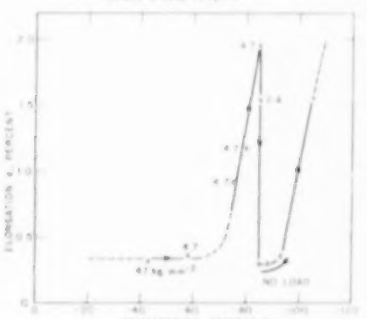

Fig. 2—The elongation of a specimen containing 60.49 pct Cu and 39.51 pct Zn by weight is shown as a function of temperature and stress in the region of incipient transformation.

E. J. SUONINEN is Graduate Student, Dept. of Metallurgy, Massachusetts Institute of Technology, R. M. GENEVRAY was formerly associated with Dept. of Metallurgy, Massachusetts Institute of Technology, and M. B. BEVER, Member AIME, is Associate Professor, Dept. of Metallurgy, Massachusetts Institute of Technology, Cambridge, Mass.

TN 298E. Manuscript, June 24, 1955.

This note is based on theses by E. J. Suoninen and R. M. Genevray submitted, in partial fulfillment of the requirements for the degree of Master of Science, to Massachusetts Institute of Technology.

Acknowledgments

The authors are greatly indebted to Professor M. Cohen for his advice and encouragement. They also thank F. Paxton for assistance. Thanks are due the American Brass Co. which supplied the alloys.

References

[1] E. Kaminsky and G. V. Kurdjumov: *Zhur. Tekhn. Fiziki SSSR* (1936) **6**, p. 984.

[2] A. B. Greninger and V. G. Mooradian: *Trans.* AIME (1938) **128**, p. 337.

[3] J. E. Reynolds, Jr. and M. B. Bever: *Trans.* AIME (1952) **194**, p. 1065; JOURNAL OF METALS (October 1952).

[4] A. L. Titchener and M. B. Bever: *Trans.* AIME (1954) **200**, p. 303; JOURNAL OF METALS (February 1954).

[5] S. A. Kulin, M. Cohen, and B. L. Averbach: *Trans.* AIME (1952) **194**, p. 661; JOURNAL OF METALS (June 1952).

[6] J. R. Patel and M. Cohen: *Acta Metallurgica* (1953) **1**, p. 531.

[7] C. Crussard: *Comptes Rendus* (1953) **237**, p. 1709.

[8] G. V. Kurdjumov: *Zhur. Tekhn. Fiziki SSSR* (1948) **18**, p. 999.

[9] G. V. Kurdjumov and L. G. Khandros: *Dokl. Akad. Nauk. SSSR* (1949) **66**, p. 211.

Preparation of Metallic Titanium by Film Boiling

The van Arkel-deBoer method for producing ductile titanium by thermal decomposition of TiI_4 vapor and deposition on an electrically heated filament is modified by film boiling TiI_4 liquid on a heated filament, resulting in similar titanium deposition on the filament and liberation of gaseous iodine. The deposition rate is higher and the energy requirement smaller than in the van Arkel process. Many problems must be solved before the process is commercially feasible.

by A. W. Petersen and L. A. Bromley

TITANIUM of 99.9 pct purity, called *ductile titanium*, has been produced by a modification of the van Arkel-deBoer[1] method. In the van Arkel-deBoer method, an electrically heated wire is suspended from two electrodes, which are placed in a container holding TiI, vapor at a low[2] vapor pressure (usually <5 mm Hg). The vapor diffuses to the hot wire, usually maintained at 1100° to 1600°C,[2] and decomposes according to the reaction

$$TiI_4 \rightarrow Ti + 4I$$

liberating gaseous atomic iodine and depositing solid crystalline titanium on the wire. Estimations,[2, 3] based on the data of Runnalls and Pidgeon,[3] indicate that the rate-controlling step is the diffusion of atomic iodine away from the wire. There appears to be nearly thermodynamic equilibrium at the wire with TiI, and iodine as the main gaseous species. TiI_4 is almost certainly an important gaseous species in the cooler regions.[4] The liberated iodine diffuses to a heated source of crude titanium and reacts to form more TiI, vapor, which again diffuses to the hot wire and completes the cyclic process.

The foregoing process may be modified by suspending the hot wire in liquid TiI_4, instead of the vapor, and obtaining film boiling. This type of boiling is characterized by the formation of a continuous film of vapor over the wire surface. Since only vapor contacts the wire surface, the temperature of this surface may be raised as high as desirable, within the limit of mechanical strength requirements for the wire. By properly adjusting the input voltage, the temperature of the wire may be maintained above 1100°C; and by evacuating the vessel holding the liquid TiI, and maintaining a suitable condenser temperature, the vapor pressure of TiI, may be held low. Thus, the conditions of operation of the van Arkel-deBoer method may be approximated with film boiling; and hence, it is postulated that ductile titanium may be produced by this method.

Preparation of TiI_4

There are many[5-17] methods available for the preparation of TiI_4; that used in this research was prepared by the direct reaction of titanium sponge in controlled amounts with liquid iodine. Although no difficulty was encountered with this reaction, it has since been pointed out that this method is sometimes dangerous and should be used with caution. The resulting TiI, was purified by distillation.

A. W. PETERSEN, formerly associated with Radiation Laboratory and Dept. of Chemistry & Chemical Engineering, University of California, is now in the U. S. Signal Corps, assigned to Signal Corps Engineering Laboratories, Ft. Monmouth, N. J., and L. A. BROMLEY is associated with Radiation Laboratory and Dept. of Chemistry & Chemical Engineering, University of California, Berkeley, Calif.

Discussion of this paper, TP 4095D, may be sent, 2 copies, to AIME by Jan. 1, 1956. Manuscript, July 12, 1954. Chicago Meeting, February 1955.

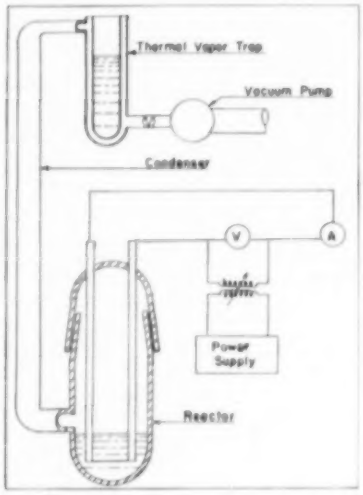

Fig. 1 — Diagram shows the first reactor built for preparation of titanium by film boiling.

First Film Boiling Experiments

Apparatus: The apparatus shown in Fig. 1 was used for film boiling TiI, on short wire filaments. The current to the filament was supplied through a bank of three 5 kva transformers connected in parallel. The current was controlled by adjusting the voltage over a 0 to 67.5 v range with a 7 kva variable transformer on the low voltage side of the bank of transformers. The current and voltage were measured by Weston meters. The sealed-in-glass tungsten electrodes were hard-soldered to the filament for the film boiling of TiI_4. The bottom part of the reactor, containing TiI_4, was wrapped with nichrome heating wires to maintain the TiI, in the liquid state. An ice or liquid nitrogen trap, for solidifying I_2 vapor and any TiI, not condensed, was attached to the low pressure side of the air-cooled condenser. A Megavac vacuum pump was used.

Procedure: A 0.010 in. diam tungsten filament was hard-soldered to the tungsten electrodes. TiI, was melted (mp 156°C) and poured into the reactor chamber; the top of the reactor chamber, containing the electrodes, was replaced. Freezing of the TiI, was prevented by controlling the current to the nichrome wires wrapped around the reactor with a 1 kva variable transformer. The mechanical vacuum pump was started and the system evacuated to about 2 mm Hg TiI, vapor pressure. The current to the filament was turned on and the impressed voltage slowly increased with the variable transformer. A sudden drop in current at nearly constant im-

pressed voltage indicated that film boiling had started, since, as the wire temperature rapidly increased, the resistance also increased, resulting in a current decrease. The variable transformer was then set so that the total resistance corresponded to a temperature in the range 1100° to 1600°C. The 0.010 in. diam filament usually fused after only about 30 sec of operation. The apparatus was then disassembled and the characteristics of the deposit were noted.

Results: The first metallic titanium prepared was deposited on a 0.010 in. diam tungsten wire 0.81 in. long between electrodes. The deposition rate was calculated from the diameter of the uniform deposit, 0.019 in., on the short large-diameter middle section of the wire and from the deposition time of 20 sec; this corresponds to an average deposition rate for titanium of about 9000 mg per cm³ per hr. This result is only qualitative, however, as the deposit was not uniform over the length of the wire.

The initial current was 9.5 amp and the total voltage drop was 2.0 v; this corresponds to a power input of 4 kw-hr per lb Ti. The current increased slightly as the run progressed, due to the increased cross-section and resulting decreased resistance.

Two breaks in the wire resulted during the experiment from handling the tungsten, which had become somewhat brittle from being heated.

The titanium sample was analyzed spectrographically for iron and tungsten and found to contain less than 0.1 pct of either.

Second Film Boiling Experiments

Apparatus: The apparatus shown in Fig. 2 was used for film boiling TiI, on long wire filaments. The current supply and electrical instruments were the same as for the apparatus for short wires, except that the variable transformer was on the high voltage side of the bank of three transformers. The current was conducted to the wire filament through teflon plugs on the ends of the reactor.

Nichrome heaters wrapped around the reactor were used to liquify the TiI, and to adjust the liquid temperature to any desired value at the beginning of a run. The liquid and vapor temperature was measured with a chromel-alumel thermocouple immersed in a wax-filled well and recorded continuously with a Speedomax recorder.

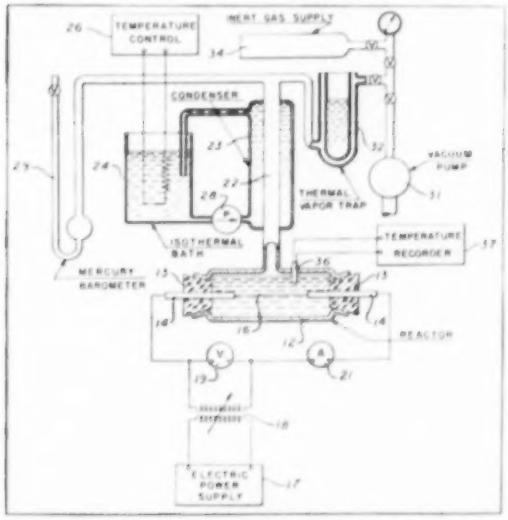

Fig. 2—Apparatus shown in Fig. 1 was modified for the second run of experiments. Equipment is used for the preparation of metallic titanium by film boiling.

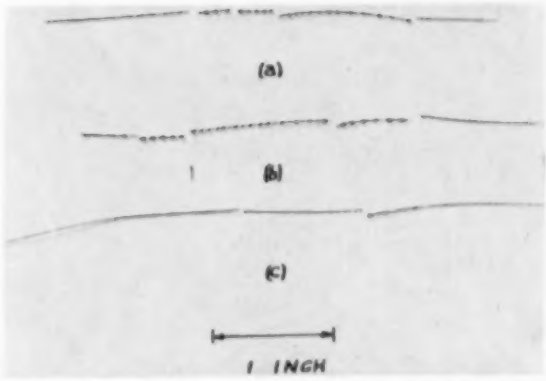

Fig. 3—Samples *a*, *b*, and *c* are titanium deposited on tungsten wires. One of the breaks in each wire resulted from fusion, while the other breaks were from handling.

The reactor was attached to the condenser by a ball joint, lubricated with high vacuum silicone grease. The condenser temperature was maintained ±2°C by circulating wax from a constant temperature bath. An ice trap for corrosive vapors was inserted between the condenser and the mechanical vacuum pump. A cylinder was attached near the ice trap for filling the system with inert gas when necessary.

Procedure: The wire filament was hard-soldered to the electrodes and this assembly was put into the reactor. TiI, was melted and siphoned into the reactor, filling it about ⅞ full. The reactor was attached to the condenser and the system slowly evacuated to the desired pressure as indicated by the mercury barometer; this pressure was maintained by carefully adjusting the stopcock to the vacuum pump. The ice trap was filled and wax was started cycling through the condenser. The current was turned on and the impressed voltage slowly increased in small increments. A sudden decrease in current at constant impressed voltage indicated film boiling had started. The current and total voltage were then set so that the wire resistance corresponded to a filament temperature in the range 1100° to 1600°C; this was estimated by a previous calibration using an optical pyrometer, with the filament in vacuo. A slightly increasing current at constant impressed voltage indicated that titanium was depositing. The run was continued until the wire fused; the apparatus was disassembled, and the characteristics of the deposit were noted.

Results: Film boiling was obtained on 0.010 in. diam and 5.75 in. long tungsten wires in the apparatus shown in Fig. 2. The titanium deposit, as shown in Figs. 3a, 3b, and 3c, was in globules; attempts to obtain a smooth deposit with a 0.010 in. diam wire were unsuccessful. The deposit appeared only on short sections of the wire. One break in each wire resulted from fusion, which necessarily terminated the experiment, the other breaks were from handling.

An attempt was made to obtain film boiling on a 0.020 in. Ti wire. Film boiling was momentarily attained. However, experiments on titanium wire were discontinued because of very sensitive control of the impressed voltage required to prevent the wire from fusing.

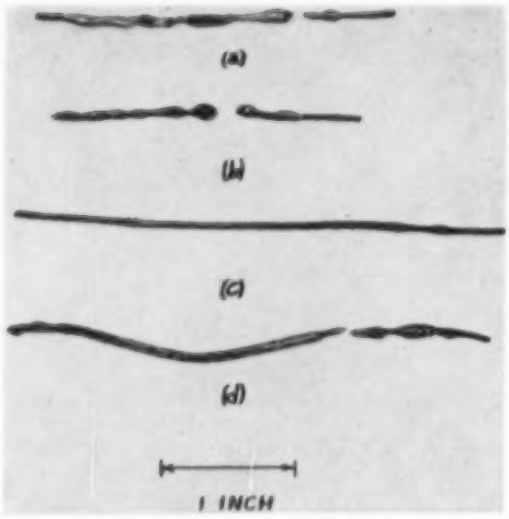

Fig. 4—Samples *a* through *d* are titanium deposited on tantalum wires. a—Part of the deposit was lumpy, indicating that the temperature of the filament had reached the melting point of titanium, 1690°C. b—The entire deposit was lumpy. c—The small crystalline deposit was obtained at a temperature below the melting point of titanium. d—By carefully controlling the impressed voltage in order to keep the wire temperature below the melting point of titanium, the uniform deposit was obtained.

Deposition was also obtained on 0.040 in. Ta wires 3 to 4 in. long. Deposits on tantalum wires are shown in Fig. 4.

Part of the deposit on the wire in Fig. 4a was lumpy, indicating that the temperature of the filament had reached the melting point of titanium—1690°C; this made the deposit sag on part of the wire. The cross-section of this deposit was somewhat elliptical, being 0.082 in. in vertical diameter and 0.074 in. in horizontal diameter; the deposit was porous and rough, indicating that it had not melted.

The deposit shown in Fig. 4b was entirely lumpy. The small crystalline deposit in Fig. 4c was obtained at a temperature below the melting point of titanium. This wire did not fuse because the hard solder connection became loose after a short time, necessarily terminating the run.

The uniform deposit in Fig. 4d was obtained by careful control of the impressed voltage to keep the wire temperature below the melting point of titanium. The deposit did not sag and formed almost concentrically around the wire to a diameter of 0.064 in. Near the end of the run, the impressed voltage was raised considerably, resulting in local overheating and fusion near one end of the wire, terminating the experiment.

Spectrographic analysis of some of the titanium which had melted (Fig. 4a) showed a gain of 15 pct Ta.

Results and Conclusions

Titanium metal has been prepared by film boiling TiI, from a hot wire.

The deposition rates calculated from the experimental data ranged from 1,600 to 12,000 mg per cm^2 per hr, but these calculated results are extremely uncertain due to experimental difficulties. The corresponding power consumption ranged from 2 to 19 kw-hr per lb of titanium and, although equally uncertain, indicated a power saving over the conventional van Arkel-deBoer process (40 to 60 kw-hr per lb).[11] However, it should be cautioned that there are many practical problems to be solved before the film boiling process could be made commercially feasible.

Discussion of this paper, if any, will appear in JOURNAL OF METALS, November 1956, and in AIME Metals Branch Transactions, Vol. **206**, 1956.

References

[1] A. E. Van Arkel and J. H. deBoer: U.S. Patent 1,671,213 (1928).
[2] O. J. C. Runnalls and L. M. Pidgeon: *Trans.* AIME (1952) **194**, pp. 843-847; JOURNAL OF METALS (August 1952).
[3] A. W. Petersen: Master's Thesis in Chemical Engineering, University of California (1954).
[4] J. D. Fast: *Recueil des travaux chimiques* (1939) **58**, pp. 174-180.
[5] J. D. Fast: *Ztsch. fur Anorg. Allgem. Chemie* (1925) **148**, p. 345.
[6] P. Hautefeuille: *Comptes Rendus* (1863) **57**, p. 151.
[7] H. Moissan: *Comptes Rendus* (1895) **120**, p. 290.
[8] L. Hoch and W. Z. Knauff: *Ztsch. für Anorg. Allgem. Chemie* (1936) **228**, pp. 204-208.
[9] P. Pascal: *Traite de Chimie Minerale.* (1932) **V**, p. 566. Paris, Masson et Cie.
[10] W. B. Blumenthal and H. Smith: *Industrial Engineering Chemistry* (1950) **42**, pp. 249-251.
[11] B. W. Gonser et al: *Report 523* Battelle Memorial Institute (March 1951).
[12] J. M. Blocher and I. E. Campbell: *Journal* Amer. Chemical Soc. (1947) **69**, pp. 2100-2101.
[13] J. M. Blocher and I. E. Campbell: *Journal* Amer. Chemical Soc. (1949) **71**, p. 4046.
[14] L. A. Bromley: *Chemical Engineering Progress* (1950) **46**, pp. 221-227.
[15] L. L. Quill: *Chemistry and Metallurgy of Miscellaneous Materials: Thermodynamics.* (1950).
[16] C. R. Wilke: *Industrial Engineering Chemistry* (1951) **43**, p. 1641.

Technical Note

Liquid Emulsion Autoradiography of Metals

by Jack C. Bokros and Philip C. Rosenthal

DEVELOPMENT of the autoradiographic method in metallurgical research has been directed mainly toward gaining higher resolution, i.e., toward being able to locate segregation of a radioactive isotope on a finer scale. In the investigation reported, the liquid emulsion autoradiographic technique[1] used in the biological science was adapted to the autoradiography of metals. The distribution of carbon-14 in pure iron after various treatments was studied using this technique.

Amorphous carbon uniformly labelled with carbon-14 at a specific activity of 6.95 microcuries per millimole was obtained from Tracerlab Inc. Carbon-14 emits β particles having a maximum energy of 157 kev and an average energy of about 50 kev. These βs have a maximum range of about 30 mg per cm^2 and a half-thickness of about 3 mg per cm^2.

The iron used was spectroscopically pure electrolytic iron prepared by the Oak Ridge National Laboratory.

Unhardened nuclear track emulsion, type NTB', was kindly supplied by the Eastman Kodak Co. This emulsion contains approximately 80 pct Ag halide,

J. C. BOKROS, Student Associate AIME, and P. C. ROSENTHAL, Member AIME, are Graduate Student and Professor of Metallurgical Engineering, respectively, University of Wisconsin, Madison, Wis.

TN 306E. Manuscript, May 16, 1955.

This paper is based on a portion of a thesis by J. C. Bokros submitted, in partial fulfillment of the requirements for the degree of Master of Science, to the University of Wisconsin.

Fig. 1 — Autoradiograph shows pearlite carburized at 927°C and furnace cooled. X100. Area reduced approximately 35 pct for reproduction.

has a grain size of 0.1 to 0.5 μ and is sensitive to β particles having energies up to 400 kev. This emulsion was kept fresh by storing in a refrigerator at from 2° to 7°C until the time of use.

Pure iron specimens were made of $\frac{1}{8}$ in. thick plate, $\frac{5}{8}$ in. sq., in which a shallow 5/16 in. hole was drilled in one face to contain the carburizing compound. The hole was sealed by bolting another *pure* iron plate over the top. The carburizing compound consisted of tagged amorphous carbon plus 18 pct $BaCO_3$ energizer. The capsule was loaded with 8 to 10 mg of carburizing compound. In order to get satisfactory carburization at each temperature, carburization was carried out for 91 hr at 838°, 22.7 hr at 927°, 3.5 hr at 1093°, and 2.0 hr at 1204°C. After carburization, the capsules were removed and quenched in water. Specimens which were carburized below the α-to-γ transformation temperature in pure iron and water quenched had microstructures consisting of a sharply defined layer of martensite on ferrite, while those carburized above the transformation and water quenched had microstructures consisting of a surface layer of martensite along with a poorly defined transition zone between the martensite and ferrite.

The capsules were unloaded, sectioned, and ground through No. 4/0 metallographic paper in a dry box. After final polishing, the surfaces were lightly etched with two pct nital.

For ease of correlation between the microstructure of a specimen containing a radioactive isotope and the autoradiograph, it was necessary to affix the photographic emulsion to the prepared surface of the specimen permanently in such a manner that the microstructure and the developed autoradiograph could be viewed simultaneously under the microscope. To avoid corrosion and staining of the metal specimen during the development, it was necessary to coat the surface of the specimen with a tough protective film. Towe, Gomberg, and Freeman[7] have developed such a plastic film for use in the *wet autoradiographic* process. The mounted specimens were dipped in a solution of two g Vinylite VYNS, (a 90:10 copolymer of vinyl chloride and vinyl acetate) dissolved in 100 ml of methyl ethyl ketone, which gave a plastic film on the metallographic specimen about 1μ thick. The specimen was heated at 100°C for about 30 min in an oven to remove all of the solvent.

The unhardened Eastman Kodak NTB2 Nuclear Track emulsion was melted by placing a small amount in a beaker and heating in a water bath at 38°C. The specimens were painted with the emulsion using a No. 7 camel's hair brush. The thickness of the emulsion was kept very thin (3 to 5μ) by controlling the amount of emulsion on the brush. After the coating was allowed to gel at room temperature, it was dried in a gentle dust-free air current. The specimens were then placed in a light-tight container along with a small beaker of $CaSO_4$—high humidities greatly impair sensitivity—and refrigerated at from 2° to 7°C for exposure.

After a ten day exposure period, the specimens were removed and developed. Because these emulsions disintegrate rapidly in aqueous solutions above 20°, the processing solutions were kept at 18°C. The autoradiographs were developed for 4 min in Eastman Kodak D-19 developer and fixed in Eastman Kodak F-5 acid fixer with hardener for twice the time to clear. The autoradiographs were dried in a gentle air current. At this point the emulsions wrinkled if they were too thick, resulting in the displacement of the image from the active areas by a small amount; however, when the emulsions were thin enough to clear in about 30 sec in the F-5 fixer, no wrinkling or shifting occurred.

An illustrative autoradiograph shown in Fig. 1 is of pearlite at X100. Fig. 2 is an autoradiograph of the martensite-ferrite interface obtained by carburizing below the transformation temperature.

The autoradiograph shown in Fig. 3 shows very high grain boundary activity produced in ferrite by annealing a carburized specimen for 138 hr at 538°C followed by a water quench. This iron specimen had been carburized at 838°C for 91 hr and water quenched before the 138 hr anneal. The grain boundary activity varied from boundary to boundary, indicating a possible orientation effect. This grain boundary activity is probably due to reduced solubility of carbon in ferrite at annealing temperature.

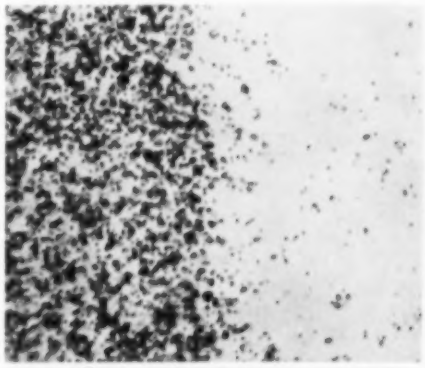

Fig. 2—Autoradiograph shows the martensite-ferrite interface. Specimen was carburized at 838°C and water quenched. X1000. Area reduced approximately 35 pct for reproduction.

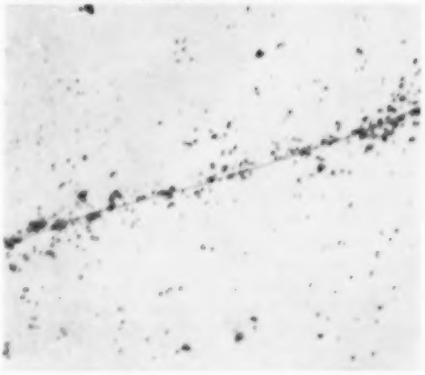

Fig. 3—Autoradiograph shows specimen carburized at 838°C, water quenched, and annealed at 538°C for 138 hr. X1000. Area reduced approximately 35 pct for reproduction.

Autoradiographs of martensite indicate a random distribution of carbon in austenite with no abnormal grain boundary effects. None of the autoradiographs of specimens carburized above the α-to-γ transformation temperature in pure iron gave any evidence of accelerated grain boundary diffusion of carbon in austenite.

Acknowledgments

The authors wish to express their appreciation for the helpful discussions with J. E. Willard, Professor of Radio-Chemistry at the University of Wisconsin, and Walter V. Green, Graduate Student at the University of Wisconsin, and for the Nuclear Track Emulsions kindly supplied by Eastman Kodak Co.

References

[1] J. S. Arnold: An Improved Technique for Liquid Emulsion Autoradiography. *Proceedings* Soc. for Experimental Biology and Medicine (1954) 85, pp. 113-116.

[2] G. C. Towe, H. J. Gomberg, and J. W. Freeman: High Resolution Autoradiography. *Technical Note 3209* NACA (July 1954).

Technical Note

Effect of Cooling Rate on Hardness of Commercial Titanium Alloys

by Howard Martens

HARDNESS behavior of commercial titanium alloys following various heat treating processes has been studied for some time. However, the hardness of such alloys following a definite measured cooling rate from the single phase β region has not been reported. Therefore, a series of experiments was conducted on the three alloys: 150A, 130A, and 130B. The manufacturers gave the following compositions for these alloys: Ti 150A: 0.045 pct C, 0.069 pct N, 1.32 pct Fe, and 2.68 pct Cr; RC 130A: 0.13 pct C, and 7.9 pct Mn; RC 130B: 0.11 pct C, 3.5 pct Mn, and 3.2 pct Al. A method similar to that described by Greninger[1] was used, and the cooling rate varied from 6° to 9200°F per sec. The cooling curves were recorded on a Speedomax or a recording oscillograph, and the hardness was measured on a Tukon hardness tester using a Knoop indentor with a 500 g load.

The curves of Fig. 1 show the variation of the Knoop hardness with the cooling rate for these three alloys. The alloys 150A and 130B behave in a similar manner, as shown by the curves. In neither of these alloys was it possible to retain the high temperature β phases, even by the most rapid cooling rate. The slow cooling rates produced a typical $\alpha+\beta$ structure in these two alloys. As the cooling was increased, these phases became more finely dispersed and the hardness increased. This increase in hardness with cooling rate continued for the 150A alloy until a rate of approximately 1000°F per sec was reached. At this cooling rate, the structure showed the result of the diffusionless transformation of the β solid solution to the supersaturated α solid solution which is referred to as α'. At higher cooling rates, the structure showed no change and the hardness showed no great change, as indicated by the dotted portion of the curve in Fig. 1. The increase in hardness with cooling rate for the 130B alloy continued until a rate of approximately 300°F per sec was reached. At this rate the α' structure was produced and the maximum hardness was reached. Higher cooling rates caused no marked changes in hardness or structure.

The alloy 130A behaved in a different manner, as shown by the curve of Fig. 1. The structure produced by the slow cooling rates was a typical $\alpha+\beta$ structure, which became finely dispersed as the cooling rate increased. The hardness increased with cooling rate and reached a maximum at approximately 120°F per sec. At this maximum hardness, the structure showed the result of the decomposition of the β phase into the $\beta+\omega$ phase structure. As the cooling rate was increased, smaller amounts of the ω phase were formed and the alloy became softer. For cooling rates of 3000°F per sec and above, the high temperature β phase was retained and the hardness of the alloy did not change markedly.

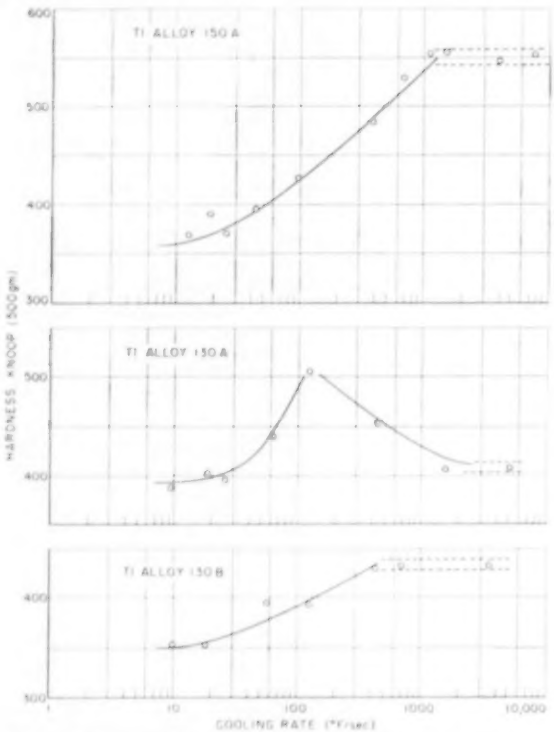

Fig. 1—Curves show the variation of Knoop hardness with cooling rates from 2000°F for alloys Ti 150A, RC 130A, and RC 130B.

Acknowledgment

This paper presents the results of one phase of research carried out at the Jet Propulsion Laboratory, California Institute of Technology, under Contract No. DA-04-495-Ord 18, sponsored by the Dept. of the Army, Ordnance Corps.

H. MARTENS is Research Engineer, Jet Propulsion Laboratory, California Institute of Technology, Pasadena, Calif.

TN 292E. Manuscript, June 27, 1955.

[1] A. B. Greninger: The Martensite Thermal Arrest in Iron-Carbon Alloys and Plain Carbon Steels. *Trans.* ASM (1942) 30, pp. 1-26.

AIME OFFICERS:
President—H. DeWitt Smith
Vice-Presidents—T. B. Counselman, W. A. Dean, Harold Decker, L. E. Elkins, A. B. Kinzel, W. W. Mein, Jr.
President-Elect—C. E. Reistle, Jr.
Treasurer—G. F. Moulton
Secretary—Ernest Kirkendall
AIME STAFF:
Secretary Emeritus—E. H. Robie
Ass't. Secretaries—J. B. Alford, H. N. Appleton, E. J. Kennedy, Jr.
Ass't. Treasurer—P. J. Apol
Field Secretary & Ass't. Secy—R. E. O'Brien, 707 Newhouse Bldg., Salt Lake City 1, Utah

aime NEWS

949 Attend Electric Furnace Steel Conference

New attendance records were set at the 13th Electric Furnace Steel Conference, held in Pittsburgh on Dec. 7, 8, and 9, 1955. The registration for the Conference totalled 949, a new high. Registration in 1954 was 882.

A feature of the conference was the plant trip to the Allegheny Ludlum Steel Corp. plant, Brackenridge, Pa., on Wednesday, December 7. Upon arrival at Brackenridge, Allegheny Ludlum provided lunch and as groups completed lunch, buses transported the visitors to the plant. Guides were provided for each group of 12. Visitors were escorted through the electric furnace and open hearth depts., and to the blooming and hot strip dept., hot sheet mill and sheet finishing depts., cold strip dept., and lamination dept. The Brackenridge plant occupies 100 acres and employees 5000 workers. It is one of the largest stainless steel producing plants in the world. A long-range expansion and modernization program was completed recently with the installation of a four-high, four-stand tandem cold rolling mill. Approximately 280 made the trip to Brackenridge.

The Annual Dinner on Thursday evening was attended by some 650, another record-breaker. At the dinner, C. F. Staley, Chairman of the Executive Committee, was presented a 400-day clock and a permanent certificate of registration by Conference Chairman C. E. Sims in appreciation of his service to the Electric Furnace Steel Committee. A. W. Thornton served as Toastmaster at the dinner, and introduced the speaker of the evening, E. J. Hanley, president of Allegheny Ludlum Steel Corp. His topic, *How Shall We Charge Tomorrow's Furnaces*, was a searching economic study of the problems facing steel companies financially in their expansion of facilities to meet ever increasing demands for steel.

A joint technical session on *Degasification* Thursday afternoon attracted many interested in the vacuum process practiced at Bochumer Verein in Germany. This paper was presented by Werner Coupette, chief of the research laboratory, Gusstahlwerke Bochumer Verein. Excellent motion pictures of the process was shown. A second paper on degasification was given at this session by Adam J. Texter of Firth Sterling Inc.

Better Utilization of Electrode Furnace Electrodes Through Shop Training Program was the topic at a joint session on electrodes, Thursday morning. Talks were given by representatives of National Carbon Co. and of Great Lakes Carbon Corp.

On Friday, simultaneous technical sessions were held in the morning and afternoon on ingot practices and on castings practices.

A dinner meeting of the Electric Furnace Steel Executive and Conference Committees was held at the William Penn Hotel on Wednesday evening of the Conference.

The Local Committee on Arrangements, for whom much credit for the success of the Conference is due, was headed by L. Roger Burke. Other committee members were C. E. Ahl, Jr., J. J. Golden, J. T. Richey, and R. B. Shaw.

Nuclear Metallurgy Vol. II Published

The six papers to be presented during the Annual Meeting at the Symposium on Nuclear Metallurgy, Monday, February 20, are being printed in book form. Purchase your copy at the Registration Desk, Hotel New Yorker, during the Annual Meeting. This is the second volume on *Nuclear Metallurgy*, published by the Institute of Metals Div.

Bessemer Centennial To Be Celebrated

In celebration of the 100 years of the Bessemer converter, a special Bessemer Centennial Luncheon will be held during the AIME Annual Meeting. This is scheduled for Thursday, February 23, at 12:15 pm in the North Ball Room of the Hotel New Yorker. It is planned to have a number of individuals long associated with Bessemer steelmaking attend this function and tell something of the "good old days." The luncheon will follow the Basic Bessemer Session, Iron and Steel Div. program.

To the Members of the American Institute of Mining and Metallurgical Engineers:

The regular Annual Business Meeting of the Institute will be held at 4:00 pm on the 21st day of February 1956 in the Ivy Suite of the Statler Hotel in New York City.

PLEASE TAKE NOTICE that a Special Meeting of the members of the AIME has been called for the 21st day of February 1956, to be held at the Statler Hotel in the City of New York at 4:45 pm for the purpose of considering and voting upon the following resolutions:

RESOLVED, that the name of this corporation shall be changed to AMERICAN INSTITUTE OF MINING, METALLURGICAL, AND PETROLEUM ENGINEERS, INC. and further

RESOLVED, that the second clause of Section 1 of Article I of the Certificate of Incorporation be amended to read:

"Its corporate name is AMERICAN INSTITUTE OF MINING, METALLURGICAL, AND PETROLEUM ENGINEERS, INC. and its abbreviated title is AIME." and further

RESOLVED, that the President and Secretary be and hereby are authorized and empowered to execute and file any and all documents and do all things necessary and proper to accomplish this change of name.

Dated: Dec. 21, 1955
New York, N. Y.

By Order of the Board,
Ernest Kirkendall, Secretary

AIME Elects 1956 President From Petroleum Branch

THE sixth President of the Institute to represent the petroleum membership is Carl E. Reistle, Jr., of Houston. A vice president and member of the board of directors of the Humble Oil & Refining Co., in charge of the production dept., he is a respected executive in the oil industry and a man of distinctive personal and professional achievements.

Born in Denver in 1901, he later moved with his parents to Oklahoma City. He became intrigued with chemistry through his father's photoengraving business, but the romance of the booming oil industry in Oklahoma held an irresistible attraction for him. Deciding to combine the two, he entered the University of Oklahoma in 1918 to study chemical engineering, and worked as a roustabout during summer vacations. Upon graduation in 1922, Reistle joined the Petroleum Div. of the U. S. Bureau of Mines and was soon sent to the Salt Creek Field in Wyoming to develop an easy way to determine the gravity of oil. This work brought his assignment to the Laramie Station of the USBM when it was established in 1924. He was keenly interested in a number of factors concerned with the production of oil, and later that year he and D. B. Dow conducted some of the first experiments on the solubility of gas in oil. A paper on the work published in *Mining & Metallurgy* interested the late Henry L. Doherty, pioneer in this field, and was a forerunner to work that followed on the problem.

With 1931 came the discovery of the great East Texas oil field, the nation's largest. The drilling of thousands of wells there, overproduction, and 10¢ oil brought chaos from which order had to be restored. By then Reistle's ability had become evident to the U. S. Bureau of Mines, and he was assigned to work on this job in 1932. He began by attempting to measure reservoir pressures in the field and organize them on a systematic basis. When the East Texas Engineering Assn. was formed by operators in the field in 1933 to further this work, Reistle was invited to become its first field chairman. The cooperative effort that followed, in which he played a leading part, led to the launching of a water injection program in the field in 1942. The end product will be a tremendous increase in the recovery of oil from this field.

The Humble Co. was one of the largest operators in the East Texas Field, and upon observing his work there, the company invited him to become engineer-in-charge of its Petroleum Engineering Div. in 1936. His subsequent rise in the company attests to his ability: to head of the Petroleum Engineering Div. in 1940, to manager of production in 1945, to director in 1948, and to vice president in 1955. His present responsibilities cover the wide range of activities involved in directing the production operations for the nation's largest domestic oil producing company.

Warm personality traits have made friends for him everywhere he has gone. His good humor and fun-loving nature are revealed in a story Mrs. Reistle tells about when she accompanied him as a young bride to Laramie in 1924. As it was her first trip west, snow fences were new to her, and curiosity getting the upper hand, she asked Carl why such fences were built. He blandly told her that because the country was so flat the cows didn't have much exercise and the fences were put up for the cows to get exercise in jumping over them. She doubtfully accepted this and had to find out the truth later for herself.

Carl Reistle has been active in AIME and professional work during his entire career. He attended his first AIME meeting in 1924, presented his first paper before the Petroleum Div. in 1927, and has since been one of the strongest advocates of the Institute. He is noted for clearing the way for engineers in his company to participate in AIME, and one of the largest contingents at the Petroleum Branch Fall Meeting each year is the Humble Co. group. Through 15 published technical papers and a variety of articles and speeches, he has been a continuing contributor to engineering literature. His creative mind has produced technical tools and processes for which he now holds seven patents.

Our friend is an avid hunter and fisherman. His eagerness here, combined with his personal habit of being early for appointments, got him into some difficulty recently when he and a companion went to the mouth of the Mississippi off Louisiana for the opening of the duck season. They shared double-decker bunks in a lodge, with Carl in the top one, and agreed to arise at 3:00 am. Upon awakening during the night, Carl read his watch to be this uncomfortable hour. He bounded off the top deck, shook his companion, and went into the bath. After hurrying through a quick shave, he went back to arouse the companion in the lower bunk. This person looked at his own watch and discovered the hour to be 12:30 am—Carl had mistaken the hands of his watch at 12:15 to read 3:00 am. Under a barrage of invective, our anxious nimrod climbed back into the top bunk to caress his fresh shave and sleep out the remaining hours.

Carl Reistle characterizes the modern corporate executive: intellectual acumen, calm temperament, sound judgment, and the ability to assimilate the complexity of big business. Yet, a corporation is more than assets and balance sheets to him—it is people. He is genuinely concerned with the welfare of the people all up and down the line in a company, and is intensely loyal to those who work for and with him. Blessed with a happy family of four children, he has a keen interest in young people, and has served as president of the Houston Branch of Junior Achievement. He is now on the national board of directors of that organization.

His concept of AIME is that it is the professional society for engineering in all of the mineral industries, and he believes that all engineers in these industries have common ties. He feels that members of the Board of Directors must be concerned with the welfare of all Branches and Divisions of the Institute. He believes that the Institute has a great opportunity for the future, which will be realized by all members and groups working together for common goals. His own contribution, as President in 1956, will form a distinct page in the continuing record of the Institute.—*Joe B. Alford*

CARL E. REISTLE, JR.

PRESIDENT OF AIME IN 1956

AIME Annual Meeting Program, Feb. 18 to 23, 1956

New Yorker and Statler Hotels, New York

Names of Divisions and Subdivisions are coded as follows: MIED—Mineral Industry Education Div. MED—Mineral Economics Div. M—Mining Subdiv. G—Geology Subdiv. Geophys.—Geophysics Subdiv. IndM—Industrial Minerals Div. Coal—Coal Div. MBD—Minerals Beneficiation Div. EMD—Extractive Metallurgy Div. IMD—Institute of Metals Div. ISD—Iron & Steel Div. Petroleum Branch—Named as such. SEG—Society of Economic Geologists.

SATURDAY, FEBRUARY 18

10 am
Council of Section Delegates
5:30 pm
National Membership Steering Committee

SUNDAY, FEBRUARY 19

9:30 am
National Membership Committee
11:00 am
Inter-Branch Council
12:30 pm
National Membership Committee Luncheon
2:00 pm
Registration
Board of Directors
MIED
IMD—Metallurgical Education
4:30 pm
IMD Program Committee
5:00 pm
MIED Fellowship Hour and Buffet Supper
6:00 pm
SEG Council
7:30 pm
MIED, IMD—Metallurgical Education Committee

MONDAY, FEBRUARY 20

8:00 am
Registration
8:45 am
Meeting of presiding officers and authors
9:30 am
Petroleum Branch Executive Committee
MIED—Training Engineers for Management
ISD—Sintering
EMD—Refractories
9:45 am
IMD—Research in Progress
IMD—Theory of Alloys; Constitution
10:00 am
MBD Business Meeting
Metals Branch Council
12:15 pm
Welcoming Luncheon
2:00 pm
JOURNAL OF METALS Editorial Advisory Committee
2:30 pm
Petroleum Branch—1955 Oil and Gas Developments
MBD—Concentration
MBD—Material Handling; Operating Control
EMD, ISD—Slags, Mattes, and Fused Salts
EMD—Zinc Smelting
IMD—Research Summaries; Phase Transformations
IMD—Symposium: Nuclear Metallurgy
3:30 pm
IMD Publications Committee
4:00 pm
Coal Div. Executive Committee
MGG Executive Committee
4:30 pm
IMD Membership Committee
6:00
Cocktail Party
8:00 pm
Dinner-Smoker

TUESDAY, FEBRUARY 21

7:30 am
EMD Executive Committee Breakfast Meeting
8:00 am
MBD Scotch Breakfast
8:15 am
Meeting of presiding officers and authors
9:00 am
MED—Business Outlook; Trends
Petroleum Branch—Technical Session
EMD—Lead, Zinc, Cadmium
EMD—Physical Chemistry of Roasting
ISD—Oxygen Steelmaking
IMD—Symposium on Semiconductors
IMD—Research Summaries; Diffusion and Internal Friction
9:30 am
MBD—Concentration
MBD, IndM—Air Separation of Nonmetallic Ores
10:00 am
Mining Branch Council
10:45 am
ISD Business Meeting
11:00 am
Howe Memorial Lecture
12:15 pm
MGGD Luncheon
Coal Div. Luncheon
IMD Executive Committee Luncheon
Committee on Physical Chemistry of Steelmaking Luncheon
2:00 pm
MIED Business Meeting
Petroleum Branch—Technical Session
MED—Strategic Minerals Session
MBD—Hydrometallurgy—Solution and Precipitation
MBD—Mill Design
EMD—Lead Smelting
EMD—Fused Salt Systems
ISD—Mechanical Working
IMD—Flow and Fracture at Various Temperatures
IMD—Symposium on Semiconductors
3:00 pm
Executive Committee, IndM
4:00 pm
Annual Institute Business Meeting
4:45 pm
Special Institute Business Meeting
5:00 pm
Directors' Meeting, Executive
6:00 pm
Metals, Mining, and Petroleum Branch Social Hours
7:00 pm
Metals, Mining, and Petroleum Branch Dinners
9:00 pm
Informal Dance

WEDNESDAY, FEBRUARY 22

7:30
ISD Executive Committee Breakfast Meeting
EMD Committee Chairmen Breakfast Meeting
8:15
Meeting of presiding officers and authors
9:00 am
MED—Canadian-U.S. Economic Trends
Petroleum Branch—Technical Session
MBD—Concentration
MBD—Crushing and Grinding
Council of Section Delegates
ISD—Physical Chemistry
EMD—Symposium on Titanium
EMD—Pyrometallurgy
ISD, IMD—Hydrogen Embrittlement
Woman's Auxiliary Annual Meeting
10:45 am
IMD Annual Business Meeting
11:00 am
IMD Lecture
12:15 pm
Mineral Economics Div. Luncheon
Mining and Metallurgical Society of America Luncheon
IndM Luncheon
EMD Luncheon
IMD Titanium Committee Luncheon
2:00 pm
MBD—Starting a New Mill
MED—General Session
EMD—Extractive Metallurgy of Uranium
EMD—Copper Converting and Refining
IMD—Deformation and Recrystallization
IMD, ISD—Hydrogen in Steel
IMD—Nuclear Metallurgy Committee
Woman's Auxiliary Annual Meeting
3:00 pm
Committee on Physical Chemistry of Extractive Metallurgy
AIME Nominating Committee
7:00 pm
Annual Banquet and President's Reception

THURSDAY, FEBRUARY 23

8:15 am
Meeting of presiding officers and authors
9:00 am
MBD—Solids-Fluids Separation, Pyrolysis
MBD—Crushing and Grinding
EMD—New Methods in Hydrometallurgy
EMD—Fused Salt Electrolysis
IMD—Powder Metallurgy
IMD—Research in Progress
ISD—Basic Bessemer
Geophys—Geochemistry
12:15 pm
MBD Luncheon
IMD Powder Metallurgy Luncheon
Bessemer Centennial Luncheon
2:00 pm
MBD—Richards Award
ISD—Physical Chemistry
EMD—Physical Chemistry of Hydrometallurgy
IMD—Equilibrium Diagrams and Microstructures
IMD—Powder Metallurgy
3:00 pm
MBD—Cleanup Session

Regional Reactive Metals Conference

Hotel Statler, Buffalo, N. Y.—March 19, 20, 21, 1956
AIME—Niagara Frontier Section

REACTIVE metals—those metals, such as titanium, zirconium, columbium, rhenium, tantalum, beryllium, uranium, and thorium, that are either rare or difficult to process by conventional means—will be discussed at a Regional Conference of AIME, sponsored by the Niagara Frontier Section. The three day meeting will be held at Hotel Statler, Buffalo, Mar. 19, 20, and 21, 1956.

On Monday and Tuesday, March 19 and 20, technical sessions will be held on the extraction, melting, fabrication, applications, and research on this important family of new metals. Papers scheduled will be authored by leading authorities. Monday evening will be devoted to a panel discussion on "Reactive Metals in Atomic Energy." Tuesday evening will feature a banquet. Willy Ley, well known rocket expert, will be the principal speaker. On Wednesday, plant visitations will be made.

Exhibits by leading manufacturers in the field can be viewed at the Statler.

Registration

Registration fee to attend the Conference is $5.00 for AIME members; $7.00 for nonmembers. Advance registration can be made by writing to D. L. Clark, Regional Reactive Metals Conference AIME, 155 Franklin St., Buffalo 2, N. Y.

Hotel reservations should be made directly with Hotel Statler or other Buffalo hotels.

MONDAY, MARCH 19

9:00 am

Melting, Fabrication, and Applications

Welcoming Address: D. C. Hilty, General Chairman and David Swan, Section Chairman

Arc Melting of Reactive Metals: J. L. Ham and C. B. Sibley, National Research Corp.

The Potential Merits of Titanium and Titanium Alloys Produced by the Oxide Reduction Process: H. A. Timm, Dominion Magnesium, Ltd.

Preliminary Data on the Properties of Sodium Reduced Titanium: C. M. Brown, R. L. Folkman, and M. Schussler, Electro Metallurgical Co.

2:00 pm

Fabrication and Application

Processing of Titanium into Wrought Form: L. S. Busch, Mallory-Sharon Titanium Corp.

Production Forming of Titanium: A. E. Leach, Bell Aircraft Corp.

Columbium, Beryllium, Titanium, Zirconium, and Molybdenum in Reactor Development: W. D. Manly, Oak Ridge National Laboratory.

Non-Defense Applications for Titanium: L. J. Barron, Pigment Div., E. I. du Pont de Nemours & Co., Inc.

2:00 pm

Research

Zone Purification of Reactive Metals: R. L. Smith and J. Rutherford, Franklin Institute

Observation on the Mechanical Properties of Hydrogenated Vanadium: B. Roberts and H. Rogers, General Electric Research Laboratories

Oxidation and High-Temperature Properties of Columbium: H. Inouye, Oak Ridge National Laboratory

Recrystallization and Grain Growth of Iodide Zirconium: R. M. Treco, Bridgeport Brass Co.

8:00 pm

Panel Discussion: Reactive Metals in Atomic Energy

Moderator: John Chipman, Massachusetts Institute of Technology

Panelists:

Frank Foote, Argonne National Laboratory
A. R. Kaufman, Nuclear Metals, Inc.
Benjamin Lustman, Westinghouse Electric Corp.
Harley A. Wilhelm, Iowa State College

TUESDAY, MARCH 20

9:00 am

General Metallurgy of Reactive Metals

Reactive Metals in Canada: W. K. Buck, Bureau of Mines, Ottawa, Canada

The Properties and Applications of Rhenium: C. T. Sims, Battelle Memorial Institute

Some Salient Properties of Zirconium: R. Hilkert, Titanium Alloy Mfg. Div., National Lead Co.

Vanadium Metallurgy: W. Rostoker, Armour Research Foundation

2:00 pm

Fabrication and Application

Powder Metallurgy of Titanium and Zirconium: H. H. Hausner, Nuclear Engineering Div., Penn-Texas Corp.

Extraction, Chemistry, and Applications of Tantalum in the Chemical Industry: C. A. Hampel, Fansteel Metallurgical Corp.

Metallurgical Characteristics of Tantalum and Their Relationship to the Fabrication of Tantalum Products: R. W. Yancey, Fansteel Metallurgical Corp.

The Extrusion of Zirconium: P. Loewenstein, Nuclear Metals, Inc.

2:00 pm

Research

Tensile Properties of Titanium as a Function of Annealing Temperature and Testing Temperature: J. H. Keeler and R. W. Guard, General Electric Research Laboratory

The Influence of Small Iron Additions on the Behavior of Titanium: C. R. McKinsey and R. C. Martin, Electro Metallurgical Co.

Heat-Treatment and Mechanical Properties of Ti-Mo Alloys: F. C. Holden, H. R. Ogden, and R. I. Jaffee, Battelle Memorial Institute

An Evaluation of the Structural Stability of Ti-Mo-V Alloys: W. F. Carew, F. A. Crossley, and H. D. Kessler, Armour Research Foundation

WEDNESDAY, MARCH 21

Plant Visitations

Plant trips will be featured on Wednesday. In the morning, the Metals Research Laboratories of Electro Metallurgical Co. at Niagara Falls will be visited. Lunch will be served at the Buffalo Trap and Field Club. In the afternoon, an inspection will be made of the Cornell Aeronautical Laboratories in Buffalo.

Personals

LAWRENCE J. HALDERMAN

Lawrence J. Halderman, Timken Roller Bearing Co., has been appointed director of the general components div., business and defense services administration, U. S. Dept. of Commerce. He will serve actively for six months, after which he will be available as a trained reservist.

E. B. Suydam has been appointed president of Linde Air Products Co., New York. Mr. Suydam succeeds **T. D. Cartledge** who continues as a vice president of UCC.

Gilbert R. Semans was appointed assistant director of metallurgy and research, Jessop Steel Co., Washington, Pa. Mr. Semans was formerly a research associate at Universal-Cyclops Steel Corp., Bridgeville, Pa.

Ralph A. Happe, former chief metallurgist, Kwikset Locks, Inc., Anaheim, Calif., has joined North American Aviation, Inc., Inglewood, Calif.

Gerald O. Loach, assistant manager of the plant, Electro Metallurgical Co. of Canada, Welland, Ontario, has been named president, Electro Metallurgical Co., div. UCC, Welland, Ontario, Canada.

Chester Hadley is metallurgist for the Bridgeport Brass Co., Bridgeport, Conn., in the laminating div. Mr. Hadley had been associated with the federated metals div., American Smelting & Refining Co., Newark, N. J.

Paul D. Hale is with the Phelps Dodge Refining Corp., El Paso, Texas, as plant engineer.

K. Sudo has joined the Nuffield Research Group, extraction metallurgy, Royal School of Mines, London, England. He had been on the staff of Tohoku University, Sendai, Japan.

Edward M. Grala has resigned from the staff of the National Advisory Committee for Aeronautics, Cleveland. He is now with the Glenn L. Martin Co., nuclear div., Baltimore.

Warren P. Chernock has joined the reactor development div., Combustion Engineering, Inc., New York.

Richard F. Lupi has resigned from Utica Drop Forge & Tool Corp., Utica, N. Y., as assistant plant manager. He has accepted the position as a metallurgist at the Knolls Atomic Power Laboratory, General Electric Co., Schenectady.

R. W. Rebholz has joined the Union Carbide Nuclear Co., New York. He had been with the Vanadium Corp. of America, Cambridge, Ohio.

EDMUND M. WISE

Edmund M. Wise has been promoted to assistant to the vice president, manager, development and research div., International Nickel Co., Inc., New York.

D. W. Johnson, Reynolds Metals Co., Troutdale, Ore., has been promoted to assistant plant manager. He had been carbon plant manager.

Ralph G. Wells, U. S. Steel Corp., applied research laboratory, Monroeville, Pa., is on the staff of the University of Michigan, Engineering Research Institute, Ann Arbor, Mich.

Bernard J. Esarey has been named general superintendent, heavy alloy fabricast div., General Motors Corp., Bedford, Ind. Mr. Esarey had been chief engineer, national bearing div., American Brake Shoe Co., St. Louis.

W. L. Schalliol, Northern Indiana Brass Co., Elkhart, Ind., has been promoted from manager of branches to director of engineering.

W. D'Orville Doty, U. S. Steel Corp., has been transferred from Pittsburgh to the applied research laboratory at Monroeville, Pa.

T. Stevens Daugherty has resigned from the Ford Motor Co., Dearborn, Mich. He is now with the Bohn Aluminum & Brass Corp., Greensburg, Ind.

Harry W. Highriter has joined the staff of Fansteel Metallurgical Corp., North Chicago, as vice president and technical director. Mr. Highriter had been associated with the Vascoloy-Ramet Corp., Waukegan, Ill.

Charles E. H. Halle, Cerro de Pasco Corp., La Oroya, Peru, has been named superintendent of lead smelting. Mr. Halle had been smelter metallurgist for the company.

Hubert C. Smith is now with the Colorado Fuel & Iron Corp., Claymont, Del. He had been assistant vice president in charge of metallurgical control for Great Lakes Steel Corp., Detroit.

Alexander Leipper, Reynolds Metals Corp., is manager of the Patterson plant at Arkadelphia, Ark. He had been at the Troutdale, Ore., plant.

Charles Locke has joined Westelectric Castings, Inc., Los Angeles. Mr. Locke had been with the West Michigan Steel Foundry Co., Muskegon, Mich.

Harry C. Fuller, U. S. Bureau of Mines, Boulder City, Nev., has been transferred to Salt Lake City as supervising extractive metallurgist.

Charles G. McCabe, supervisor technical service, Wheeling Steel Corp., has been transferred from Wheeling, W. Va., to Steubenville, Ohio.

James C. Buck, American Smelting & Refining Co., has been transferred to the New York ore purchasing dept. He had been located at the Garfield plant, Garfield, Utah.

Frank A. Zorko is now plant metallurgist for the lamp div., General Electric Co., Cleveland. Mr. Zorko had been associated with the Cleveland Graphite Bronze Co., Cleveland.

Apr. 15, 1956, is the deadline for papers that are to be presented at the Institute of Metals Div. Fall Meeting in Cleveland, Oct. 8 to 10, 1956. Papers received by this deadline but requiring revision may not be processed in time to permit scheduling for this meeting.

Obituaries

Clarence Aldro Wright

An Appreciation by
David L. Forrester

The passing of C. A. Wright (Member 1912) on June 10, 1955 at the age of 69 was a real loss not only to his many friends but to the mining profession.

Mr. Wright was a native of Marquette, Mich. He was a graduate of the George Washington University, the Yale Sheffield School, and did postgraduate work at the Royal School of Mines in Berlin.

He was associated with the Bureau of Mines from 1911 to 1920, first in charge of research in ore-dressing at the Experimental Station in Joplin, Mo.; then in charge of the Bureau's Experimental Station in Moscow, Idaho; and later at the Salt Lake City Station. From 1920 to 1928 he was employed by the Atesina Mining Co. in northern Italy where he was in charge of building concentrating mills and later became manager of the company.

Returning to the U. S., he was employed by the Standard Oil Co. of New Jersey in research on hydrogeneration of coal. He returned to federal service with the Bureau of Mines and in 1941 joined the Office of Production Management and subsequently was with the War Production Board. He continued with the Government until he retired in 1953.

He was a member of the Mining and Metallurgical Society of America, the Cosmos Club of Washington, D. C., and the Chi Phi Fraternity at Yale.

During his Federal service, he was particularly helpful to the young engineers and metallurgists entering the Government service.

Survivors are his widow, Dorothy Gibson Wright; two daughters, Mrs. William A. Van Allen and Mrs. David W. Heron; five grandchildren; and his brother, Charles Will Wright.

Aaron B. Bagsar (Member 1924) died Oct. 7, 1955. He was chief metallurgist for the Sun Oil Co., Philadelphia, until his retirement two years ago. Mr. Bagsar was born in Armenia in 1896, received a B.S. from the University of California in 1924 and an M.S. from the University of Idaho in 1925. Shortly after receiving a Ph.D. from Columbia University in 1927, he joined International Nickel Co., Huntington, W. Va., as a research metallurgical engineer. Mr. Bagsar was later employed by Babcock & Wilcox Co. in Bayonne, N. J. In 1932 he joined Sun Oil Co. as manager of the metal and inspection dept. and also began serving as consulting metallurgical engineer for the Sun Shipbuilding Co., Chester, Pa. Mr. Bagsar was the author of many technical articles and held U. S. and Canadian patents.

Keith F. Finlay (Member 1947) was killed in an airplane crash in Wyoming, Oct. 6, 1955. At the time of his death, Mr. Finlay was employed by Northrop Aircraft Inc., Hawthorne, Calif. Born in Victoria, B. C., in 1913, he received a B.S. from Oregon State College in 1937. A short time later Mr. Finlay went to South America as junior engineer for Chile Exploration Co., Chuquicamata, Chile. Returning to the U. S., he joined Phelps Dodge Co., Morenci, Ariz., as superintendent of materials. Later Mr. Finlay was associated with Airesearch Mfg. Co., Los Angeles. Prior to joining Northrop Aircraft Inc., he was manager, Southwestern Mines Inc., Douglas, Ariz. For a number of years Mr. Finlay was a member of Latterly, Keith F. Finlay Engineering Service, acting as consulting industrial metallurgist.

Victor A. Giesey (Member 1951) died Nov. 5, 1955. He was president of Narco Products Co., Pittsburgh. Mr. Giesey was born in Pittsburgh in 1883 and gained his early experience there with Drake & Stratton Contractors and Harbison-Walker Refractories Co. He was later associated with Gas Machinery Co., Cleveland; Portsmouth Refractories Co., Portsmouth, Ohio; and U. S. Refractories Co., Mt. Union, Pa. Mr. Giesey was also president of National Refractories Co., Cleveland. Prior to joining Narco Products Co. in 1937, he was works manager, Egan Webster Co., Pittsburgh.

Harold B. Makin (Member 1942) died Oct. 12, 1955 at Provo, Utah, after a brief illness. Mr. Makin was division superintendent at the Geneva Works, U. S. Steel Corp., Columbia-Geneva Steel Div., Provo, Utah. He was born in Alabama in 1892. After attending the University of Alabama, Mr. Makin joined Woodward Iron Co., Woodward, Ala. Later he was employed by Corrigan McKinney Steel Co., Cleveland, and Gulf States Steel Co., Gadsdan, Ala. In 1918 Mr. Makin became associated with Colorado Fuel & Iron Co., Pueblo, Colo., where he rose to general foreman of the byproducts dept. In 1924 he was employed as general coke plant foreman by Columbia Steel Co., Provo, Utah, which later became part of the U. S. Steel Corp. In 1937 Mr. Makin was promoted to superintendent of blast furnaces and became division superintendent of Geneva Works furnaces in 1952.

Charles B. Willmore (Member 1948) technical consultant, Kaiser Aluminum & Chemical Sales Co., Newark,

Proposed for Membership
— Metals Branch AIME —

Total AIME membership on Nov. 30, 1955 was 23,526; in addition 2284 Student Associates were enrolled.

ADMISSIONS COMMITTEE

P. D. Wilson, Chairman; F. A. Ayer, Vice-Chairman; A. C. Brinker, R. H. Dickson, T. D. Jones, F. T. Hanson, Sidney Rolle, O. B. J. Fraser, F. T. Sisco, Frank T. Weems, R. L. Zieyfield, R. B. Caples, F. W. McQuiston, Jr., A. R. Lytle, H. R. Wheeler, L. P. Warriner, J. H. Scuff.

The Institute desires to extend its privileges to every person to whom it can be of service, but does not desire as members persons who are unqualified. Institute members are urged to review this list as soon as possible and immediately to inform the Secretary's office if names of people are found who are known to be unqualified for AIME membership.

Members

Earl V. Akerlow, Oakland, Calif.
Heinz W. Balster, WittenRuhr, Germany
Jack Bateman, Ferndale, Mich.
Ernesto Beyer, Monclova, Coahuila, Mexico
O. Norman Carlson, Ames, Iowa
Jean Coudsl, Mont-sur-Marchienne, Belgium
Harry U. Glimer, Birmingham, Ala.
Robert C. Hilprecht, Jr., Detroit, Mich.
John W. Holden, Milford, Near Derby, England
Richard W. Hyde, Lexington, Mass.
Walter L. Kerlie, Monroeville, Pa.
Stanley V. Margolin, Brookline, Mass.
Blair L. Molander, Downey, Calif.
Kent I. Newman, Columbia Falls, Mont.
Walter E. Rager, Lark, Utah
Wilhelm E. Schwabe, Niagara Falls, N. Y.
David A. Sharp, Wantagh, N. Y.
Charles R. Skinker, Summit, N. J.
Antonio S. Tarnawiecki, Lima, Peru
Delmar E. Trout, Cheshire, Conn.
Carl A. Westerdahl, Baguio, P. I.
Russell C. Weymier, Chesterton, Ind.

Associate Members

Lawrence J. Burlett, Leetsdale, Pa.
Samuel A. Constantino, Jr., Moab, Utah
Anthony F. Corbetta, Grand Junction, Colo.
Bruce A. Fountain, White Plains, N. Y.
Urban W. Howard, New York, N. Y.
Donald L. Johnson, Cambridge, Ohio
James F. Jones, Newark, Ohio
Louis R. Matricardi, Cambridge, Ohio
Eugene A. Mogentale, Meadowlands, Pa.
Walter W. Nash, Springfield, Pa.
T. Vaughan Simpkinson, Warren, Ohio
Stanley A. Tucker, New York, N. Y.
John Shepherd, Pittsburgh, Pa.

Junior Members

Allan K. Booth, Jr., Linden, N. J.
Merwyn B. Brodsky, Upton, L. I., N. Y.
David L. Douglass, Columbus, Ohio
Neal R. Griffing, Niagara Falls, N. Y.
Robert W. Hogue, Pittsburgh, Pa.
Edward E. Hucke, Ann Arbor, Mich.
Robert H. Lascheid, Trumbull, Canada
Bruno F. Peters, Victoria, B. C., Canada
John P. Rowe, Ann Arbor, Mich.
Charles A. Sutherland, Trail, B. C., Canada
William R. Yario, Chicago, Ill.

REINSTATEMENTS

Members

Louis G. Klinker, Joliet, Ill.
Jack B. McConnell, Copper Cliff, Ont., Canada

Associate to Member

Vincente Chiaverini, Sao Paulo, Brazil

Junior to Member

William O. Alexander, Sea Cliff, L. I., N. Y.

Student to Member

Ben T. Collins, Crawfordsville, Ind.
Horace J. Corigliano, Wantagh, N. Y.
Donald G. Treilhard, Nkana, N. Rhodesia

Junior to Associate

Thomas F. Kaveney, Albany, N. Y.

CHANGE OF STATUS

Associate to Member

Paul T. Aylward, Bethlehem, Pa.
James Y. Dong, Anaconda, Mont.
Donald N. Rosenblatt, Salt Lake City, Utah
Italo S. Servi, Niagara Falls, N. Y.

Ohio, died in October 1955. Born in Marion, Ind., in 1893, he received a B.S. from the University of Wisconsin in 1916 and a Ch.E. in 1924. Mr. Willmore also attended Carnegie Institute of Technology. Shortly after receiving his B.S., he joined Aluminum Co. of America, Massena, N. Y., as chief chemist. Mr. Willmore became assistant chief of Alcoa's Chemical Development Div., New Kensington, Pa., in 1930, and assistant chief of the Process Metallurgy Div. in 1942. He joined William F. Jobbins Inc., Aurora, Ill., as chief metallurgist in charge of research before serving as technical consultant to Kaiser Aluminum & Chemical Sales Co. Mr. Willmore was a member of AIChE, American Chemical Society, American Foundrymen's Association, and ASM.

Necrology

Date of Election	Name	Date of Death
1941	Richard G. Amidon	Unknown
1936	Benjamin V. Becker	Feb. 5, 1955
1943	D. F. Brown	November 1955
1906	Milton A. Caine	Dec. 25, 1955
1947	Keith F. Finlay	Oct. 6, 1955
1937	Teodoro Flores	February 1955
1927	Adnah G. Kostenbauder	Unknown
1931	H. H. Lester	Nov. 11, 1955
1952	V. H. Montgomery	Unknown
1921	R. Hartley Sherwood	Dec. 2, 1955
1948	A. A. Smith	Nov. 26, 1955
1950	Irving S. Tillotson	Apr. 8, 1955
1912	Carl J. Trauerman	Unknown
1920	Marshall S. Walker	Dec. 2, 1955
1905	Samuel S. Wyer	Nov. 30, 1955

PROFESSIONAL SERVICES

Limited to AIME members, or to companies that have at least one AIME member on their staffs. Rates $40 per year per inch.

LEDOUX & COMPANY
Chemists Assayers Spectroscopists
SHIPPERS REPRESENTATIVES
Mine Examination Analyses
359 Alfred Ave. Teaneck, New Jersey

MAX STERN
Consulting Engineer
Expert for Scrap Recovery and Shipwrecking — Modernization of Plants and Yards for Ferrous and Nonferrous Metal Scrap
149 Broadway New York 6, N. Y.

H. L. TALBOT
Consulting Metallurgical Engineer
Extraction and Refining of Base Metals Specializing in Cobalt and Copper
Room 330, 84 State St., Boston 9, Mass.

DR. E. TSUTSUMI
Registered Japanese Patent Attorney & Metallurgical Consulting Engineer
Patent Matters—Research . . . technical text translated from Japanese into English or vice versa: 2¢ per English word.
C. P. O. Box 1545 Tokyo, Japan

— Coming Events —

Feb. 16, AIME, Cleveland Section, dinner meeting, Hotel Manger, Cleveland.

Feb. 20-23, AIME, annual meeting, Statler and New Yorker Hotels, New York.

Feb. 26-29, American Institute of Chemical Engineers, Statler Hotel, Los Angeles.

Feb. 27-Mar. 2, ASTM, committee week, Statler Hotel, Buffalo.

Mar. 6, AIME, NOHC, Northern Ohio Local Section, Youngstown, Ohio.

Mar. 15, AIME, Cleveland Section, dinner meeting, Hotel Manger, Cleveland.

Mar. 15-16, Steel Founders' Society of America, annual meeting, Drake Hotel, Chicago.

Mar. 19-21, AIME, Niagara Frontier Local Section, Regional Meeting on Reactive Metals, Statler Hotel, Buffalo.

Mar. 19-23, ASTE, national convention and industrial exposition, International Amphitheatre, Chicago.

Mar. 21, AIME, NOHC, Western Section, Rodger Young Auditorium, Los Angeles.

Mar. 22-23, Institution of Mining and Metallurgy, extractive metallurgy symposium, Royal Society of Arts, London, England.

Apr. 2-7, International Union of Crystallography, Madrid, Spain.

Apr. 9-11, AIME, Blast Furnace, Coke Oven, and Raw Materials and National Open Hearth Steel Conferences, Netherland-Plaza Hotel, Cincinnati.

Apr. 10-12, Metal Powder Association, annual meeting and Metal Powder Show, Hotel Cleveland, Cleveland.

Apr. 18-20, National Industrial Research Conference, Armour Research Foundation, Illinois Institute of Technology, Chicago.

Apr. 19, AIME, Cleveland Section, dinner meeting, Hotel Manger, Cleveland.

Apr. 20-21, AIME, New England Regional Conference, Waverly Inn, Cheshire, Conn.

Apr. 22-26, American Ceramic Society, Statler Hotel, New York.

Apr. 26-27, American Insitute of Electrical Engineers, national meeting, Bradford Hotel, Boston.

Apr. 29-May 3, Electrochemical Society, Inc., Mark-Hopkins Hotel, San Francisco.

May 6-9, American Institute of Chemical Engineers, Roosevelt Hotel, New Orleans.

May 14-17, Design Engineering Show, Convention Hall, Philadelphia.

May 16, AIME, Western Section NOHC, Rodger Young Auditorium, Los Angeles.

May 22-25. Societe de Chimie Physique (Society of Physical Chemistry), annual reunion, Paris, France.

June 4-7, Material Handling Institute, show, Public Auditorium, Cleveland.

June 5, AIME, NOHC, Buffalo Section, golf party.

June 13, AIME, NOHC, Pittsburgh Section, golf party, Pittsburgh Field Club.

June 16-23, Fifth World Power Conference, Vienna, Austria.

June 17-22, ASTM, annual meeting, Hotel Chalfonte-Haddon Hall, Atlantic City.

June 22-July 6, International Machine Tool Exhibition, Olympia, London, England.

Aug. 23-25, National Council of State Boards of Engineering Examiners, Hotel Statler, Los Angeles.

Sept. 26-28, AIME, Rocky Mountain Minerals Conference, Salt Lake City. Technical papers will represent all branches.

Oct. 8-10, AIME, IMD fall meeting, Hotel Carter, Cleveland.

Advertisers' Index

Ajax Electrothermic Corp. *The Harry P. Bridge Co.*	*
Ajax Engineering Corp. *Eldridge, Inc.*	230
American Bridge Div., U. S. Steel Corp. *Batten, Barton, Durstine & Osborn, Inc.*	229
Bailey Co., Wm. M. *Downing Industrial Adv., Inc.*	*
Basic Refractories Inc. *The Griswold-Eshleman Co.*	*
Bell Telephone Labs. *N. W. Ayer & Son, Inc.*	225
Buehler Ltd. *Kreicker & Meloan, Inc.*	228
Consolidated Vacuum Corp. *Charles L. Rumrill & Co., Inc.*	*
Dow Chemical Co. *MacManus, John & Adams, Inc.*	*
Electro Met. Div., Union Carbide & Carbon Corp. *J. M. Mathes, Inc.*	Second Cover
General Electric Co., X-Ray Dept. *Klau, Van Pietersom-Dunlap Assoc.*	*
Great Lakes Carbon Corp. *Davis, Parsons & Strohmeier, Inc.*	227
Harbison-Walker Refractories Co. *Downing Industrial Adv., Inc.*	*
International Nickel Co. *Marschalk & Pratt*	232
Jet Propulsion Laboratory, Caltech *Frank Barrett Cole, Adv.*	226
Leitz, Inc., E. *L. W. Frohlich & Co., Inc.*	221
Molybdenum Corp. of America *Smith, Taylor & Jenkins, Inc.*	*
Morgan Construction Co. *Davis Press, Inc., The*	220
National Research Corp. *Sutherland-Abbott Adv.*	*
North American Philips Co. *Anders Assoc. Adv.*	*
Pittsburgh Lectromelt Furnace Corp. *The Griswold-Eshleman Co.*	Third Cover
Shieldalloy Corp. *Harold Schor Assoc.*	*
Smeeth-Harwood Co. *Allbright Associates Adv.*	224
Steel City Testing Machines, Inc. *Whipple & Black Adv. Co.*	218
Stokes Machine Co., F. J. *The Aitkin-Kynett Co.*	222, 223
Swindell-Dressler Corp. *Downing Industrial Adv., Inc.*	*
Titanium Alloy Mfg. Div. *Comstock & Co.*	*
United States Graphite Co., The *Price, Tanner & Willox, Inc.*	Fourth Cover
U. S. Steel Corp. Columbia-Geneva Steel Div. Tennessee Coal & Iron Div. U. S. Steel Supply Div. U. S. Steel Export Co. *Batten, Barton, Durstine & Osborn, Inc.*	*
Utica Drop Forge and Tool Corp. *Wilson, Haight, Welch & Grover, Inc.*	*
Wyman-Gordon Co. *John W. Odlin Co., Inc.*	*

* Previous issue

LECTROMELT* FURNACES

for smelting and refining range from 50 to 24,000 KVA for electrothermic production of...

- COPPER MATTE
- NICKEL MATTE
- TIN
- TUNGSTEN
- VANADIUM
- COBALT
- LEAD
- SILICON
- ZINC
- TITANIFEROUS AND NICKEL-BEARING IRON ORE
- CALCIUM CARBIDE
- PHOSPHOROUS
- FERRO-SILICON
- FERRO MANGANESE
- PIG IRON
- FERRO-CHROMIUM
- ABRASIVES
- FUSED REFRACTORIES

LECTROMELT engineers have been conducting continuing research for years on electrothermic reductions—have designed and built many furnaces for various branches of the metallurgical and chemical industries. They can advise you on many of those operations.

Lectromelt furnace components are strong and sturdy—electrode clamps and controls are positive and fast acting, but micro-accurate—charging methods are developed to a high degree—electrical equipment and substations are built to withstand tremendous overloads.

Catalog No. 105 describes Lectromelt equipment. For a copy, write Pittsburgh Lectromelt Furnace Corporation, 326 32nd Street, Pittsburgh 30, Pennsylvania.

Manufactured in... GERMANY: Friedrich Kocks GMBH, Dusseldorf... ENGLAND: Birlec, Ltd., Birmingham ... FRANCE: Stein et Roubaix, Paris... BELGIUM: S. A. Belge Stein et Roubaix, Bressoux-Liege... SPAIN: General Electrica Espanola, Bilbao... ITALY: Forni Stein, Genoa. JAPAN: Daido Steel Co., Ltd., Nagoya

*REG. T. M. U. S. PAT. OFF.

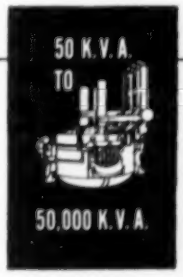

WHEN YOU MELT... MOORE RAPID *Lectromelt*

NEW!

a memo to Melters, Open Hearth Superintendents, Metallurgists and others concerned with quality steel making . . . If you haven't tried RECARB-X and want the full facts on the best recarburizer for steel making, write for the new Engineering Bulletin No. 11, use the convenient coupon below.

SEND ME ENGINEERING BULLETIN NO. 11

NAME _____

TITLE _____

FIRM _____

ADDRESS _____

CITY _____ STATE _____

210

THE UNITED STATES GRAPHITE COMPANY

DIVISION OF THE WICKES CORPORATION • SAGINAW, MICHIGAN